SPRINGER BRIEFS IN ECOLOGY

James R. Miller
Christopher G. Adams
Paul A. Weston
Jeffrey H. Schenker

Trapping of Small Organisms Moving Randomly

Principles and Applications to Pest Monitoring and Management

Springer

SpringerBriefs in Ecology

SpringerBriefs present concise summaries of cutting-edge research and practical applications across a wide spectrum of fields. Featuring compact volumes of 50 to 125 pages, the series covers a range of content from professional to academic.

Typical topics might include:

- A timely report of state-of-the art analytical techniques
- A bridge between new research results, as published in journal articles, and a contextual literature review
- A snapshot of a hot or emerging topic
- An in-depth case study or clinical example
- A presentation of core concepts that students must understand in order to make independent contributions

More information about this series at http://www.springer.com/series/10157

James R. Miller • Christopher G. Adams
Paul A. Weston • Jeffrey H. Schenker

Trapping of Small Organisms Moving Randomly

Principles and Applications to Pest Monitoring and Management

Springer

James R. Miller
Department of Entomology
Michigan State University
East Lansing
Michigan
USA

Paul A. Weston
School of Agricultural and Wine Sciences
Charles Sturt University
Wagga Wagga
New South Wales
Australia

Christopher G. Adams
Department of Entomology
Michigan State University
East Lansing
Michigan
USA

Jeffrey H. Schenker
Department of Mathematics
Michigan State University
East Lansing
Michigan
USA

Any opinions, findings, and conclusions or recommendations expressed in this material are those of the author(s) and do not necessarily reflect the views of the National Science Foundation. who now funds this research program under Grant RC104081 to J.H.S. and J.R.M

ISSN 2192-4759 ISSN 2192-4767 (electronic)
SpringerBriefs in Ecology
ISBN 978-3-319-12993-8 ISBN 978-3-319-12994-5 (eBook)
DOI 10.1007/978-3-319-12994-5

Library of Congress Control Number: 2014959858

Springer Cham Heidelberg New York Dordrecht London

Printed on acid-free paper

Springer is part of Springer Science+Business Media (www.springer.com)

The senior author dedicates this book to the three wonderful scientific educators/mentors most responsible for his scientific development and career success: **Dr. William Yurkiewicz** *(Department of Biology, Millersville University; undergraduate advisor and person who, despite my dubious grade point average, extended the invitation to join him in real research leading to peer-reviewed publications);* **Dr. Ralph Mumma** *(Department of Entomology, Penn State University; Ph.D. Major Professor); and* **Dr. Wendell Roelofs** *(Department of Entomology, Cornell University; Post-doc mentor). This book is a product of the superb example you set for creativity and innovation, critical thinking, rigorous experimentation, and the seamless integration of fundamental and applied research. Your passion for research and demonstration that science can be great fun has been a lifelong gift, nearly as important as your unwavering belief in me and my potential.*

—J. R. Miller

Preface

This SpringerBrief focuses on how the numbers of randomly moving organisms caught in monitoring traps can be translated into reliable estimates of their absolute rather than just relative density. Quick and inexpensive methods for establishing absolute density are sorely needed to enable pest managers to sharpen their decisions about when pesticides are or are not justified, thereby boosting profits as well as human and environmental safety.

This book grew out of seemingly disparate experiences by Dr. James Miller during a research and teaching career as a quantitative insect behaviorist and chemical ecologist working at Michigan State University, a Land-Grant University where fundamental and applied science are expected to blend seamlessly to produce knowledge that makes a difference in the world. Our applied research on how insect control might be effectively achieved using sex attractant pheromones to disrupt mate-finding led to fundamental research on the mechanisms whereby sex pheromones impact insect behavior and physiology. One highly productive approach explored parallels between mating disruption of moth pests of apple and enzyme kinetics. The goal was to determine whether mating disruption was or was not mediated principally by competition between artificial and natural point sources of pheromone ("substrates") for the attention of responsive males ("enzyme"). However, the "test tubes" for these quantitative experiments interrelating capture numbers in traps with manipulated numbers of female and male insects as well as dispensers of artificial pheromone were 20 field cages, each covering 12 full-sized apple trees. Nevertheless, striking and useful parallels were found between these inanimate and molecular vs. macroscopic and whole-organism systems. Highly reproducible patterns in the capture data convinced us that insects and molecules were behaving similarly at their given spatial scales, e.g., both diffusing randomly throughout their test tubes before complexing for measurable times with any agents for which they had affinity. Moreover, we discovered that the known absolute density of insects deployed in the cages could accurately be derived from graphical plots of the number of attractive pheromone dispensers deployed per cage against the inverse of catch per monitoring trap. That insight piqued our curiosity about whether such an approach might also be successful in the open-field situation.

Further insights into random elements in animal behavior came from teaching a graduate-level course in insect behavior. One of the laboratory exercises required students to record and analyze the tracks of dispersing insects. The picture emerging across years of data was that most insects not influenced by cues from resources, move randomly and display normal distributions of headings for new steps whose width is characteristic of the species, but varies across species. Additionally, striking matches were found between the tracks produced by real vs. the randomly-based computer-simulated movers we developed for teaching the mechanisms of insect orientation and their consequences when foraging.

Yet another line of research on egg depositional behaviors of onion flies interacting with artificial host plants of varying quality gave evidence for the existence of some sort of "random number generator" that injected randomness into the investment decisions of insect herbivores, essentially allowing them to diversify investments across the full range of resource qualities while investing most heavily in the best resources. The patterns of investment by real insects were faithfully reproduced by simple computer simulations where the strength of the positive factors promoting egg deposition was divided by the strength of any negative factors to yield a quotient then increased or decreased by a random input. A bout of oviposition was envisioned to turn on when the overall outcome fell above some threshold value.

This convergence of data from various systems points toward a central and highly valuable role for random elements within the mechanics underpinning the biology of simple organisms like insects. We elected to tackle the important puzzle of understanding the mechanics of trapping with the confidence that random elements and random outcomes would feature prominently in the problem, and that computer simulations permitting the manipulation of random elements would be an essential tool in that exploration. We also recognized that this effort would best be accomplished by a team bringing expertise from biology/behavior (J.R.M., C.G.A., P.A.W.), computer science (P.A.W.), and mathematical physics (J.H.S.). Thus, the product you are about to read represents an interdisciplinary synthesis.

September 24, 2014 J. R. Miller

Acknowledgements

We gratefully acknowledge the positive influence of many colleagues in the Department of Entomology and its administrators at Michigan State University (MSU) who created an atmosphere fully supportive of this research and the production of this book. A special and heartfelt thanks goes to Drs. Larry Gut (tree-fruit entomologist at MSU) and Peter McGhee (technician and research associate in the MSU tree-fruit entomology lab) for more than a decade of intellectually stimulating and highly productive collaborations on the chemical ecology and management of tree-fruit pests, including investigations of insect mating disruption culminating in the large-cage experiments leading to this research on trapping as explained in the preface. The accomplishments reported here would not have been possible without the fusion of fundamental and theoretical insights with the wealth of applied and practical knowledge brought by the labs of Drs. Miller and Gut respectively, which yielded a unique synergism. We thank colleagues Drs. Matthew Grieshop and Rufus Isaacs of Entomology for linking authors J.R.M. and J.H.S. (MSU mathematics professor). Special thanks is also extended to David Williams (Director of the Department of Environment and Primary Industries of the State Government of Victoria, Tatura, Australia) for the invitation and financial support permitting J.R.M. to be a visiting scholar in Tatura, during which time these investigations into trapping theory commenced under enthusiastic encouragement. Likewise, the production of this book was significantly aided by the encouragement and backing of Drs. George Kennedy and Fred Gould (North Carolina State University) as well as Jocelyn Millar (Univ. California, Riverside).

Funding for the large-cage research leading to our trapping research was provided to Drs. Miller and Gut by the USDA National Research Initiative Entomology/Nematology program. Funding for the research reported here and during the production of this book came from MSU, Michigan Project GREEEN, and the Michigan Apple Committee. Author J.H.S. was supported by a grant from the Fund for Math during his sabbatical at the Institute for Advanced Study in the 2013-2014 academic year and by the National Science Foundation under a CAREER Grant (#0846325), which predisposed him to enter this interdisciplinary collaboration on trapping research. Our MSU research on trapping is now funded by a grant from the National Science Foundation (#1411411) to authors J.H.S. and J.R.M. Critical

bridging funds were provided by Dr. Steve Pueppke, director of Michigan AgRioResearch, when funding for this research program was repeatedly denied by the USDA AFRI Foundational Entomology/Nematology Program. Author C.G.A. acknowledges a Department of Entomology Teaching Assistantship supporting him for 2 years during which he conducted codling moth trapping studies and his current research assistantship paid from the NSF Grant #1411411. Undergraduate student, Danielle Kirkpatrick, ably assisted the field research. Author P.A.W. acknowledges the stimulating and nurturing atmosphere of the Miller lab, which encouraged the fusion of his interests in computer programming and insect behavior that gave rise many years ago to the basic movement model underlying the simulations used in this book, as well as the support of his wife, who endured countless hours having her husband lost in cyberspace as he wrote and tested computer code.

The highly professional, efficient, and pleasant interactions with editors Janet Slobodien and Eric Hardy of Springer Publishing in the crafting, vetting, and production of this book are gratefully acknowledged.

Contents

Author Contributions

J.R.M. conceived and led this project, framed its concepts and approaches, conducted the simulations and analyzed their outcomes, produced the figures and tables, and wrote the main text. J.H.S. and C.G.A. collaborated closely with J.R.M. in developing and vetting the concepts, selecting and refining the experimental approaches, and interpreting all data. P.A.W. designed, wrote, debugged, and alpha-tested the computer software based upon performance specifications from J.R.M. and C.G.A. Any correspondence requesting further information about or possible access to this *MultiMover* software should be directed to pweston@csu.edu.au. J.H.S. confirmed and refined the probability and mathematical content and wrote the mathematical footnotes. The field experiments reported for the codling moth were conducted by C.G.A. All authors closely checked, improved, and approved the manuscript.

List of Abbreviations

α	angle comprised by the adjoining legs of a current and previous step of a track for a mover
ac	acre
C	number of movers caught
C_T	movers caught per one trap
c.s.d.	circular standard deviation = standard deviation as applied to a normal (Gaussian) distribution of headings where 0° is straight ahead; +/– 1 c.s.d. contains 67 % of all possible values out of the full 360°
den	density = number per area
e	Euler's number
e	efficiency = probability that a mover having arrived at a trap gets captured when used in conjunction with T
f	findability = probability that a mover arrives at a trap or resource when used in conjunction with T
ha	hectare
IPM	integrated pest management
L	a length corresponding to trap diameter
m	meter
M	mover(s)
MAG plot	graph plotting the distance movers originate from a trap on the x-axis vs. 1/proportion captured on the y-axis
Miller plot	a graph plotting the radius of a trapping annulus on the x axis vs. spT_{fer} x annulus area on the y-axis
Miller-Gut plot	a graph plotting the density of competing sources of attraction on the x-axis vs. 1/ catch on the y-axis
P_T	Proportion of all movers populating a trapping area that will be captured in the focal trap T
P_t	proportion of all movers populating a trapping area that will be captured per competing trap t that otherwise would have appeared as part of the catch in the focal trap T
Prop. C	proportion of movers captured

R	a release point for a single-trap, multiple-release experiment
R_2	regression coefficient = proportion of the total variation attributable to the variable plotted on the x-axis
r	trapping radius = maximum dispersive distance for a population of movers plus plume reach
r	retention = probability that a mover having gotten caught in a trap is retained until harvested when used in conjunction with T
s	starting point for the track of a mover
S.E.M.	standard error of the mean = standard deviation divided by square root of n
spT_{fer}	proportion of movers caught when originating at a specified distance from a trap
T	trap; refers to the reference (focal) trap when used in an equation with t
t	competing trap
T_{fer}	expected number of organisms harvested after some specified time of trap operation divided by the total number of organisms within the sampling area of the trap
TR	trapping radius
TR_{75}	a distance equivalent to 75 % of the trapping radius
x-int	x-intercept
y-int	y-intercept

Chapter 1
Why Care About Trapping Small Organisms Moving Randomly?

1.1 Most Animals Are Small and Forage Using Simple Behavioral Rules

The Earth supports a rich diversity of microbial and plant life. In turn, these primary producers are estimated to support well more than 10 million species of animals (Mora et al. 2011), the preponderance of which are smaller than a fingernail and weigh less than a gram. The resources upon which most small terrestrial animals come to specialize are patchy and often ephemeral. Life spans of small animals are short. Their capacity for and the advantages of learning and memory are of less consequence than is usual for vertebrates like humans, whose behaviors are dominated by vision, spatial maps, directed locomotion, and planning before actions.

In contrast, animals like a small butterfly explore their environments initially using what appear to be random search mechanisms. If a potential resource is encountered by chance alone, it is important that the mover has the capacity to stop, examine, and exploit the resource if appropriate. Foragers initially engaged in simple random search can also encounter meaningful cues (e.g., visual or chemical) at some distance from a potential resource and then switch to more sophisticated behaviors to steer toward the source if the cues are positive (attractive) or away if the cues are negative (repellent) (Miller et al. 2009). The effectiveness of the deceptively simple foraging rules depicted in Fig. 1.1 should not be underestimated, given the resounding success of the many organisms using them and for which it is challenging to prove that more sophisticated tactics come into play.

1.2 The Most Serious Animal Pests Are Small

An unhappy fact of life from the human perspective is that small animals like insects, mites, mollusks, and nematodes compete with us for resources. Many become severe pests. Global annual losses to insects alone for just the top ten most abundant

J. R. Miller et al., *Trapping of Small Organisms Moving Randomly,*
SpringerBriefs in Ecology, DOI 10.1007/978-3-319-12994-5_1

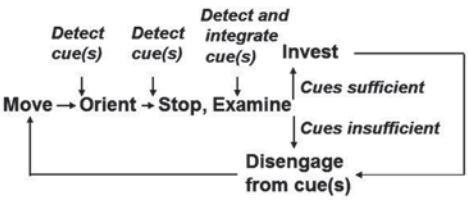

Fig. 1.1 Primitive but effective behavioral rules guiding foraging by simple organisms

food crops have been estimated at more than US $ 90 billion (Yudelman et al. 1998). In the USA alone, where some 0.5 million tons of pesticides are applied to crops annually, pests still destroy an estimated 37% of potential production (Pimentel 2005). Moreover, other small creatures cause vector diseases of plants and animals including humans. For example, mosquitoes of the genus *Anopheles* transmit human malaria, which annually kills about 1 million children in Sub-Saharan Africa alone (Breman et al. 2001). Successful management of these pests and disease vectors typically requires pesticides, which present well-known safety challenges to the human food supply, nontarget organisms, and the environment. An imperative of a civilized world is that pests and disease vectors be identified, monitored, and managed in a manner that strikes a fair compromise between the needs of humans, all of Earth's biota, and the biosphere.

1.3 Responsible Pest Management Decisions Require Knowledge of Pest Numbers

Fortunately, substantial progress toward this lofty aim has been made in the field of pest management theory and practice (Kogan 1986; Arora et al. 2012). A core concept of integrated pest management is that the control measures be applied only when sufficient numbers of pests are present to justify intervention. Thus, pest detection and monitoring programs need to be in place to identify what potential pests are present, precisely when they are active, and, ideally, their absolute abundance through time, as suggested in Fig. 1.2. The pest density at which the benefit of an intervention exceeds its cost is termed the *economic injury level* (EIL). Establishing the EIL requires both an accurate measure of pest numbers and knowledge of pest biology. For example, if adult insects are being monitored but it will be larvae that damage the crop, the pest manager must know the fecundity and mortality rates of the pest through time to predict population levels of the damaging life stage.

1.4 Current Methods of Estimating Absolute Densities of Pests Are Prohibitively Costly

Unfortunately, measuring the absolute density of organisms requires considerable time and effort; thus, it is costly. Texts on procedures for estimating animal density are readily available, e.g., (Krebs 1999; Southwood and Henderson 2000). The

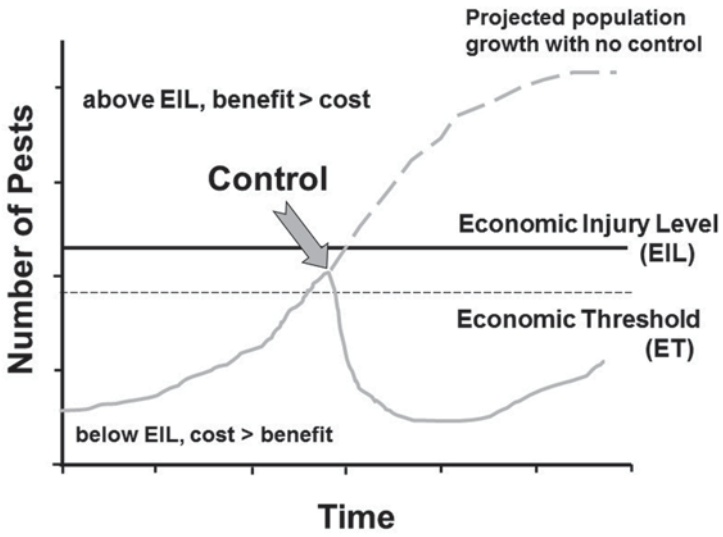

Fig. 1.2 Conceptual framework for how pest managers interrelate pest numbers and population growth over time with economics to apply a control measure only when it is actually needed and when the benefit of treatment exceeds its cost. This figure was redrawn from similar diagrams available on the web

simplest but certainly not least costly approach is direct enumeration. Here, one directly views the area over which the number of animals present is sought. For example, a researcher wishing to quantify shifts in polar bear populations in the face of global warming can pass across an expanse of polar ice in a low-flying airplane and count how many bears are sighted. Similarly, with sufficient patience and work force, researchers can count the hundreds of thousands of soybean aphids present in sections of selected fields. However, such enumerations are impossible for everyday management decisions for tiny pests.

Sampling regimes can shrink such a mammoth task. For example, reliable estimates of absolute animal density can be achieved by using transects across the area of interest and counting individuals within the selected quadrats of defined size at regular intervals along the transects. If the set of samples taken is representative of the area, overall absolute animal density can be estimated. Sequential sampling (Krebs 1999) aims to reduce sampling to the bare minimum needed for an estimate of animal density at some specified level of confidence sufficient for an informed pest management decision.

A quite different approach is mark-release-recapture (Krebs 1999; Southwood and Henderson 2000). Here, animals are collected from their habitat, distinctively marked, and released back into the existing population. After ample time for mixing, the population is sampled for the ratio of marked vs. unmarked individuals. Equations have been developed whose solutions yield an estimate of the total population density. This technique was first conceptualized and explored by Lincoln (1930) for birds. Various improvements on the original Lincoln Index have since been devised in attempts to improve its accuracy across a range of spatial contexts.

However, neither this nor any of the above techniques provide the quick, inexpensive, and reliable estimates of the absolute population density of animal pests needed for everyday pest management applications.

1.5 Can Traps and Trapping Fill This Need?

Enthusiasm for this approach as applied to insects ran high with the identification and synthesis of potent sex attractant pheromones of diverse pests (Roelofs and Cardé 1977). Pheromone-baited monitoring traps such as those pictured in Fig. 1.3 are indeed a boon to insect pest management because they reveal exactly what pest species are present and when they are active. Such information is critical to timing of sprays for maximum effect (Judd and Gardiner 1997). However, the initial expectation that catch numbers might be translated into accurate estimates of absolute pest density went unfulfilled. A key impediment has been that the trapping process is insufficiently understood to establish convincing links between numbers trapped with total numbers present in the area from which responders came. For most researchers, pest managers, and growers, trapping remains a "black box."

Rather than making control decisions on the basis of actual pest numbers, as the *y*-axis of Fig. 1.2 suggests, pest managers and growers rely on relative thresholds for control decisions. For example, our colleague Dr. Larry Gut is responsible for research and extension for insect pests of tree fruit in Michigan. He recommends deploying one codling moth monitoring trap like that in Fig. 1.3 for every ca. 5 ac of orchard. However, growers seeking to cut production costs usually deploy only several traps per 100 ac. Control measures are recommended if three or more codling moths are trapped for any 1 week of the growing season. This threshold is based on expert judgment accumulated over years of correlating moth captures in

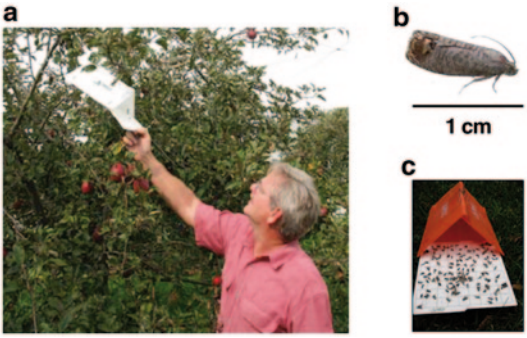

Fig. 1.3 **(a)** Trap for monitoring adult moth pests of tree fruit, in this case codling moth **(b)** in apple. A wire hanger permits the trap to be attached to an outer branch high in the tree canopy. The trap is open at the two ends; male moths are attracted to the trap by sex pheromone released from a small piece of rubber pinned inside the trap roof. Moths are ensnared on a glue-coated insert lining the inside bottom. The insert is partially withdrawn in **(a)** as the trap is being checked by the senior author. A high number of captured moths on the partially withdrawn insert is shown in **(c)**

monitoring traps with spray records and recorded damage to apple crops at the end of the growing season. Codling moth infestation of apples must be suppressed to less than 0.5%, or the crop will be rejected by the fresh-market processor and diverted to juice at substantial economic loss.

1.6 Aims and Approach of This Book

Our motivation for this book was the conviction that traps and trapping have much more potential to sharpen pest management decisions than has been achieved to date. Doing so requires deep understanding of the trapping process, including how both the trapping targets (movers) and trapping devices each contribute to catch. We will take a mechanistic approach that goes well beyond the richly historical and more descriptive volume by Muirhead-Thomson (1991)—*Trap Responses of Flying Insects.* Our investigation of trapping dynamics was greatly aided by computer simulations that capture the core elements of the trapping problem. Cyber tools made it possible to recreate the "black box" of trapping and then to quantify its outputs. We then systematically disassembled it to understand the overall effects of changes to its "gears, springs, and switches." The computer simulations reported here were conducted in a matter of months and represent research that would have occupied most of a career if completed only on real animals.

This book then integrates the insights gained from the cyber studies with real-world animal studies conducted in the field. We build on and extend the findings of various researchers who have already identified and assembled pieces of this intellectually challenging and important puzzle. However, the current treatment is not a comprehensive literature review. Rather, we aim for a succinct coverage that includes just the material necessary and sufficient to achieve the above aims.

As most of its authors are entomologists, this book is slanted toward insect examples. But, the principles explained here will hopefully find applications across a wide range of disciplines. Our chief applied aim is to provide the knowledge sufficient for translation of captured numbers into accurate estimates of absolute densities of small animals useful in sharpening pest management decisions. The principles uncovered for trapping are also highly relevant to the ecology of resource finding. These topics will be intertwined as the text progresses.

Many of the relationships encountered in this investigation are most efficiently conveyed by mathematical expressions. Moreover, solving equations for an unknown variable when the others are known is an intellectual tool whose power must be wielded in research on trapping. Thus, mathematics is inescapable. Only algebra will be employed in the main text so that all readers can follow the complete story line and use this knowledge without special training. Nevertheless, the trapping of random movers is a problem that lends itself naturally to mathematical analysis and that will ultimately require more advanced mathematics for full characterization. We note some of the mathematical issues related to trapping in optional footnotes intended for the more mathematically inclined readers.

Chapter 2
Trap Function and Overview of the Trapping Process

2.1 Definition and Functions of Traps

Finding no formal scientific definition in the literature, we define traps as devices that delimit the displacement of previously free-ranging entities in space through time. Many types of animal traps have been invented. Long before the arrival of humans, living organisms were trapping prey (see examples in Fig. 2.1). In such cases, traps assist with capture and retention of prey until it can be fully subdued and consumed.

Traps prolong visits of animals to points in space. For example, a conventional hunter can rely on real-time encounters with prey to make the occasional harvest. However, a trapper can set multiple snares so as to greatly increase the probability of prey encounters while walking just the trap line. The time for which snared prey occupies dangerous space is stretched, whereas the time required for the trapper to realize prey encounters shrinks. Likewise, the pest manager wishing to assess codling moth populations in an apple orchard could walk about with a flashlight early at night when moths are active and attempt to count them. But, such an endeavor would be ill-advised, given typical codling moth low numbers, tiny size, and their ability to fade into the vegetation before identifications can be made. It is a far better idea to deploy traps like those in Fig. 1.3 and then check them all in a short interval after appreciable catch has accumulated.

Traps can also serve as removal or killing devices. Live trapping is done with the intent of inflicting no permanent harm and releasing the animal where it can no longer be a pest. Trap-and-kill devices operate by, e.g., electrocution (bug zapper), drowning (pitfall trap for garden slugs), delivering a killing blow (mouse trap), permanently ensnaring (fly paper), or poisoning (cockroach trap). The intent here is for the traps to reduce pest populations to tolerable levels quickly without requiring some additional control measures.

J. R. Miller et al., *Trapping of Small Organisms Moving Randomly,*
SpringerBriefs in Ecology, DOI 10.1007/978-3-319-12994-5_2

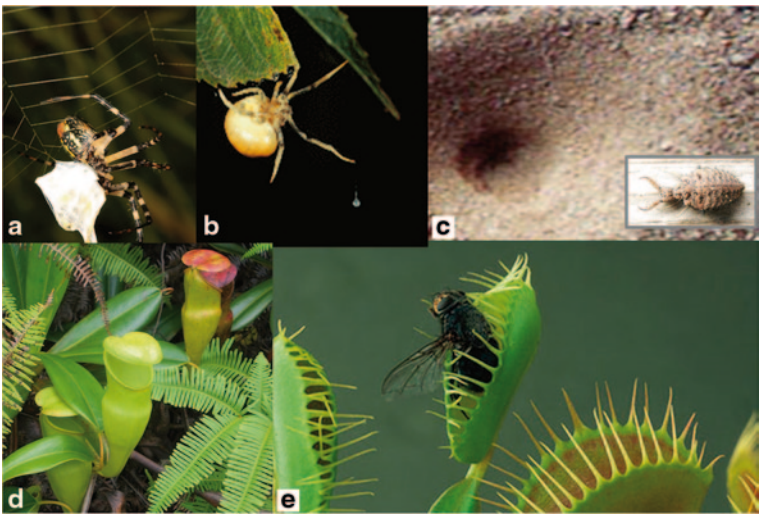

Fig. 2.1 Examples of trapping devices employed by living organisms for millions of years before humans invented their first trap. **(a)** Orb-weaver spider wrapping prey on its web. © Dr. Joseph Spencer, Illinois Natural History Survey, Univ. Illinois Campus. **(b)** Bolas spider lying in wait while dangling a sticky drop emitting moth sex pheromones. © K.F. Haynes and K.V. Yeargan, University of Kentucky. **(c)** Ant lion immature next to its sand trap. © Christopher G. Adams. **(d)** Pitcher plant. **(e)** Venus fly trap with captured fly. ©Ernie Janes/Alamy

2.2 Overview of the Trapping Process

A key feature of all trapping is intersection of a trap with its targets at some point in space. Because traps are typically stationary, it is their targets that must move so as to either approach the trap by a chance encounter or be lured there after chance encounters with attractive cues emitted by the trap. The latter case is diagrammed in Fig. 2.2 for the situation where the odorant from the trap diffuses equally in all directions and its concentration then falls with the square of distance. Responders can then be led to the source by steering up-gradient.

Only one of the four movers released near the trap in Fig. 2.2 encountered the odor, approached the trap, and got caught. The reason for low capture probability is that more space in Fig. 2.2 is devoid of odorant rather than containing it. Emission of odor effectively increases the size of a trap; yet, empty space predominates. Baiting the trap with a lure having further reach would elevate the probability that the trap is found, as would increasing foraging time. However, short-lived small organisms experience real limits on how far they can travel while avoiding environmental threats such as predation. Catch is influenced by trap size, attractant reach, mover meander (amount of turning per distance traveled), foraging time, and total distance movers displace all influence catch.

Figure 2.3 extends this scenario to the more usual case of a trap emitting an attractant into the breeze and where the responders can forage by flying or walking.

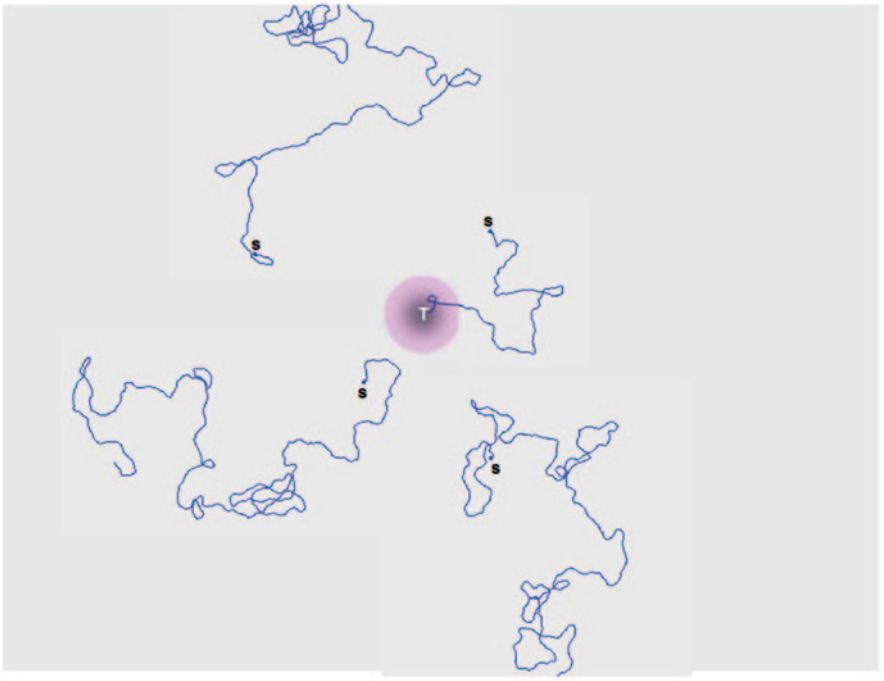

Fig. 2.2 Paths of four computer-simulated movers typical of insects and released at arbitrary distances from a trap (*T*) emitting an attractive odorant into still air. Displacement beginning at each *s* was random until chance encounter with the odor plume. Details of the computer program are given in Chap. 3

Here, the odor plume becomes elongated. Because locally foraging small animals such as insects responding to sex pheromones concentrate their search mainly to a layer near the top of a crop (Taylor 1974; Witzgall et al. 1999), the trapping problem remains essentially two-dimensional. Aerial plumes present a surprisingly flat concentration gradient along their length (Justus et al. 2002). Responders contacting a plume get little information about which direction is toward vs. away from the source. Therefore, they must use visual or tactile information to determine which direction is upwind and then be guided by the plume's borders as detected upon zigzagging in and out of a plume. Swimmers can also do this. Nevertheless, the above assessment that there is far more plume-free area around a trap than area occupied by the plume still holds. Again, trap size, plume reach, mover meander, foraging time, and total distance movers displace all strongly influence catch.

The series of steps that must occur for a target organism to be harvested as catch in a trap is listed in Fig. 2.3b. The overall probability of catch is the product of the probabilities for the requisite individual steps—steps 1 and 2 and 3 … and 6.

Findability (*f*) refers to the composite probability of only those steps bringing a target organism to the trapping mechanism. Efficiency (*e*) is reserved exclusively

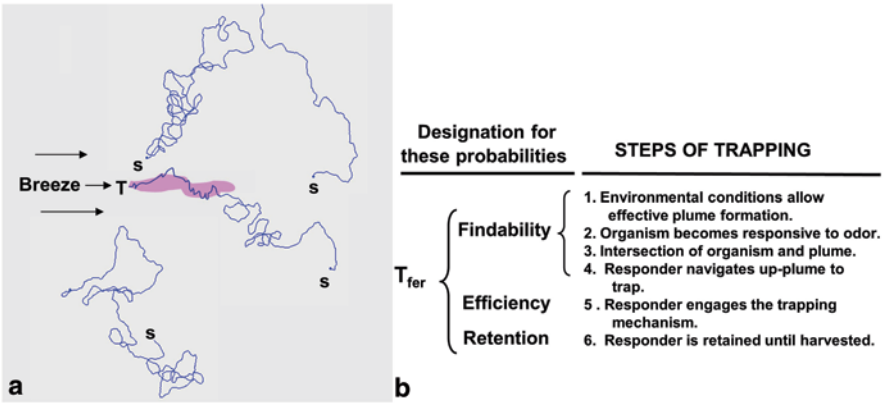

Fig. 2.3 **(a)** Paths of four computer-simulated movers exhibiting meander typical of insects and released at arbitrary distances from a trap (*T*) emitting an attractive odorant into moving air so as to generate a plume (*pink*). Displacement beginning at each *s* was random until a chance encounter with the odor plume. **(b)** Chain of steps required for a target animal to be caught in a trap emitting an attractant and designations for their probabilities

for the probability that the responder is caught by the trap once it has arrived. Step 6, retention (*r*), is the probability that the organism remains trapped until harvested. As introduced by Miller et al. (2010), we abbreviate the overall catch probability as T_{fer} where *T* stands for trap. T_{fer} equals the expected number of organisms harvested after some specified time of trap operation divided by the total number of organisms within the sampling range of the trap.

Of the three probabilities comprising T_{fer}, findability is subject to the most variation for two main reasons. First, plume reach varies with wind speed. Plume reach under a constant release of attractant will be greater under lower wind velocities than higher wind velocities. Packets of air passing slowly over the odorant source get loaded with a higher concentration of chemical so as to survive longer above the detection threshold. Additionally, greater turbulence under higher wind velocities dissipates the odorant more rapidly. But, zero wind flow is also suboptimal. Then, plume spread depends entirely upon diffusion, which is extremely slow for large odorant molecules such as sex-attractant pheromones (Gut et al. 2004). Optimal wind velocity for long-distance attraction is usually less than 1 m/s. Second, an animal's willingness or ability to forage can rise and fall with factors such as wind velocity, rainfall, humidity, and temperature. For example, codling moths cease flight whenever the air temperature falls below 16 °C (Batiste et al. 1973), perhaps because operating the flight muscles becomes energetically inefficient.

Efficiency of a given trap type should be more constant than findability. If environmental conditions allow responders to arrive at the trap, they are likely to remain favorable over the few minutes it may take to engage the trapping mechanism. But efficiencies across trap types will vary with the degree to which their engineering matches the proclivity of the responder to engage the capture

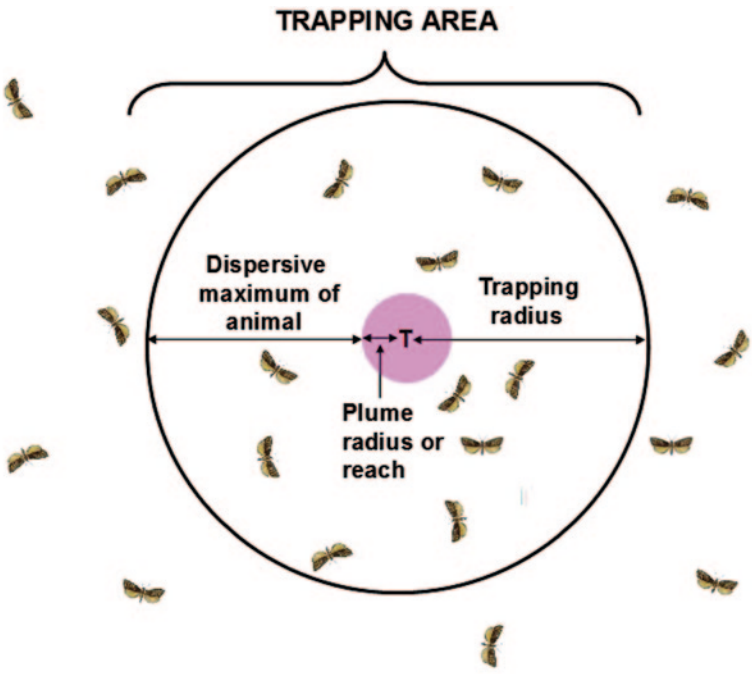

Fig. 2.4 Spatial relationships between dispersion of the target animal, plume reach, and trapping area for animals moving randomly before being attracted to the trap after contacting the plume. The trapping area would become slightly elliptical if the plume were an ellipse rather than a *disk* as *above*; but, the overall concept holds

mechanism (Muirhead-Thomson 1991). For moths responding to pheromone-baited monitoring traps, efficiencies can be as high as 0.7 (Elkinton and Childs 1983; Huang et al. unpublished data).

Retentions of the traps designed by humans are usually high because retention is easy to measure and remedy when faulty. Animals can be placed directly into the trapping mechanism and then observed to see how many escape and how they manage to do so. Countermeasures can then be taken.

The maximum net distance most randomly dispersing animals displace from their point of origin greatly exceeds the reach of an attractive plume (examples offered in Chap. 5). Thus, trapping radius is determined largely by the net dispersive radius of the target organisms plus plume reach (Fig. 2.4). All the moths depicted in Fig. 2.4 might reach the trap if they flew exclusively in straight lines (ballistically) and always toward the trap. However, because of path meander and limitations on flying time, only the encircled moths in Fig. 2.4 are suggested to have a measurable probability of reaching the trap and thus being within the *trapping area*. Even so, only some out of all the moths in the trapping area will be unlucky enough to string together a chain of turns that brings them to the plume of the trap rather than leading them out of the trapping area.

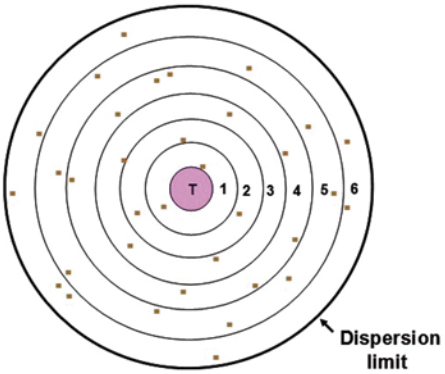

Fig. 2.5 Figure 2.4 is redrawn so that the sampling area of the trap is divided into six annuli of equal width. Here, the trap's sampling area is shown with a higher density of randomly distributed target organisms, now shown as *dots,* and none are depicted outside the dispersion limit. The dispersion limit indicates that organisms do not have the locomotory capacity to reach the trap from distances further than the *heavy circle*

It is well established (Wolf et al. 1991; Berg 1993; Turchin and Odendall 1996; Östrand and Anderbrant 2003) that the probability of capturing random walkers declines with increasing distance from which the movers originate from a trap. For example, moths originating nearest to the plume as shown in Fig. 2.4 vs. the limit of the dispersive distance (heavy circle) might be captured with probabilities >0.5 vs. <0.05, respectively, depending upon the mover meander and foraging time. We refer to the probability of capture of movers originating at a specified distance away from a trap as *specific* T_{fer}, abbreviated as spT_{fer}. Characterizing and understanding the probability function for spT_{fer} vs. distance of animal origin from a trap is critical to understanding and interpreting trapping outcomes.

We can predict catch for the full trapping area by the following procedure that does not require calculus. First, break the trapping disk in Fig. 2.4 into annuli (Fig. 2.5). If spT_{fer} for each annulus of Fig. 2.5 below were known, catch per annulus would be given by $spT_{fer} \times$ the number of animals per annulus. Catch (C) for the full trapping area would be the sum of catches for all six annuli. When the annuli of Fig. 2.5 are labeled 1–6, then C per trapping area is given by[1]:

[1] Readers familiar with calculus may recognize the right-hand side of Eq. (2.1) as a Riemann sum approximation of the integral

$$\int_0^{R_{\max}} spT_{fer}(r) D 2\pi r dr,$$

where $R_{\max}$ is the trapping radius, $spT_{fer}(r)$ is *specific* T_{fer} at distance r from the trap and D is density of movers (number per area). Here, $2\pi rdr$ is the area of an "infinitesimal" annulus at distance r from the trap. In general, spT_{fer} might depend on the absolute position of the mover relative to the trap, in which case Eq. (2.1) would be replaced by the relation

$$C = \int_{Trapping\ area} spT_{fer}(x, y) D dx dy.$$

$$C = \sum_{i=1}^{6} spT_{fer}^{(j)} \times M^{(j)}, \tag{2.1}$$

where $spT_{fer}^{(j)}$ is the specific T_{fer} for the jth annulus and $M^{(j)}$ is the number of movers in the jth annulus.

Equation 2.1 is not the only trapping equation that will be offered in this book, but the relationships it embodies are keys to an understanding trapping. As we shall see in Chap. 5, spT_{fer} can be measured by releasing known numbers of animals at specified distances from a trap and recording the proportion recovered. This measure is an important building block for other useful measures of trapping. Specific T_{fer} is an effect caused by properties of: (i) the mover (distance originating from the trap, meander during search for the plume, foraging time, and total distance movers can displace from their starting points) and (ii) the trap (size, plume reach). Each of these causes and their interactions require further scrutiny if the process of trapping is to be well understood.

Chapter 3
Random Displacement in the Absence of Cues

3.1 The Classical Random Walk

The random walk is a well-characterized phenomenon both behaviorally and mathematically (Feller 1968; Spitzer 1976; Berg 1993). This term can apply to any form of locomotion arising when headings for displacement steps are selected randomly, be it walking, flying, or swimming. The concise book by H.C. Berg (1993) provides an excellent introduction to random walks in biology, prime examples of which are the spatial displacements through time (*tracks*) of simple animals foraging without the benefit of cues from potential resources. Figure 3.1a exhibits two-dimensional random walks that we generated using a computer program written by P. A.W. The initial versions of this software (Weston 1986) were used for demonstrating orientation mechanisms in an insect behavior course at Michigan State University. Byers (1993) also developed similar software and used it well to characterize aspects of the dynamics of mass trapping and mating disruption. Beginning at a set point of origin, the Weston software uses a computer's random number generator to pick a heading for a first step from the full 360° range of possibilities. One step of set length is taken. Then, the computer randomly picks headings for next steps of length equal to the first step from a normal distribution centered on the heading just executed. Mover meander (amount of turning) for different simulations can be increased or decreased by expanding or contracting the width of the normal distribution from which new headings are picked (Fig. 3.1b). Even though the same distribution of permissible headings was being used for all replicate runs of Fig. 3.1a, the overall shapes of cumulative tracks differ across runs because of additive randomness in the selection of actual headings for each step.

The random walks shown in Fig. 3.1a are of the "classical" type, typical of diffusing molecules or tiny particles exhibiting Brownian motion visible under a microscope at very high magnification. Little forward bias is noted when spatial displacement is driven mainly by random collisions of submicroscopic particles. Any new heading is equally likely, including complete reversal.

J. R. Miller et al., *Trapping of Small Organisms Moving Randomly*,
SpringerBriefs in Ecology, DOI 10.1007/978-3-319-12994-5_3

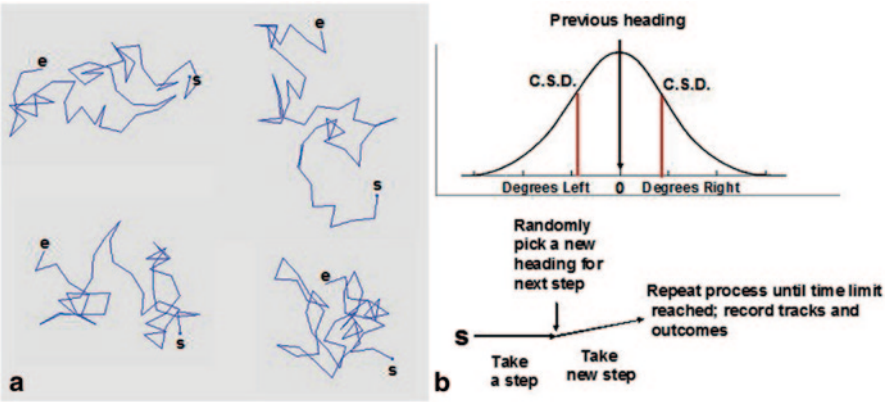

Fig. 3.1 **(a)** Four different tracks (each beginning at *s* and ending at *e*) of computer-simulated random walkers taking a total of 50 steps. *Straight segments* reflect individual steps. After each step, the computer's random number generator picked a new heading. In **(a)**, all directions out of a full 360° were equally probable for each pick. **(b)** Explanation of the Weston mover simulation program showing an important biological feature—new headings are randomly picked from a normal distribution centered on the previous heading and the possibilities can be broadened or narrowed by manipulating the circular standard deviation (c.s.d.). For all directions to be equally probable (as in **(a)**), the c.s.d. must approach 200°

3.2 The Correlated Random Walk

Spatial displacement by organisms is not collision-based. Here, movers carry a forward bias due to both their inertia and use of propulsive apparatus evolved mainly for forward rather than sidewise or backward displacement. An example of antlike (15° c.s.d.) correlated random walks can be viewed in Fig. 2.2, where the step length was much shorter and the run time longer than that shown in Fig. 3.1a. Such *correlated random walks* share attributes with classical random walks, e.g., both exhibit stochastic properties, and summed degrees for all of the left vs. all of the right turns become equal through time. Indeed, all types of random walks are mechanistically more similar than different. The classical random walk happens to lie on the extreme of a continuum (Fig. 3.3b) where forward bias is zero. However, the behavioral and ecological consequences of displacing with and without forward bias can be dramatic over the short foraging intervals typical of small organisms, as we shall see in Chap. 4.

Viewed over prolonged periods from afar, tracks of correlated random walkers appear similar but are not identical to those of classical random walks viewed up close. This effect is demonstrated in Fig. 3.2, where a random walker moving with a c.s.d. of 5° produces a track having low meander when viewed at high magnification (Fig. 3.2b) but high apparent meander when viewed at low magnification (Fig. 3.2a). From the perspective of its body size, an animal may be moving quite straightly, but small turns accumulating over time cause the overall track to turn back on itself when viewed at a larger scale. Hence, the old adage—"a lost person

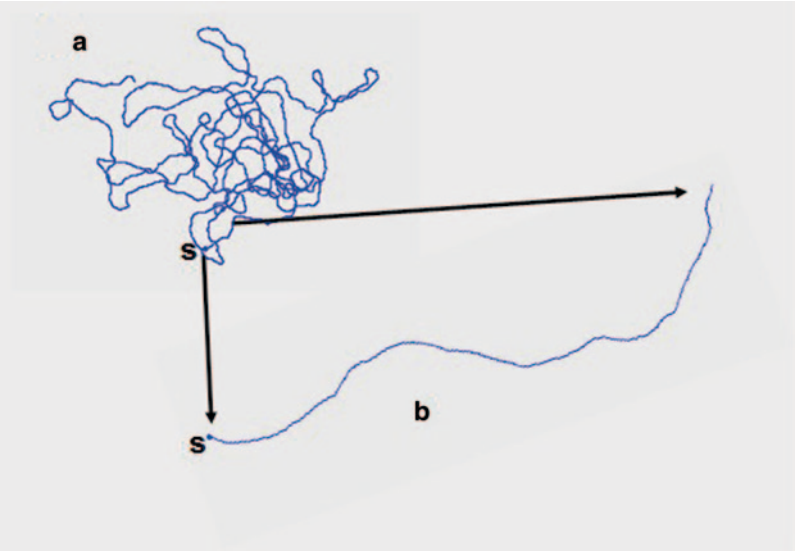

Fig. 3.2 Tracks of a Weston random walker starting at s and displacing with a c.s.d. of 5° for 30,000 steps of length 0.1 in **(a)** and 500 steps of length 1.0 in **(b)**. The overall effect is that the track segment of **(a)** that is expanded in **(b)** is magnified 10×

walks in circles." In fact, it is impossible for any biological mover to maintain a straight course over appreciable distance without using some distant reference point to adjust the course for inevitable drift away from the heading at the outset. While ballistic (straight-line) movement is the rule for particles such as photons, it is an oddity for organisms. Although the tracks of a classical random walker viewed up close and that of a correlated random walker viewed from afar may appear similar, the probability of intersection with objects near the former will be higher because a locally wider track is being cut (compare Fig. 3.1a to 3.2b). Movers with high c.s.d. values are better local searchers, whereas those with low c.s.d. are better at finding distant resources.

3.3 Outward Dispersion as Influenced by c.s.d.

Dispersion by random walkers is dramatically affected by the c.s.d. of the distribution from which new headings are randomly picked. Tracks for a population of ballistic movers released from a common point generate a wheel with randomly spaced spokes (Fig. 3.3a). As the c.s.d. opens, the spokes twist increasingly; by 10° they become a tangled disk having an irregular leading edge (Fig. 3.3a). Disk diameters for common run times shrink with increasing c.s.d. until they reach a minimum when all angles for new headings are equally probable. Clearly, maximum net dispersion falls with increasing c.s.d. and the drop is most dramatic for c.s.d. values between 5–40° (Fig. 3.3b.), the zone of biological random walking.

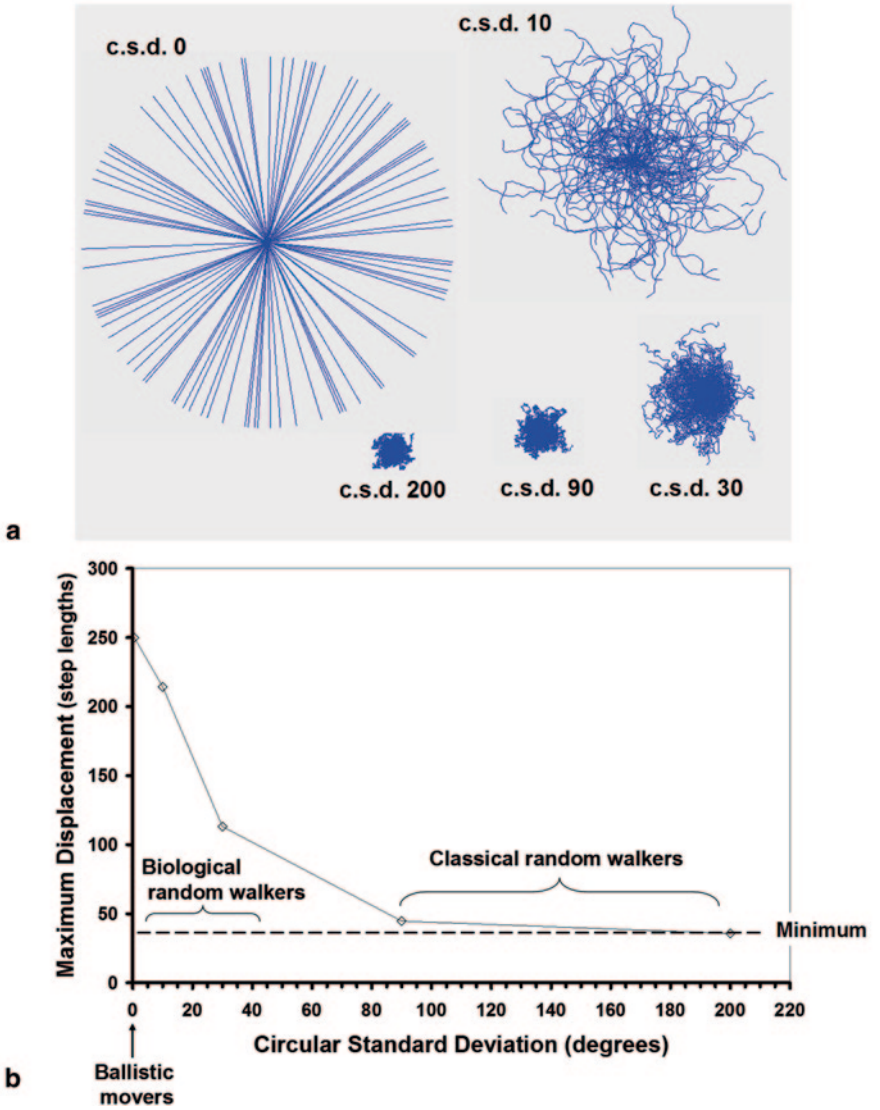

Fig. 3.3 **(a)** Data taken from records of the overlaid tracks for 100 computer-simulated random walkers released at the center of each array and taking 250 steps, each of length 1/10th that of the steps in Fig. 3.1a. Dispersion decreases with rising c.s.d. as shown in **(b)**, where c.s.d. is plotted against the greatest distance any of the 100 individuals in each array displaced from the starting point

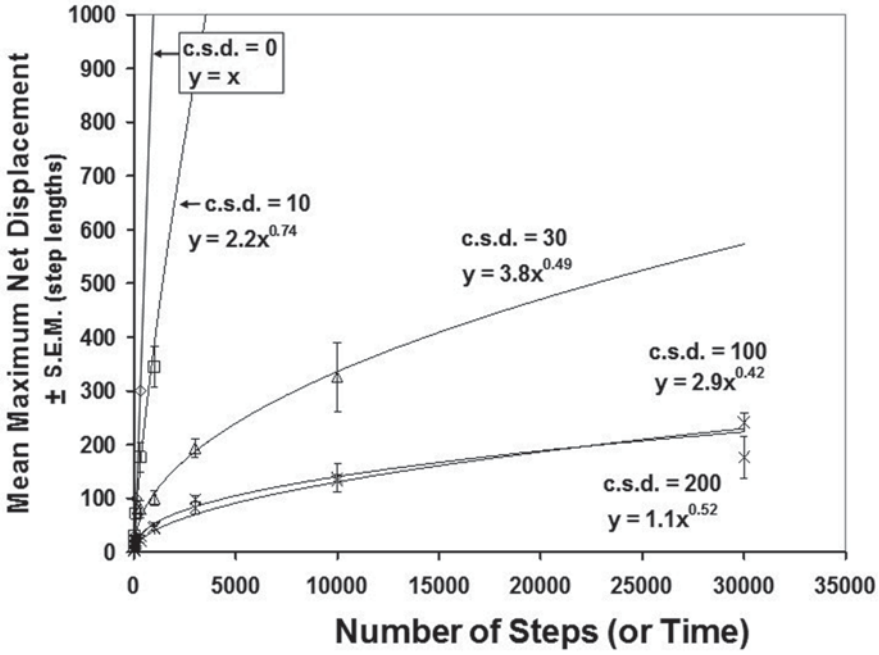

Fig. 3.4 Mean maximum net displacement for individual random walkers as a function of elapsed time and c.s.d.; $n = 5$ for each datum

3.4 Outward Dispersion as Influenced by Time

The rate of increase for maximum net displacement of a population of random walkers taking a constant number of steps per unit of time drops with elapsed time of locomotion (Fig. 3.4). At the start of any run, all movement is outward and backtracking is impossible because no track exists to overwrite. As time passes, however, the probability of backtracking progressively rises because more and more track exists upon which to backtrack. Therefore, the rate of progression into new territory falls with elapsed time. It is well established that the dispersion for classical random walkers grows as the square root of the elapsed time, or $t^{0.5}$. This observation, first noted in the eighteenth century, can be found in many standard mathematics and physics textbooks, e.g., Feynman et al. (1963). The 30, 100, and 200° c.s.d. data of Fig. 3.4 support this rule, as evidenced by their regression equation exponents of ca. 0.5. However, the regression exponent over a fixed run time must rise to 1.0 as the c.s.d. drops to zero. Thus, over the relatively short run time displayed for the movers of Fig. 3.4 with a c.s.d. of 10°, it is not surprising to see an exponent of 0.74.

3.5 Does a Population of Random Walkers Spread Indefinitely Away from the Point of Origin and, If So, Why?

The answer to this question is yes, based upon physical theory, computer simulations, and long-running experiments. As evident from Fig. 3.3a, populations of random walkers dispersing in two dimensions from a common origin will form a disk that expands ever more slowly with increasing elapsed time; and, such expansion will continue indefinitely. The disk will remain internally populated, and its highest average density will always be at the origin, although the density gradient over distance will become flat with extended run times.

Introductions to diffusion in chemistry classes often emphasize that outward dispersion of diffusing molecules occurs because of collisions among them. The argument is commonly made that the rate of outward progression of a population of molecules slows because the frequency of collisions falls as the molecules spread. But, the random walkers considered here never collide, and thus the concentration of movers behaving independently can have no effect on outward dispersion.

The reason spread occurs even without collision is quite simple. Unvisited area in an unbounded arena will always exceed visited area. Thus, on average, the probability of moving into unvisited area (outward relative to the movers' point of origin) will always exceed the probability of moving into visited area (backward) when new headings are always picked randomly. Likewise, the average diffusing molecule will continue to disperse outwards even when collisions with like molecules are too infrequent to be the main driver of spread. So, all populations of randomly moving objects in unbounded space form an ever-expanding universe unless acted upon by some counterbalancing force.

3.6 Maximum Net Outward Dispersion as Influenced by Mover Sample Size

Among the variables identified in Chap. 2 that must be known for full interpretation of catch in traps is the maximum distance a population of random walkers can displace from an origin over the time a trap operates. This measure, combined with plume reach, establishes the trapping radius or sampling range of the trap (Fig. 2.4). Maximum dispersion can be measured experimentally by releasing a population of marked individuals, allowing them to disperse for a defined time, and then recapturing them using a dense trapping grid immediately after dispersion. A question that follows is—how many movers must be released from a common origin to accurately assess measures such as maximum dispersal range? The computer simulations shown in Fig. 3.5 suggest that ca. 100 individuals will suffice for biological as

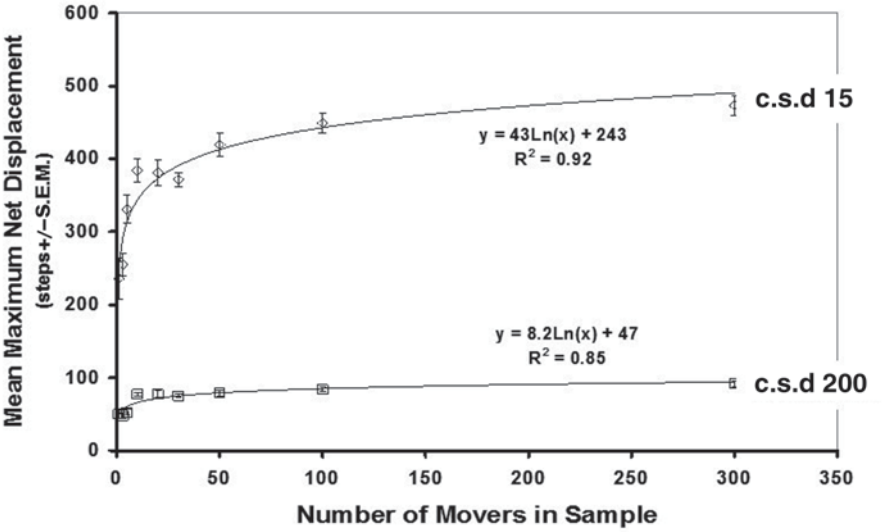

Fig. 3.5 Mean maximum net displacement from the starting point for simulated random walkers with low and high meander displacing for 1,000 steps of length 0.5 as influenced by the number of movers in the sample. $N = 8$—each datum resulted from eight runs

well as classical random walkers.[1] The considerable variability in maximum mover displacement across sample sizes of less than 50 movers (Fig. 3.5) suggests that measurable trapping radius can shrink significantly as the mover population density falls. This knowledge must be considered when interpreting low catch numbers associated with very low populations of movers.

3.7 Patterns in Random-Walker Ending Positions After a Short Period of Dispersion as Influenced by c.s.d.

The terminal positions of random walkers are of interest, as is the maximum net outward dispersion they can achieve. Figure 3.6 demonstrates how the pattern of terminal positions shifts with c.s.d. when 100 Weston movers were displaced for only 250 steps. As the c.s.d. opened from 0°, terminal positions shifted from a perfect circle to an increasingly diffuse circle. By c.s.d. of 10°, the terminal distribution became quite uniform throughout the dispersion disk. By c.s.d. 30° and greater (data not shown), the density of movers becomes greatest in the interior and sparse around the disk perimeter. This knowledge suggests how the meander of real animals moving

[1] In fact, the maximum net outward dispersion will continue to grow with increased sample size, approaching the ballistic value as the sample size approaches infinity. However, one may show mathematically that this growth is logarithmic, and hence extremely slow. In particular, to see a value of the maximal dispersion close to the ballistic value, one would need to consider a sample size $2^{\text{number of time steps}}$, which is unrealistically large for runs of the durations seen in this study.

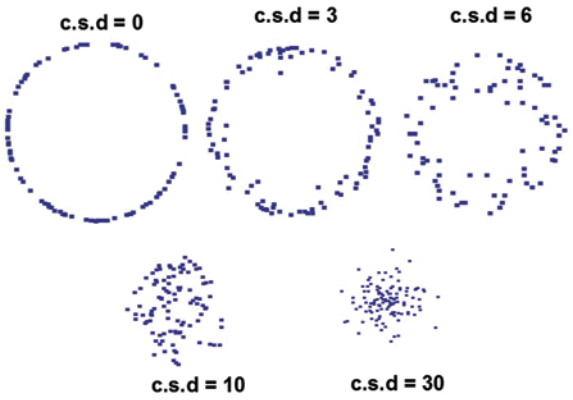

Fig. 3.6 Ending positions of 100 Weston movers after 250 steps of displacing from the center of each array as influenced by c.s.d. Mover size for c.s.d. 30 was reduced to minimize eclipsing

in the field might be judged if they could be located immediately after a short period of dispersal by, e.g., then inserting a dense trapping grid. With longer elapsed times for dispersion, the empty spaces within the dispersion circles for the random walkers would become less apparent and this type of analysis would become less useful.[2]

3.8 Experimental Analyses of Tracks and Measures of Meander for Individuals

Locomotory tracks of small animals can be captured in a variety of ways. The senior author does this as a laboratory exercise in insect behavior class simply by introducing a walker into the middle of a featureless arena covered by Plexiglas™ overlaid with clear acetate sheets. The animal's track in real time can be traced by felt pen onto the acetate. Tick marks at regular periods along the track provide a time stamp for measures of velocity. However, the standard method for track-capture is video recording using a system that provides a time stamp for each frame and known magnification. Video technology is required for fliers; however, obtaining meaningful amounts of video footage of small fliers dispersing in the field remains an unexplored (albeit worthy) research area because it requires specialized and therefore expensive equipment.

Experimentalists wishing to quantify the distribution of headings for steps comprising the tracks of real animals face an important operational question—into what lengths should the track be broken? We suggest that the animal's body length, including sensory apparatus such as antennae, is a reasonable unit for such analyses. Use of

[2] Random walks are well studied in the mathematics literature, see, e.g., (Spitzer 1976; Feller 1968). In particular, it is well understood that, provided the c.s.d. is nonzero, each of the correlated random walks considered here "looks like" an uncorrelated random walk over sufficiently large time and space scales. This fact, already illustrated in Figure 3.2, follows from an *invariance principle* stating that the long-time behavior of a wide variety of random evolutions is effectively described by Brownian motion (the Wiener process). An invariance principle was originally proved by Donsker (1951) for uncorrelated random walks, but has been generalized to a wide variety of correlated walks, see, e.g., (Billingsly 1956; Newman and Wright 1981). However, the biological problems considered here force us to consider these walks over fixed finite time and space scales too short for this universal limit to be completely descriptive.

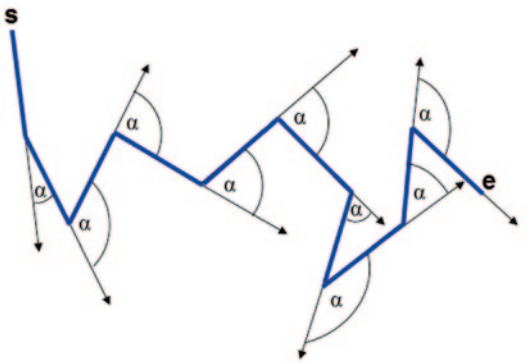

Fig. 3.7 Demonstration of how angular headings for new steps are computed for a section of the track of a classical random walker. *s* = start; *e* = end; *α* = subtended angle

larger track segments overlooks points in space that the animal actually visited along the way to a segment endpoint and will underestimate meander. Analyzing fractions of a body length leads to inclusion of wobble in the gait of the mover that may be irrelevant to overall heading.

Tracks are quantified as follows: a track is broken into segments of declared length (e.g., body length); the positions of track segment ends are recorded using, e.g., a digitizer; the angle comprised by a preceding vs. current segment of track (Fig. 3.7) is measured or computed; and a frequency histogram of headings is constructed (Fig. 3.8). It can be tested for fit to a normal or some alternative

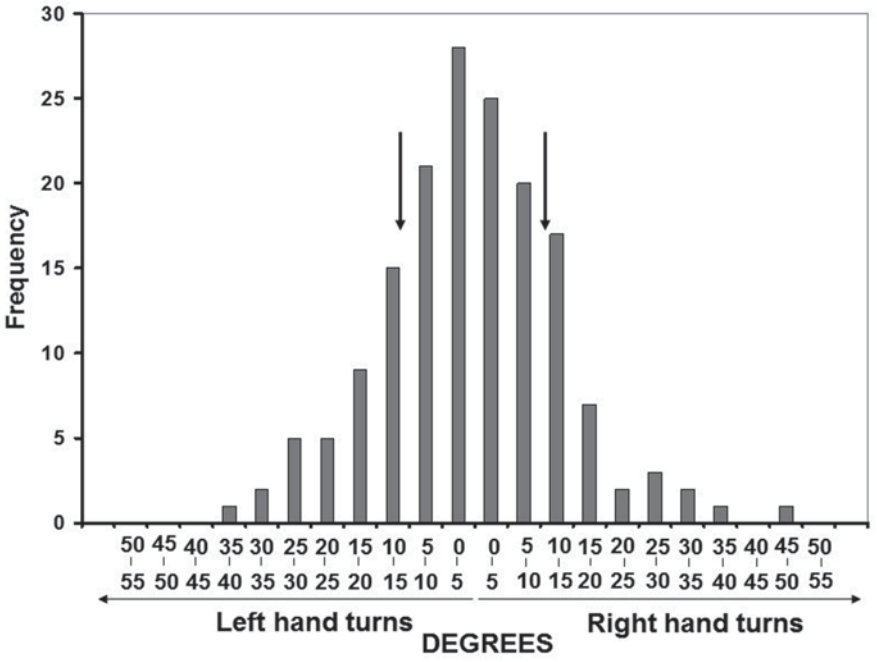

Fig. 3.8 Example of a frequency histogram for headings of track steps for a random walker having a c.s.d. of ca. 13°. *Arrows* reflect 1 standard deviation to the *right* and *left* of 0°, which represents the previous heading

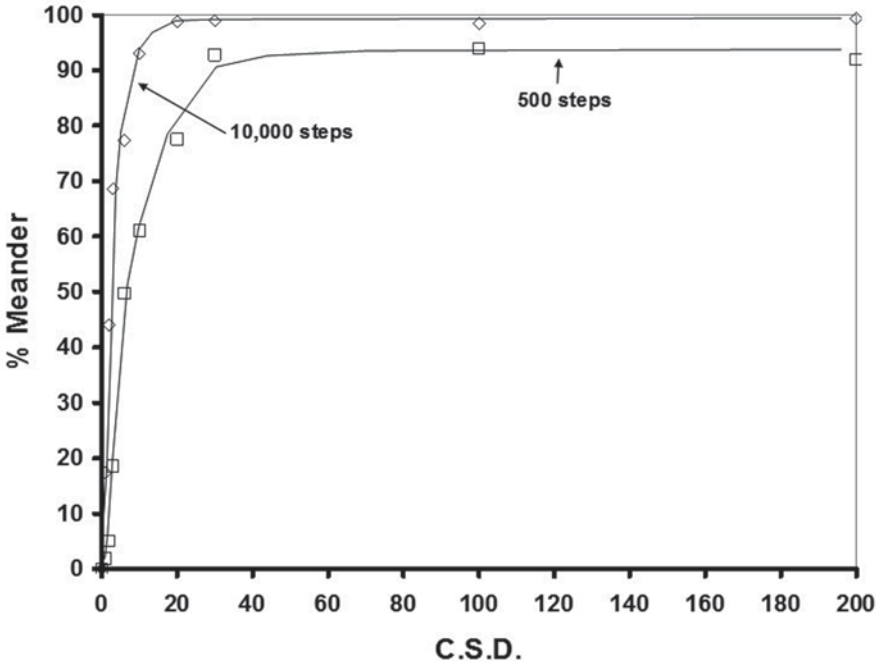

Fig. 3.9 Percentage of meander computed as per Eq. 3.1 for Weston random walkers displacing for short and long intervals as a function of varying c.s.d. value. Over all run times, percentage meander values are high except for movers with tiny c.s.d. values

distribution and then parameters such as c.s.d. can be computed as a measure of meander. Alternative measures of meander are mean absolute value of degrees turned per track segment (degrees/distance) or degrees per time (angular velocity). We also offer % meander as an additional meander measure; it is computed as:

$$\%\ \text{meander} = (1 - (\text{net displacement} / \text{total displacement})) \times 100 \qquad (3.1)$$

Figure 3.9 demonstrates that % meander values are extremely high over both long and short intervals for all random walkers except those moving with tiny c.s.d. values (virtually ballistic). Finally, distance per unit time (velocity) is always of interest in track analyses, as is constancy or shifts in any of the above measures through time.

Chapter 4
Intersections of Movers with Traps

4.1 Ballistic Movers—The Simplest Case

Let us deploy a trap having a diameter of length L at distance r from the common origin o of 100 ballistic movers (Fig. 4.1). Simple inspection reveals that the proportion of movers intercepting the trap and defined here as caught (*Prop. C*) is well approximated by L divided by the circumference of the circle centered on o and bisecting the trap, or:

$$Prop.\,C = L/2\pi r \tag{4.1}$$

Prop. C falls nonlinearly with rising r as graphed in Fig. 4.2a; it is extremely sensitive to small differences in r near the trap, but changes little across large r values. This effect can be experienced by holding a thumb very close to one's eye, and then noting the apparent size of the thumbnail when moving slowly out to arm's length and back. This relationship is nonlinear because r resides in the denominator of Eq. (4.1), rather than in the numerator. However, graphical output becomes linear (Fig. 4.2b) when Eq. (4.1) is inverted to yield Eq. (4.2):

$$\frac{1}{Prop.\,C} = \frac{2\pi r}{L} \tag{4.2}$$

and $1/Prop.\ C$ is plotted against r (Fig. 4.2b; hereafter referred to as a Miller–Adams–McGhee (MAG) plot). Opportunity is thereby afforded for computing L from data on *Prop. C* as a function of r from an experiment using a single-trap, multiple-release configuration like that of Fig. 4.3. Since the slopes of MAG plots (Fig. 4.2b) generated by ballistic movers consist of $2\pi/L$, L is revealed by dividing 2π by the MAG plot slope:

$$\frac{2\pi}{\frac{2\pi}{L}} = \cancel{2\pi} \times \frac{L}{\cancel{2\pi}} = \mathrm{L} \tag{4.3}$$

J. R. Miller et al., *Trapping of Small Organisms Moving Randomly,*
SpringerBriefs in Ecology, DOI 10.1007/978-3-319-12994-5_4

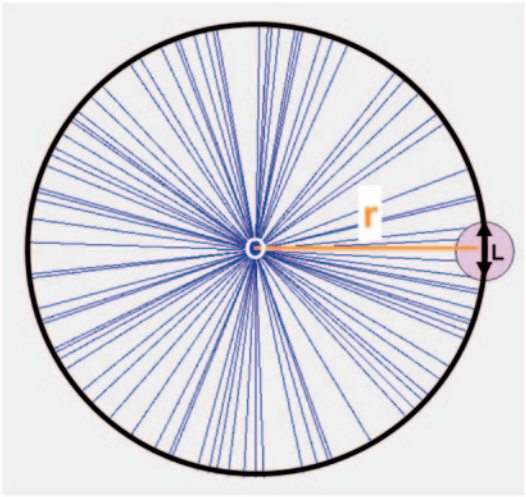

Fig. 4.1 Trap of diameter *L* at distance *r* from the common origin *o* of 100 ballistic movers. The proportion of ballistic movers intersecting the trap is well approximated by *L*/circumference of the circle centered on *o* and bisecting the trap

4.2 Random Walkers

So long as they have the capacity to reach the trap, more random walkers intercept a trap than do ballistic movers under otherwise identical conditions (Fig. 4.4a). With increases in c.s.d., random walkers lay more track in the vicinity of a trap and are able to approach it laterally and from the rear, as well as frontally (Fig. 4.4a (2)). These behaviors enhance catch. The equivalent effect of random walking vs. foraging in straight lines is diagrammed in Fig. 4.4b. It is like putting side panels (black rectangles) on the outward tracks of ballistic movers (red arrows) so that more angles leading away from the origin produce intersections.

The approach developed above for deriving trap length or plume reach from the MAG plot data for ballistic movers (Fig. 4.2b) can be applied to random walkers. However, when 2π is divided by the MAG plot slope for random walkers as per Eq. (4.3), the resultant *L* value includes plume reach plus additional apparent length that we term *gain*, as diagrammed in Fig. 4.4b. Gain can be calculated from data graphed as a MAG plot by dividing 2π by the MAG plot slope and then subtracting the actual trap diameter, or:

$$\text{Gain} = L - \text{trap } \left(\text{or plume}\right) \text{ diameter} \tag{4.4}$$

A specific example of this procedure is provided in Fig. 4.5. Gain comprised nearly 70 % of *L* in this example. And, the proportion of *L* being gain was found to be ca. 70–80 % across a range of biological c.s.d. values (see Fig. 3.3b), trap diameters, and run times (data generated from the simulation experiments described below). This finding is notable because it offers a means to estimate plume reach. First, an uncorrected *L* value can be computed from by dividing 2π by the slope of a MAG plot of spT_{fer} data. Then, the ca. 75 % of *L* that is gain is subtracted to estimate plume

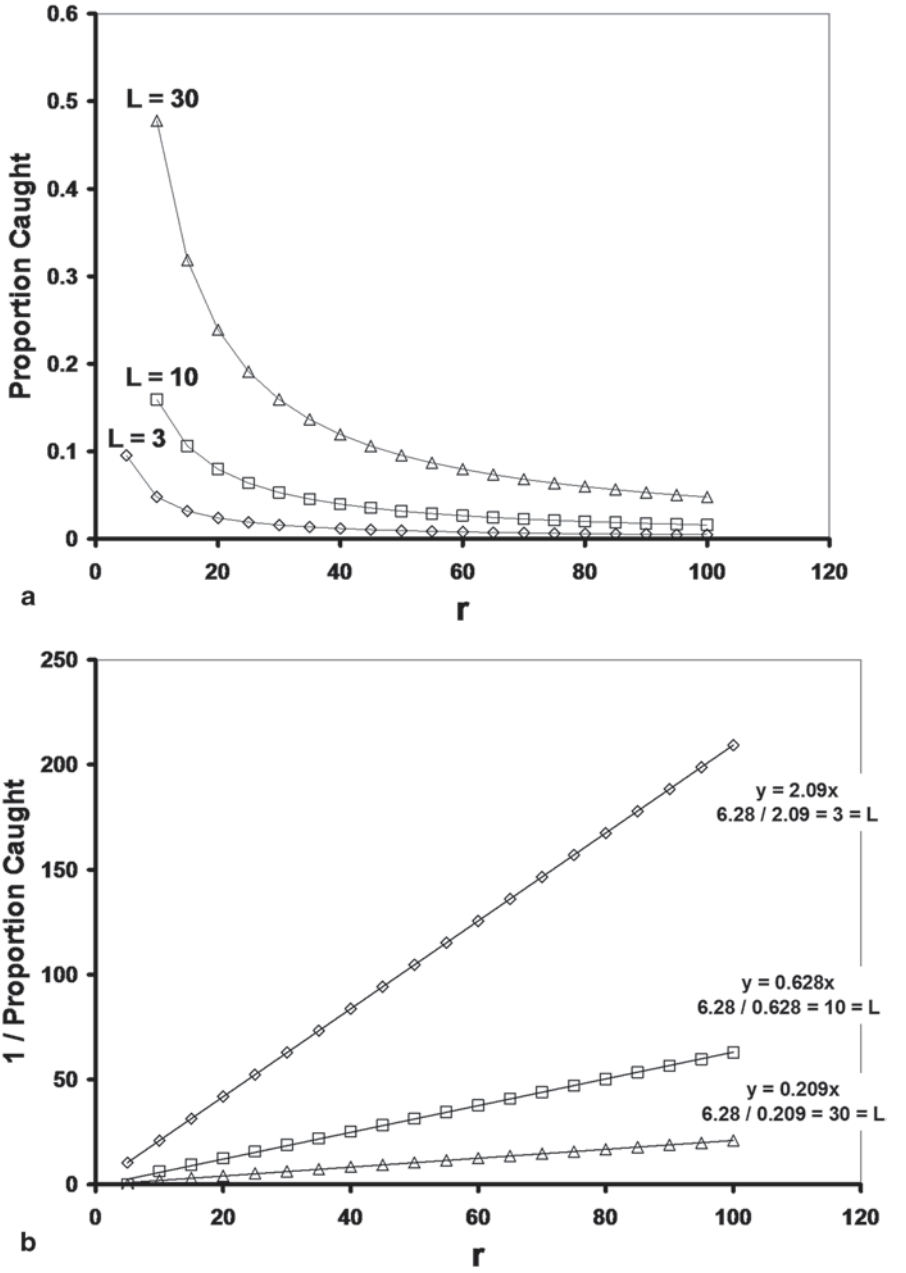

Fig. 4.2 **(a)** Untransformed graph of the proportion of ballistic movers trapped when originating from various distances *r* from traps of varying diameter indicated by *L*. **(b)** Inverse plot of the same data. This type of plot is hereafter referred to as a Miller–Adams–McGhee or MAG plot

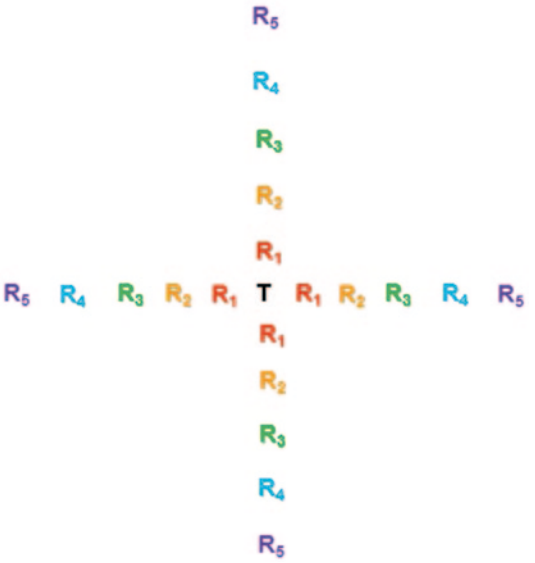

Fig. 4.3 A single-trap, multiple-release trapping configuration typical of that used in field experiments covered in Chap. 5. *T* trap, *R* a point of release for a set number of movers at a given distance from the trap. Movers originating from a common distance share a particular marking

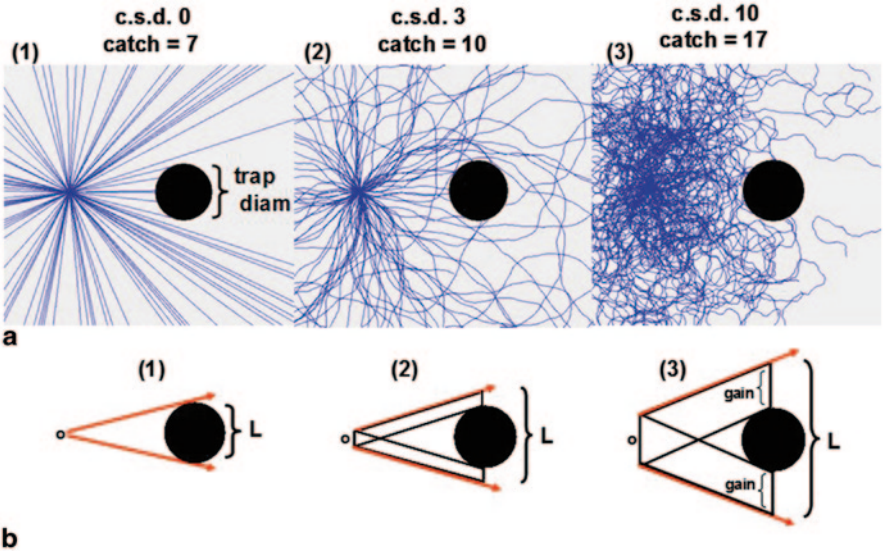

Fig. 4.4 **(a)** Tracks and catches of 100 computer-simulated movers operating at each of 3 c.s.d. values and released 200 units from a trap of diameter 100 units and taking 1,000 steps of 1 unit. **(b)** Top-down view of the net effect of meander; it is equivalent to broadening the outgoing track of a ballistic mover so that it intercepts the trap over a wider range of angles than it otherwise would have. By definition, ballistic movers which have a c.s.d. of zero **(b** (1)**)**

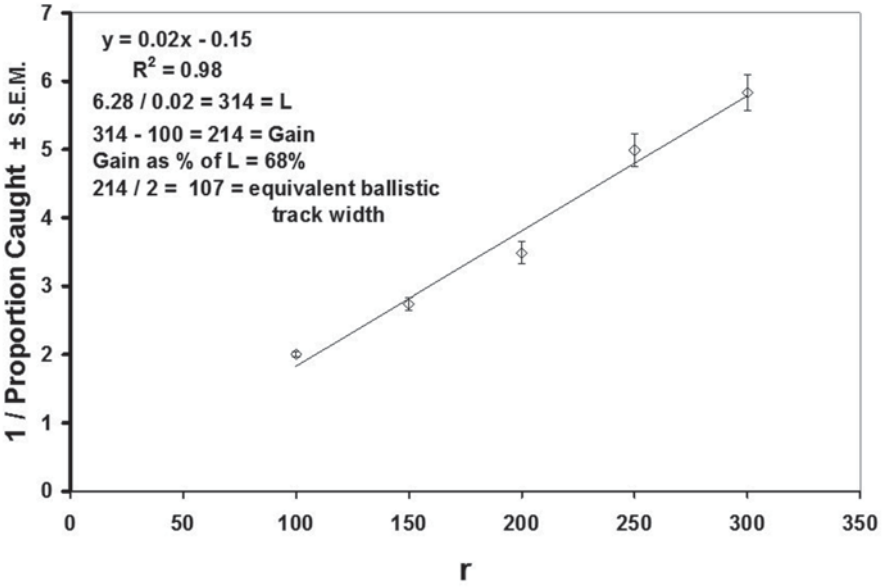

Fig. 4.5 MAG plot for 100 Weston random walkers per sample and moving 3,000 steps of 1 with a c.s.d. of 10° and intersecting a trap having a diameter of 100 units. $N=20$ runs per datum

reach in the same units as those used for setting distances of mover origin from the trap. The only other approach to estimating trap or plume reach of which we are aware is the "effective attraction radius" (EAR) procedure of Byers et al. (1989). It produces an index of plume reach by comparing catch in a baited trap to that of an unbaited trap. However, most insect monitoring traps do not catch any individuals when unbaited; thus, the EAR approach has seen limited use beyond bark beetle studies that use large vane traps.

4.3 Gain as Influenced by c.s.d. and Run Time

Gain over the foraging efficiency of a ballistic mover is strongly influenced by the c.s.d. employed. This effect is graphed in Fig. 4.6 where the diameter of the single trap was small (10 units), step length was 1 unit, and movers were released at five distances, all within 80 units of the trap. Gains were calculated from MAG plot slopes and Eq. (4.3) along with (4.4). When foraging times are extremely short, ballistic movers had the highest probability of intercepting a nearby trap (data not shown) because they were guaranteed to progress as far as the trap, a necessary condition for an interception (see Fig. 4.1). However, with increasing run times, random walkers outperformed ballistic movers and thus returned increasing gains (Fig. 4.6). The optimal c.s.d. in this experiment with a small trap was consistently ca. 25° for

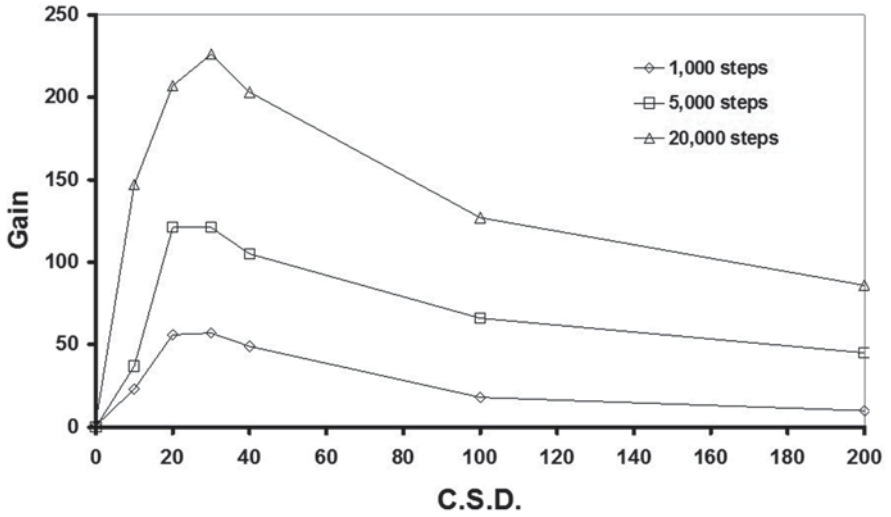

Fig. 4.6 Foraging gain as a function of c.s.d. and run time when trap diameter was 10 units and step length was 1.0. Each datum was computed from a MAG plot using 20 runs of 100 Weston movers released at 5 distances from the trap. Only the linear portions of MAG plots were used, i.e., release distances too far from the trap to be reached with high probability and thus resulting in upturning data were excluded. A gain of zero indicates a trapping rate identical to that for a ballistic mover. S.E.M. bars were ca. 10% of these means

short, medium, and long run times (Fig. 4.6). The c.s.d. that optimizes gain can be thought of as producing movement that maximizes the apparent size of the trap or reach of a plume. Doing so is clearly advantageous when foraging for resources.

The existence of a stable, optimal solution of ca. 25° c.s.d. to the problem of finding a single, small, and nearby object 10× body size raises the prospect that the c.s.d. expressed during foraging should be a biological trait selectable upon resource size, number, and distribution typically encountered. Small c.s.d. values (less meander) were inefficient in this experiment because many movers passed the trap and did not return within the allotted time (Fig. 4.7). These movers undersearched their environment as they dispersed from the origin. Very large c.s.d. values (high meander) were more efficient than tiny ones, particularly at long run times (Fig. 4.6). But movers with a very high c.s.d. oversearched as they dispersed (Fig. 4.7). The optimal c.s.d. achieves the best tradeoff in these search extremes.

4.4 Optimal c.s.d. as Influenced by Trap or Resource Size

Optimal c.s.d. for finding a single, nearby object increases as size of the object diminishes (Fig. 4.8). Smaller objects require a more thorough search if intersections are to be realized. Conversely, intersections with larger plumes are more probable

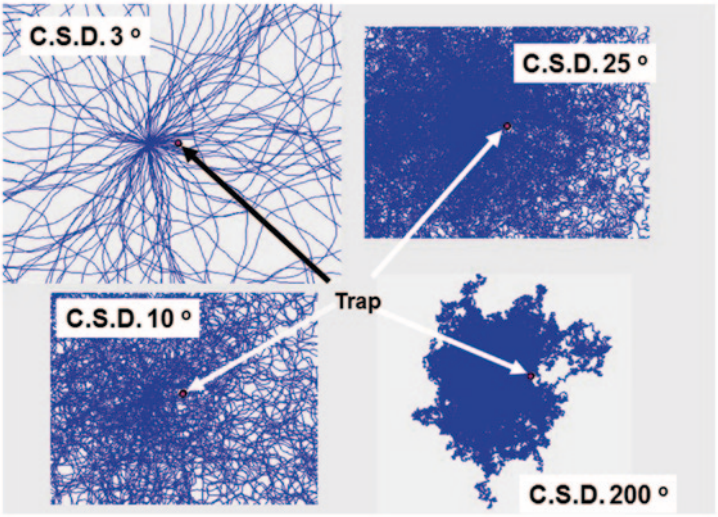

Fig. 4.7 Tracks accumulating around a trap of diameter 10 units when 100 Weston random walkers were released 40 units to the *left* of the trap in each panel. The c.s.d. of the respective movers is given with each panel. Pictures were increasingly cropped with decreasing c.s.d

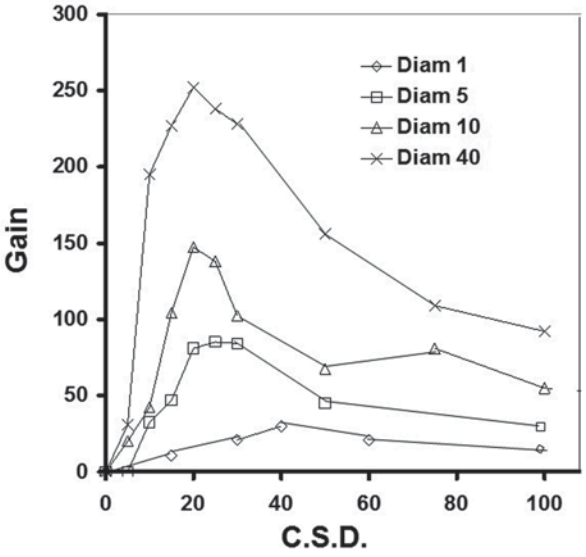

Fig. 4.8 Change in optimal c.s.d. for realizing maximal gain as influenced by trap size. Gain was measured in the manner of Fig. 4.6. S.E.M. bars averaged less than 10% of these means

because they present much more distance across which any intersection yields the whole prize. Animals foraging for large resources can therefore afford to displace with less meander, which is also likely to decrease the time required to find a given resource at some distance from the mover's origin. Gains are appreciable across a wide range of c.s.d. values and trap sizes as seen in Fig. 4.8. The existence of prominent foraging optima at particular c.s.d. values supports the legitimacy of random walking as a search tactic and presents a conceptual framework quite different from that held by previous investigators who expected that the optimal tactic for finding plumes was movement in straight lines relative to the wind direction (see references in Murlis et al. (1992)).

4.5 What Aspect of Plume Geometry Correlates Best with Capture Probability?

We answered this question by conducting the trapping simulations detailed in the caption of Fig. 4.9. The shape of the trap was a: line, circle, or square, whose length, diameter, or side was manipulated and catch recorded. Catch was very poorly correlated with object area, not tightly correlated with object length or silhouette, but well correlated with object perimeter (Fig. 4.9).[1] This finding supports the idea that trapping is fundamentally a phenomenon of intersection. A trap or plume of any shape or size can be intersected when approached from any side or angle. But only when its boundary is penetrated does an intersection occur. Thus, simple perimeter of a trap or its plume is the aspect best correlated with capture probability. Near-linearity of Fig. 4.9 when perimeters exceeded 100 units indicates that trap captures will increase approximately linearly with plume reach when mover density is constant.

[1] Intersection probabilities have been extensively studied for Brownian motion (Wiener process) and uncorrelated random walks. In particular, Spitzer (1964) proved an asymptotic formula that can be used to compute the behavior of the expected catch $C(t)$ at time $t \to \infty$, in the limit t, for a trap positioned in an infinite plane populated with a density D of Brownian movers:

$$C(t) \sim 2\pi Dt\left(\frac{1}{\ln t}+\frac{1}{(\ln t)^2}[rc(T)+1+\gamma-\ln 2]\right)$$

where $\gamma \approx 0.5772\ldots$ is Euler's constant and $rc(T)$ is "conformal radius," or "logarithmic capacity," of the trapping radius (see Kuz'mina for the definition). This result is not particularly useful for our analysis because we study correlated walks over time scales too short for this universal Brownian behavior to emerge. However, the above relation does suggest that the conformal radius of the trap might be the correct geometric parameter to correlate with capture probability, not the perimeter as considered in Sect. 4.5. In this regard, it is significant that each of the traps considered in Fig. 4.9 is a convex body (for which conformal radius and perimeter are comparable). We do not expect the relationship between perimeter and catch to extend to nonconvex traps, as such traps may have deep fjords in their boundary which greatly increase perimeter without increasing catch. Indeed, a trap with a fractal boundary could have infinite perimeter and finite catch.

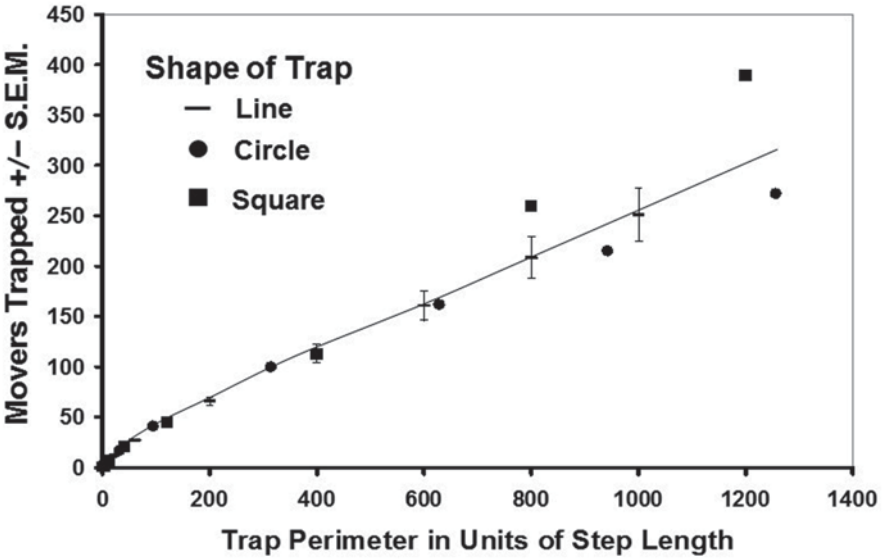

Fig. 4.9 Demonstration that catch of random walkers in a trap is well correlated with trap perimeter. A total of 5,000 Weston random walkers having a c.s.d. of 20° were randomly seeded into an environment 4 times the size of the computer screen and allowed 1,000 steps of 1 unit. The program recorded the number of movers trapped. Movers happening to originate within the confines of a trap were excluded from these data; only movers intercepting the trap when originating from outside are shown. Each datum *symbol* carries the shape of its trap but not its actual size, which varied with perimeter. S.E.M. values typical for this experiment are shown for the linear trap

4.6 Contrasts of Ellipsoid Plumes with Discoid Plumes

As introduced in Chap. 2, traps baited with attractants typically operate in moving air where the plume elongates into an ellipsoid (Fig. 4.10a) rather than a disk (Fig. 4.10b). Elongating a discoid plume into a 10 (length) × 1 (maximum width) ellipse increases the longest axis by only 1.5 fold (Fig. 4.10c) and does not change the perimeter. If movers are released equidistantly from a trap generating an ellipsoid plume, as is standard procedure in field tests of the effectiveness of attractive traps, then the simple symmetry of Fig. 4.10b for discoid plumes is disturbed. All movers are now no longer released equidistantly from the plume, as shown by the length of arrows in Fig. 4.10a and b. Rather, movers happening to originate downwind from the trap are advantaged because less travel is required to reach the plume (right side of Fig. 4.10a). When released in a circle centered on the trap, the mean distance of movers from the ellipsoid plume of Fig. 4.10a was ca. 80 % of the distance from the trap. But, ballistic movers originating upwind of the trap emitting an ellipsoid plume are disadvantaged because the plume presents only its width and not its length.

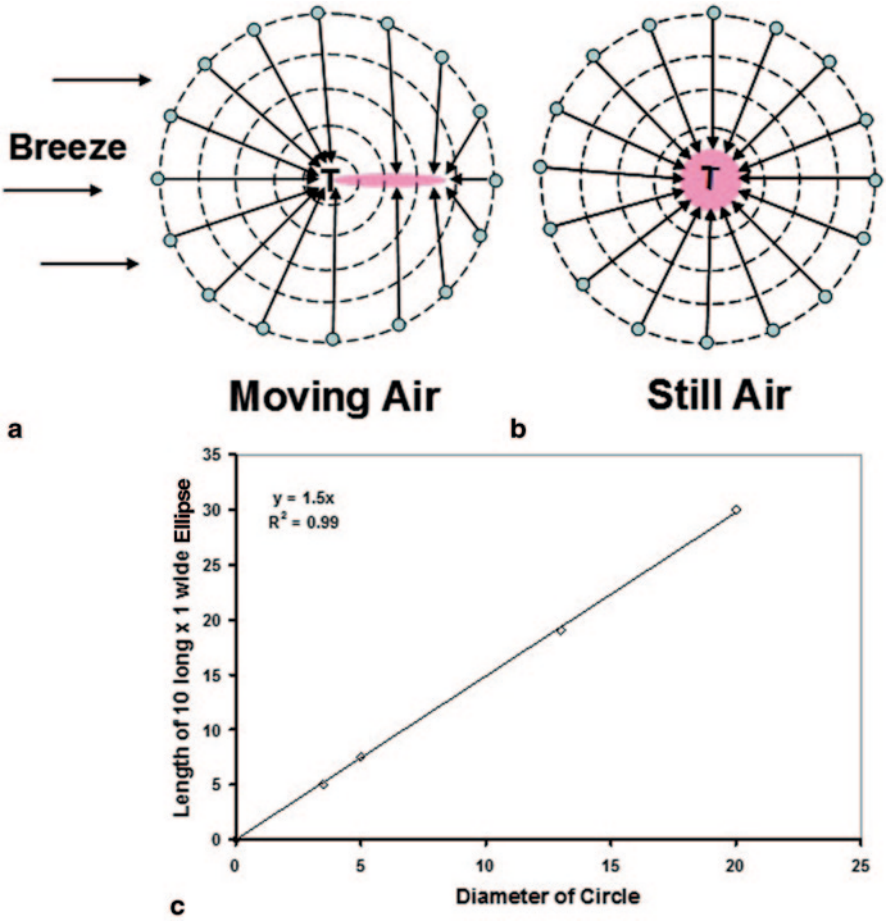

Fig. 4.10 Contrasts in the distances (*length of arrows*) movers must displace to reach plumes (*pink*) when released equidistantly from a trap in moving air **(a)** and still air **(b)**. The *tiny circles* atop the *dashed large circles* represent an arbitrary selection of positions out of 360°. **(c)** Demonstration that collapsing *circles* into 10 × 1 ellipses results in a longest axis of 1.5 times the original circle diameter. These measures were taken by ruler while manipulating rings of string

The net impact of these shifts on probability of capture and gain was quantified by simulation experiments with Weston movers. For each run ($N = 10$ runs per set of conditions), 100 movers with representative c.s.d. values spanning from 0 to 200° were released for 5,000 steps of 1 unit at 6 distances from one end of an ellipsoid plume 50 units long and 5 units at maximum width. Half of these release distances exceeded plume length. The distances of release used in data analyses were corrected for the plume proximity effect noted in Fig. 4.10a by multiplying distance from the trap by 0.8. Gain was calculated by subtracting the actual plume length (50) from L values calculated by dividing 2π by the MAG plot slopes.

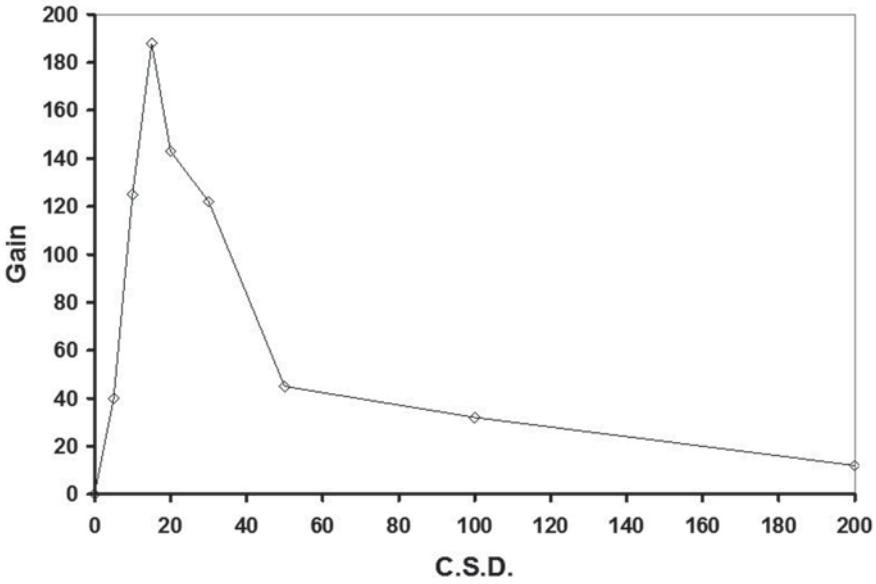

Fig. 4.11 Gain in foraging efficiency for computer-simulated random walkers released in concentric circles from one end of an ellipsoid plume 50 units long × 5 units wide as influenced by c.s.d. S.E.M. bars were ca. 10 % of these means

The *L* value measured for ballistic movers released in circles centered on one end of the 50 × 5 unit ellipsoid plume was 21 rather than the actual 50 units of length. Therefore, *L* for this ellipsoid plume approached from all angles by ballistic movers was only 42 % of its actual longest length. This reduction can be explained by the preponderance of ballistic movers that approached the plume obliquely rather than perpendicularly to the long axis (see Fig. 4.10a while envisioning arrows departing in all directions from each origin).

By contrast, random walkers were considerably less disadvantaged by originating at oblique angles to the long axis of an ellipsoid plume. The gain values recorded here (Fig. 4.11) were only slightly less than those recorded for a discoid plume of similar perimeter (see Fig. 4.8, diameter 40 units). Likewise, the c.s.d. optimum realized here of 15° nearly matched the 20° maximum for a discoid plume of similar perimeter (Fig. 4.8). The effects of ellipsoid plume size and duration of experimental runs were also very similar to those already reported for discoid plumes. Finally, simulations using Weston movers executing various c.s.d. values, various plume sizes, and run times revealed that ca. 70–90 % of *L* values were attributable to gain and the remainder to plume reach.

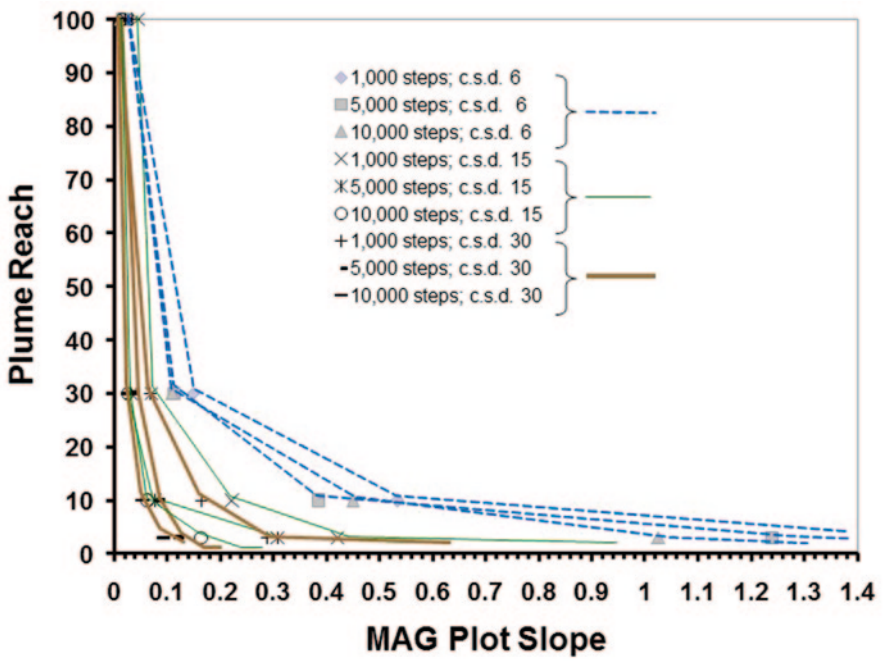

Fig. 4.12 Standard curves generated by Weston mover simulations (conditions explained *above*) and useful for converting MAG plot slopes of spT_{fer} data into estimates of plume reach. The units for plume reach would be the same as the units used for distances of release of movers from the trap

4.7 Setting the Stage for Estimating Plume Reach from Field Experiments Measuring spT_{fer}

Availability of the Weston mover simulations allowed us to generate a set of standard curves (Fig. 4.12) useful in estimating plume reaches from MAG plot slopes of spT_{fer} data (proportion of movers caught when originating at a particular distance) from field experiments with real animals. We consider this approach to be more straightforward and objective than calculating an L from MAG plots and then subtracting a percentage from it to account for gain. Figure 4.12 was produced by recording the proportion of simulated movers trapped after release in 4–5 concentric circles around one end of ellipsoid plumes of length 3, 10, 30, and 100 units and each having a greatest width of 0.1 × length. Each release employed 100 movers, and 20 such releases were completed for conditions that, in addition to plume length, included using c.s.d. values of 6, 15, and 30° and run times of 1,000, 5,000, and 10,000 steps. This range of conditions was judged likely to encompass the key variables coming into play when biological random walkers respond to an attractive trap in the field, e.g., an insect responding to a monitoring trap baited with sex pheromone. MAG plots were made of the respective spT_{fer} data and then the plume reach was plotted against the MAG slope (Fig. 4.12).

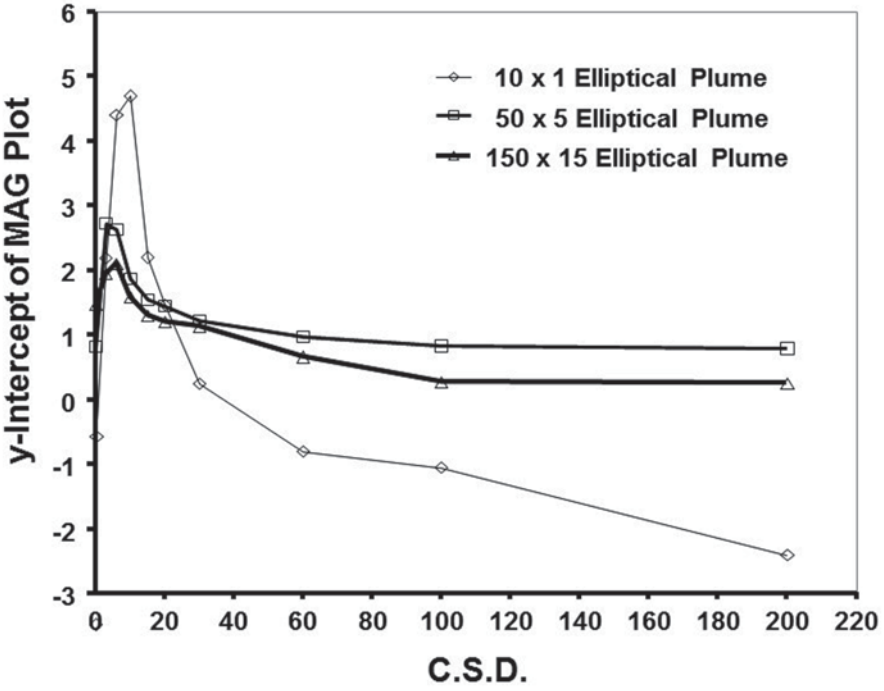

Fig. 4.13 The *y*-intercepts of MAG plots of spT_{fer} data for Weston movers displacing 1,000 steps of 1.0 and using differing c.s.d. values. Extending the run times diminished *y*-intercept values across all c.s.d. values

Figure 4.12 functions as a look-up graph for interpreting MAG plot slopes. As an hypothetical example, let us postulate that researchers are developing a trapping system for the emerald ash borer, a devastating invasive pest of ash trees in the USA (Herms and McCullough 2014). Imagine that the trap emits host-tree odors. These researchers release marked beetles at 10, 20, 30, 40, and 50 m in multiple directions from their prototype trap and record the proportion of marked beetles appearing in the trap over several days after release. They plot distance of release on the *x*-axis vs. 1/proportion of beetles recovered on the *y*-axis. Imagine that the first four data points fall in a straight line; however, the 50 m datum shows upturn. The latter point should therefore not be included for the slope analysis. Imagine that the MAG plot slope for the first four data points happened to be 1.1. We then go to this point on the *x*-axis of Fig. 4.12 and examine the possibilities for plume reach of this new trap. These researchers would find that the attractive reach of their trap was, at best, less than 10 m. Moreover, for the plume reach to be this large, the emerald ash borer must move with a small c.s.d. and not be highly active (fits only short run time of Fig. 4.12). Given that c.s.d. values of foraging insects can be larger than 6° and that these beetles are known to be active for hours on balmy days, it is highly probable that the plume reach of this hypothetical new trap was very short, meaning that it is

not a great tool for detecting this pest. On the other hand, if the MAG plot slope from this hypothetical experiment proved to be 0.1 or 0.05, such a trap could be ranked as generating a plume of 40 m or more, which would be conducive to beetle detection.

The *y*-intercepts of MAG plots of spT_{fer} data can also help estimate plume reach. Figure 4.13 demonstrates that graphical profiles of *y*-intercept vs. c.s.d. vary with the size of elliptical plumes. A *y*-intercept greater than 4 can be obtained only when the plume reach is small. Likewise, a *y*-intercept > 1.5 suggests that the movers generating those data displaced with a c.s.d. somewhere between 3 and 20°. Negative *y*-intercepts for MAG plots are associated with plumes that are very small.

The following chapter will provide actual examples of how plume reach can be estimated from spT_{fer} data generated by real animals in the field. It will also demonstrate how to estimate mover dispersive distance and absolute density for real rather than computer-simulated traps and movers.

Chapter 5
Interpreting Catch in a Single Trap

5.1 A Simple Trapping Equation

Figure 2.5 and Eq. (2.1) of Chap. 2 suggested how catch in a trap can be computed when we know: (i) the number of movers (M) present in each annulus of a trapping area (M_{den}), and (ii) the probability of catch for each annulus (spT_{fer}). Then, one sums across all annuli the spT_{fer} value multiplied by M_{den}. However, a simpler trapping equation can be formulated if the average findability × efficiency × retentiveness (abbreviated as T_{fer}) for the set of animals within the whole trapping area is known. Then, catch (C) is given simply by:

$$C = T_{fer} \times M_{den} \tag{5.1}$$

5.2 Converting spT_{fer} into T_{fer}

But, calculating T_{fer} from known spT_{fer} values is less straightforward then it might first appear. Simply averaging the spT_{fer} values for all annuli of a trapping area would overestimate T_{fer}. The flaw in doing so is that the area of the respective annuli increases with radius, albeit only with r and not r^2 as for area of a circle (Fig. 5.1). Therefore, the number of target organisms in each enlarging annulus also increases when the animals are distributed randomly across a trapping area. For example, a spT_{fer} value for a Fig. 5.1 annulus with an r of 180 applies to threefold more animals then would be true for an annulus with an r of 60. Thus, the calculation of T_{fer} requires averaging weighted by the number of animals in each annulus, or by annulus area when the number of animals is unknown. One approach for computing the weighted average is demonstrated in Table 5.1; it yields a T_{fer} of 0.12 for the experimental conditions of Table 5.1.[1]

[1] An even simpler calculation yielding the same result is to use the total of spT_{fer} × annulus area and divide by total trapping area.

J. R. Miller et al., *Trapping of Small Organisms Moving Randomly,*
SpringerBriefs in Ecology, DOI 10.1007/978-3-319-12994-5_5

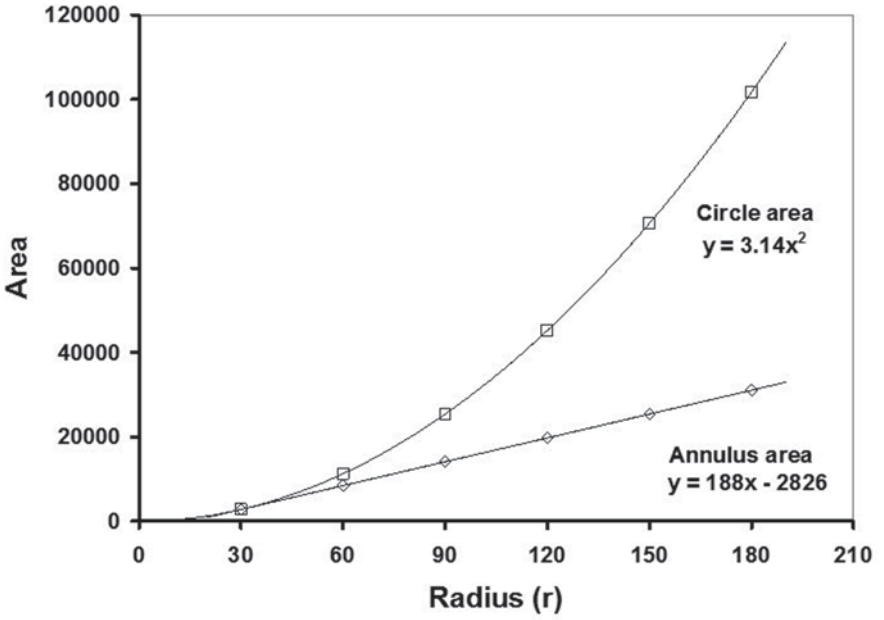

Fig. 5.1 Demonstration that the area of a disk's annuli increases linearly with radius (r) while disk area increases by πr^2. Annulus r was arbitrarily taken as the outer limit

Table 5.1 An example of how a set of spT_{fer} values can be converted to T_{fer}. The data used were generated by Weston movers displacing 5,000 steps of 0.2 with a c.s.d. of 15°. The single trap was a disk of diameter 50. Annulus radius is given as the outer limit. No movers were caught at r of 180.

	Distance movers released from trap	Annulus area	Proportion caught = spT_{fer}	spT_{fer} × annulus area
	30	2,826	0.79	2,233
	60	8,478	0.36	3,052
	90	14,130	0.16	2,261
	120	19,782	0.047	930
	150	25,434	0.005	127
Mean for column	90	14,130	0.27	1,715
				1,715/14,130 = 0.12 = T_{fer}

$$\text{Mean}(spT_{fer} \times \text{Annulus Area}) / \text{Mean Annulus Area} = T_{fer} \tag{5.2}$$

Equation (5.1) has been confirmed experimentally. One validation employed computer simulations using the conditions of Table 5.1. However, movers were not released at prescribed distances from the trap. Rather, they were seeded randomly

at known densities into a trapping area whose radius was determined by measuring maximum net displacement of a population of 100 movers under the same conditions, but released from a single point. As Eq. (5.1) prescribes, catch increased linearly with M_{den} (Fig. 5.2 a). The consistent slope of 0.12 directly reveals T_{fer} and the exact match with the 0.12 value above validates the procedure of Eq. (5.2).

However, we actually discovered Eq. (5.1) during earlier field experiments (Miller et al. 2010) using codling moths released at set densities into large field cages, each covering 12 full-sized apple trees and containing a single sex pheromone-baited trap like that of Fig. 1.3. Catch accumulating over several days after release of laboratory-reared moths increased linearly with insect density (Fig. 5.2b) in accordance with Eq. (5.1)[2]. But, the T_{fer} revealed by the slope of the regression equation for caged codling moth catch was high (0.5) because the moths were not free to emigrate. Forced proximity of moths and the trap guaranteed high spT_{fer} values for all moths within a cage, and thus an unusually high T_{fer} relative to values we shall encounter below for the open-field situation.

5.3 From Where Does most of the Catch Accumulating in a Trap Originate?

One might surmise that most of the random walkers recovered from a trap originated very near that trap. However, such an assertion would be incorrect for movers distributed randomly throughout a trapping area. As introduced in Chap. 3, and reconfirmed in Fig. 5.3 under the experimental conditions generating the results of Table 5.1, spT_{fer} for biological random-walkers initially falls nonlinearly but smoothly with distance of mover origin from a trap. However, when distances of origin are extended so far that few random walkers reach the trap within the run time of the experiment, MAG plots (Chap. 4) are not linear throughout; the departure from near-linearity is seen at the right side of Fig. 5.3b, while such a transition is undetectable in Fig. 5.3a. For this reason, only the linear portions of MAG plots

[2] For independent random movers under study here, the fundamental Equation (5.1) is provable mathematically for the expected $\overline{C}$, which corresponds by the law of large numbers to the average value of C over many repeated trials, as in Section 5.5. Indeed, the probability that a particular mover is captured is just T_{fer}. It follows that the expected catch is simply

$$\overline{C} = \sum_{j=1}^{M_{den}} T_{fer} = T_{fer} \times M_{den}$$

where as above M_{den} is the number of movers in the trapping area. This argument may make Equation (5.1) seem almost tautological. Yet, in the derivation we used in a critical way the fact that the capture events of distinct movers are "stochastically independent," which is to say that the probability of a given mover being captured is not influenced in any way by the trajectories of the other movers. This is true by fiat for the Weston movers, but is not obvious for real biological movers. However, the validity of Equation (5.1) in the cage experiments of Miller et al. (2010) strongly supports the hypothesis of stochastic independence of capture events for codling moths.

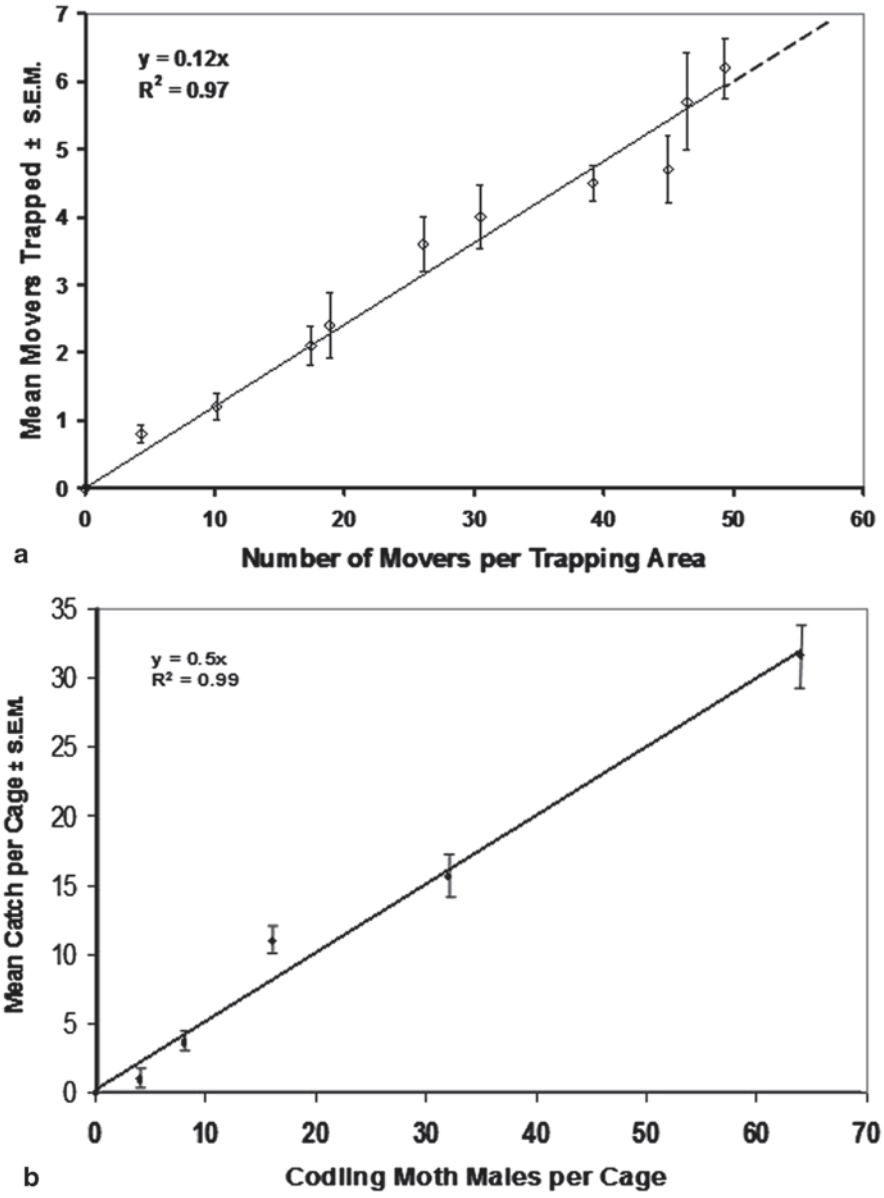

Fig. 5.2 Demonstrations that capture increases linearly with the density of Weston movers introduced into the trapping area of a single trap. **(a)** Results from computer-simulated random walkers, details in text above. **(b)** Results from large-cage experiments using codling moths (Miller et al. 2010). Such research validates Eq. (5.1) and (5.2)

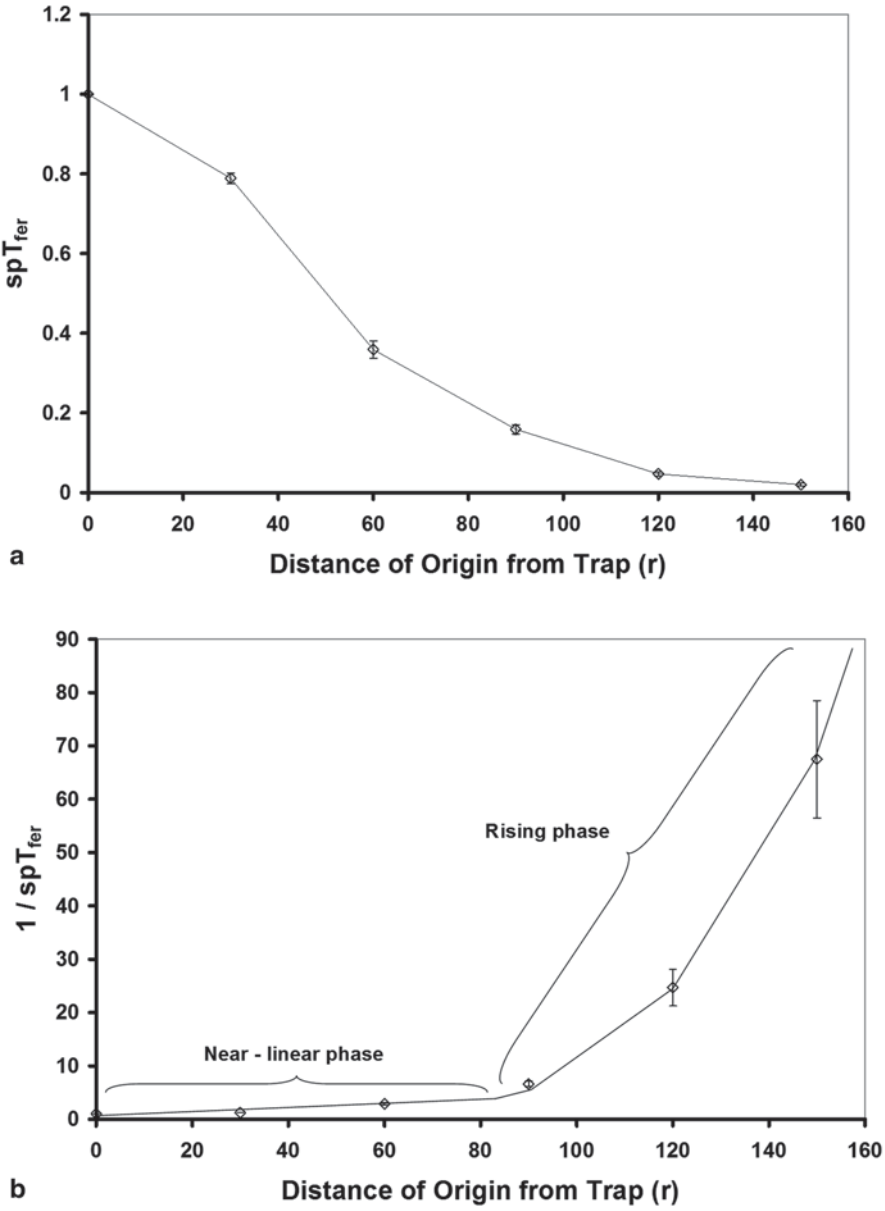

Fig. 5.3 Nontransformed **(a)** and MAG plot **(b)** of catch probability as influenced by distance of mover origin from a trap as seen across the full range of distances resulting in any catch. These data were generated by the computer simulations used for Table 5.1. No catch was obtained when *r* exceeded 150. *Error bars* indicate S.E.M.

should be used when estimating L values (Chap. 4). However, a wider range of r values, including those resulting in little catch, must be included when estimating the maximum for trapping radius or the favored zone of origin of the movers recovered from a trap.

As documented in Fig. 5.1 above, the area of the annuli comprising a trapping disk rises linearly with r, while spT_{fer} falls nonlinearly with increasing r (Fig. 5.3a). The zone producing the most catch can be identified as the maximum in a plot of (spT_{fer} × annulus area) as a function of r (referred to hereafter as a Miller plot). For biological random walkers, the zone contributing the most catch lies just short of the middle of the trapping radius (Fig. 5.4). For example, 60 % of the catch for movers with a 15°c.s.d. was drawn from between radii 30 and 90 of a trapping radius whose limit was 150. The zone close to the trap yields little catch. Even though it experiences the highest probability for plume encounter, it comprises a very small portion of the total trapping area. The zone far from the trap, but yet within the trapping area, yields little catch because spT_{fer} is fast falling even though annulus area and thus number of movers experiencing that spT_{fer} continues to rise. So, when just a few random walkers are captured in a trap, it is likely they originated from the mid-zone and not near the trap or from the perimeter of a trapping area.

Subsequent to our discovery of the "sweet-distance" phenomenon for trapping, a similar idea was found in Eq. (3) of Östrand and Anderbrant (2003) dealing with cumulative proportional catch (CPC). However, the importance and simplicity of this phenomenon seems to have gone unappreciated by the various researchers who cite this reference but do not mention CPC.

Catch of ballistic movers, on the other hand, remains constant across all zones throughout a trapping area (except for low catch near the trap) (Fig. 5.4) because spT_{fer} is never reduced by backtracking. Rather, catch of ballistic movers abruptly drops only when their dispersive capacity is exceeded.

The Fig. 5.4 experiment provided further insight into the problem of optimizing c.s.d. when foraging for resources. When a single, modestly-sized object was presented at 5,000 steps from movers, those with c.s.d. values of 0 and 5° had the highest probability of finding the resource at the greater distances. However, the picture reverses when the resource happens to be close at hand. If the density of randomly distributed resources were high, some would be guaranteed to be close at hand. Then, a larger c.s.d. might suffice and could be favored. However, the smaller c.s.d. values would be favored under low resource densities, because larger net displacements would be required. The tradeoffs encountered in this situation are obvious, further supporting the notion that, like other genetically-based traits, the c.s.d. values organisms display should be selectable upon resource density and distribution.

Some insect studies have shown that it can be advantageous for organisms to modulate c.s.d. values in accordance with how recently the forager has encountered a resource. For example, walking house flies foraging for invisible sugar deposits on a flat substrate use a particular default c.s.d. before encountering the first resource by chance (Bell 1991). After consuming that deposit, the flies displace with an opened c.s.d. promoting intense local search for other deposits that might be nearby as in a resource patch. When this tactic is no longer rewarding, the c.s.d.

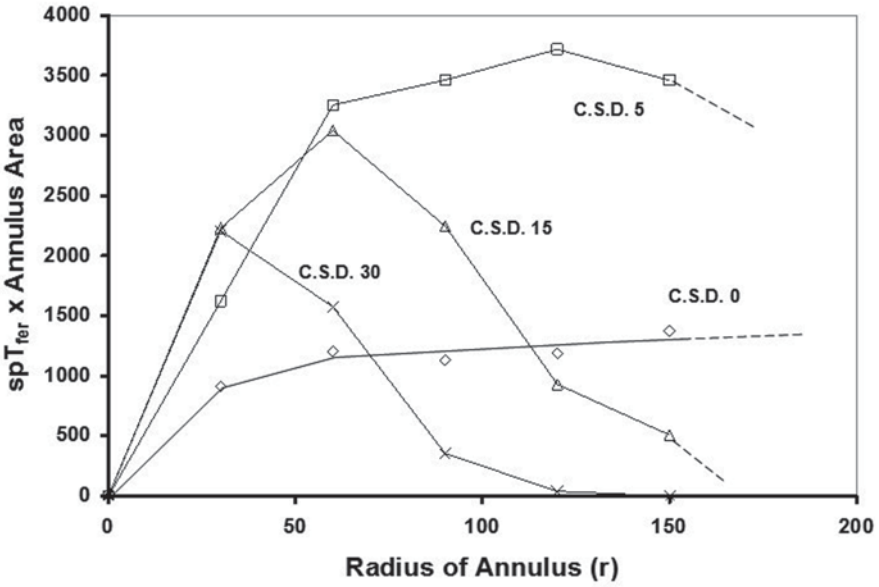

Fig. 5.4 Graphs documenting the radii for greatest capture for a single trap of diameter 50 units as influenced by mover c.s.d. Movers displaced for 5,000 steps of 0.2 units. For this run time, the chosen radii exceeded the maximum dispersion for movers with c.s.d. 30 and 15°, but not 5 and 0°. The maximal trapping radius occurs where descending graphs reach the *x*-axis. Annulus area is directly correlated with mover numbers when the mover population is distributed randomly across a trapping area. Therefore, the *y*-axis can be interpreted as relative numbers of movers caught. Large areas under segments of any curve equate to high catches. This type of graph is designated as a Miller plot. S.E.M. bars were < 20 % of the means

reverts to the smaller default value, which sensibly facilitates searching at greater distances for other patches.

5.4 Preparing to Put Eq. (5.1) to Work

The introductory chapter declared that establishing trapping methodologies to quickly, cheaply, and accurately estimate the absolute density of small animals dispersing randomly was the core applied goal of this investigation. Are we getting close to that goal? Can Eq. (5.1) do the job? And, what information must be in place to apply Eq. (5.1)?

Let's address these questions in reverse order. Equation (5.1) ($C = T_{fer} \times M_{den}$) enables one to solve for any of its three variables when any two of them are known. In practice, catch C will always be known, because some number caught (be it zero or many) always results from any trapping research. M_{den} could be experimentally varied as per Fig. 5.2 and then T_{fer} calculated as:

$$T_{fer} = C / M_{den} \tag{5.3}$$

Alternatively, M_{den} can be solved for if T_{fer} and C are known, i.e.,

$$M_{den} = C / T_{fer} \tag{5.4}$$

However, in both the cases, one needs to know the trapping radius (or area) to associate units of area to the catch. As noted in Chap. 1, pest managers harvest a plethora of catch numbers, but they do not know to what area those numbers apply.

Judged from the published literature and our above analyses, the most accessible method for establishing trapping radius is to deploy a single trap, release known numbers of marked animals at set distances and directions from the trap (see Fig. 4.3), and then trap those animals to exhaustion. The untransformed spT_{fer} data can then be plotted as in Fig. 5.3a above. A first approximation of trapping radius is offered by where catch drops to zero. However, a challenge to establishing the limit for trapping radius from a plot like Fig. 5.3a is accuracy in judging whether catch actually ceased, or whether it simply became undetectable because low sampling power resulted in false negatives, i.e., catch would have occurred if more animals were released. This problem is particularly acute for ballistic or near-ballistic movers whose capture profiles approach zero catch very slowly. However, a Miller plot (Fig. 5.4) can sharpen judgments about the limit to trapping radius. A peak followed by a smooth down-turn in such a graph indicates that the movers are non-ballistic and that the limit to trapping radius is indeed approaching. Again, that determination can be unacceptably arbitrary when using only a Fig. 5.3a plot. We also recommend against estimating sampling distance for a trap by extrapolating to zero catch after logarithmic transformation of the spT_{fer} data. Although sometimes done, this procedure seems questionable when such log graphs cut the x-axis rather than approaching it asymptotically as would the more appropriate inverse function.

We learned from Fig. 5.4 that, for biological random walkers expressing c.s.d. values greater than a few degrees, the most distant zone of the trapping area will have little impact on catch numbers because few movers from near the boundary of the trapping area arrive at the trap due to very low spT_{fer}. But, the limit placed on trapping radius will always strongly influence the area to which any catch number applies. Thus, trapping radius must always be established with care.

It is instructive to consider the potential impacts of over- vs. underestimating trapping radius when using catch numbers and Eq. (5.4) to estimate absolute density of a pest population. Overestimating trapping radius is the more dangerous error. Then, a given catch number would be interpreted as applying to an incorrectly large area; thus, the density estimate assigned would be incorrectly low. A grower would be justifiably upset if, on this basis, he or she failed to spray a highly valuable crop that was actually destined to be lost to pests. The better scenario would be that trapping radius is somewhat underestimated so that the absolute density estimate of the pest is not underestimated. Rather than emphasizing the absolute limit to trapping radius, pest managers might be better served by seeking a solid estimate of, e.g., 75 % of the trapping radius, which could be abbreviated as the TR_{75}.

A similar argument can be made for estimates of T_{fer} destined to be used in pest management decisions. Here again, it would be better that the procedures used to establish T_{fer} produce under- rather than overestimates. T_{fer} occurs in the denominator of Eq. (5.4); thus, smaller values of T_{fer} will raise rather than lower the M_{den} estimate.

5.5 Measures of Variation around Estimates of Absolute Animal Density Derived from Trapping

Measures of precision and accuracy are critical to any estimate of importance. This is certainly true for estimates of absolute pest density that will be used to make decisions of whether or not to execute control measures for serious pests. A starting point is assessment of the likelihood of obtaining a given catch number when the elapsed time for trapping runs is held constant across various densities of movers within a trapping area. To do so we used Weston movers displacing 1,000 steps of 1.0 unit under a c.s.d. of 15°. We used 300, 1,000, and 3,000 such movers randomly seeded into an unbounded cyber arena to generate an average of 50, 170, and 500 movers per trapping area (396,000 square units). If this trapping area is taken as equivalent to 20 ac (units relevant to US growers and area shown below to be realistic for locally searching flying insects), the seeded mover densities would be 3, 9, and 15 /ac, respectively. Deployed at the center of the trapping area was either one large (100 × 10 unit) or one small (10 × 1 unit) trap plume. Catch was tallied for 100 runs under each condition and analyzed for count variation.

As is to be expected for a process as stochastic as trapping, variation in catch was appreciable across replicated trapping runs for a given set of conditions (Fig. 5.5). Some of this variation can be attributed to random seeding. Simply by chance, the zone around a trap may be populated with more or less movers. The lower the average density of movers, the greater will be the probability of empty zones. Variation in catch is then expanded by the irregularities in the tracks produced by each mover upon departure from its origin, as documented in Chap. 3. Nevertheless, meaningful confidence intervals can be drawn around any given catch number. For example, a catch of zero is plausible only for a population of Fig. 5.5 movers of < 9 / ac when the plume reach is small. Provided the trap was functioning properly and the movers were active for the expected time, getting zero catch for a trap with a large plume when there are 3 animals/ac or greater is so unlikely that a grower could place this bet with supreme confidence. The bounds on the range for estimated M_{den} associated with various recorded catch categories are shown in Table 5.2. They demonstrate that the precision for these estimates improves substantially with plume reach. This knowledge suggests that, when the plume from a trap is found to have little reach, the precision of M_{den} estimates using it could be considerably tightened by deploying multiple copies of this trap closely spaced in a given location to increase the overall amount of plume perimeter without increasing time demands to visit widely spaced sites to collect the data. The total catch for, e.g., four traps

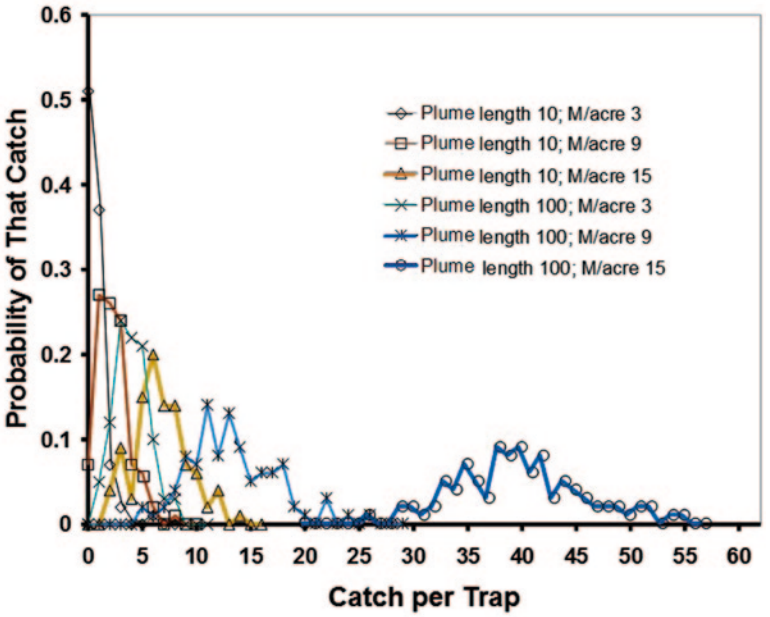

Fig. 5.5 Frequency histograms revealing variation in catch outcomes for a single trap when the duration of trapping runs was held constant. *M* = movers

could be used in place of the catch number for a single trap (see Fig. 5.6). But, the calibrations for trapping area and T_{fer} would then need to be established using the trap multiples.

5.6 Examples of Eq. 5.1 at Work

We now offer four real-world examples that collectively demonstrate how these methods and Eq. (5.1) and its derivatives can be put to practical use. The first example draws upon ongoing field research by author C. G. Adams for the codling

Table 5.2 Translation of the catch probabilities of Fig. 5.5 into estimates of the plausible range for M_{den} as calculated for a small and large plume reach

	Movers per acre	
Catch	10 unit plume	100 unit plume
0	0–9	0
1–2	0–25	1–5
3–5	3–25	2–5
6–15	10–50	5–15
15–28	–	8–20

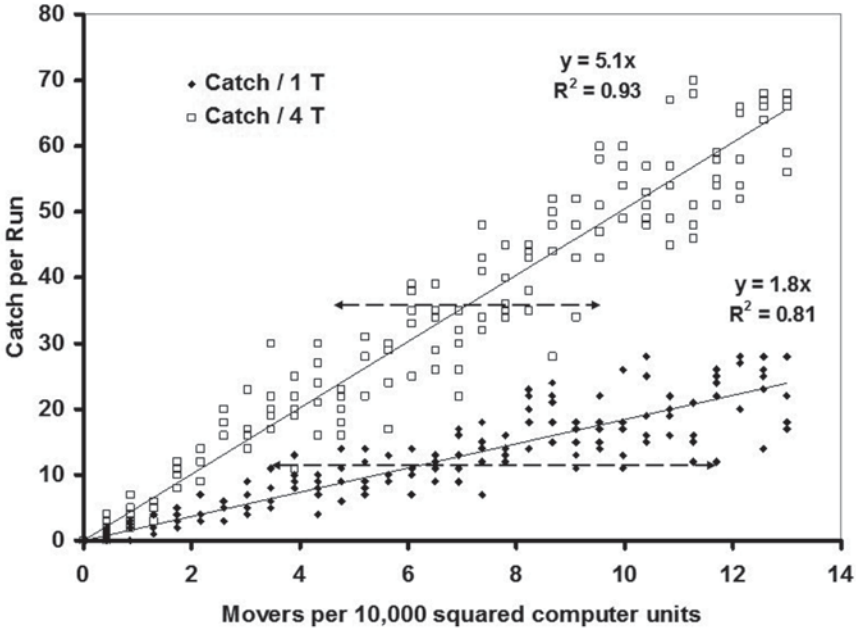

Fig. 5.6 Scatter plots of total catch per run for a single trap vs. total catch for four traps under various densities of randomly seeded Weston movers displacing 1,000 steps of 1.0 using a c.s.d. of 15°. Traps had elliptical plumes of 50 × 5 units and were separated by 70 units when deployed as multiples. Greater precision of the 4-trap metric is evidenced by a narrower range of possible seeding densities producing a given catch (*dashed double-headed arrows*) and a higher R^2 value for the regression line

moth. A trap like that of Fig. 1.3 c baited with an optimized sex pheromone lure for males of this species was deployed at the center of a large, commercial apple orchard in Western Michigan presenting uniform conditions. Approximately 140 laboratory-reared and reproductively sterilized males per site were released at 40, 80, 120, 160, and 200 m in each of the four cardinal directions from the trap. Those for each distance were marked with a distinctively colored powder that fluoresced under UV light. Catch in the trap was recorded over the following week and the moths caught were identified by release distance. We determined what proportion of the released moths were actually capable of responding to pheromone and being caught in a trap by releasing a sample of several hundred moths into a 3 × 3 × 2 m field cage holding a single trap. This step was important because the below analysis of plume reach requires knowing the proportion of *responsive* movers captured from each distance.

Most of the catch yielding the data of Table 5.3 accumulated on the first three nights after moth release. Although these given data are preliminary and the study is being replicated to arrive at central tendency, these results can be used to demonstrate recommended procedures for analyzing such data. First, the spT_{fer} data are plotted as per Fig. 5.7. Catch diminished with release distance and fell to a mere

Table 5.3 Results of a preliminary single-trap, multiple-release field test with codling moth. Experimental details are given in the text above

Release distance (m)	Annulus area (m^2)	spT_{fer}	spT_{fer} × annulus area
40	5,024	0.039	197
80	15,072	0.014	215
120	25,120	0.013	314
160	35,168	0.005	188
200	45,216	0.002	81
Mean	25,120	0.015	199

$T_{fer} = 199/25{,}120 = 0.008$

0.2% by 200 m, suggesting that the limit to trapping radius was approaching. However, because zero catch was not yet reached, release distances must be expanded in further runs of this experiment.

The down-turn by 200 m in the Miller plot of these data (Fig. 5.7b) provides strong evidence that: (i) codling moth males dispersed by correlated random walks and not ballistically, and (ii) that the limit to trapping radius was ca. 225 m. If the sampling radius of this trap was taken at 225 m, the full trapping area would be 16 ha. However, if the bulk of catch accumulates inside of 120 m, as suggested by Fig. 5.7b, the area over which this trap is most powerful would be closer to 8 ha. This finding suggests that deploying one trap every 20 ac may be sufficient for monitoring of codling moth populations using this trapping system.

Given that the trapping limit was nearly approached in the above test, we calculated T_{fer} using the method of Table 5.1 and Eq. (5.2); the value returned was 0.008 (Table 5.3), suggesting that only 0.8% of all the moths present in the full 16 ha of apples being sampled by the trap would be captured. Table 5.4 translates catch numbers for a single trap into densities scaled to units smaller than trapping area. Readers should recognize that variation similar to that documented in Table 5.2 is to be expected surrounding the listed mean values for M_{den}. Intriguingly, the number caught draws ever closer to the density number as the unit of area referenced shrinks. But, this effect is strictly an accounting phenomenon; it does not mean that trapping efficacy increased for smaller areas. For example, the ratio appears impressive when a catch of one in the trap is compared with the calculated 3 males/ac. However, that catch of one must be considered shared with all of the many other 1 ac zones within the full trapping area. It cannot be attributed to the males originating in one given acre. Here is a potential conceptual pitfall to be avoided as this knowledge is shared with practitioners.

Rather than using the maximal trapping radius to establish the units of area to which a given catch applies, we could follow the more conservative route and use the 75% trapping radius (TR_{75}). Doing so translates into a trapping radius of 168 m rather than 225 m. The trapping area then becomes 9 ha and the estimates of absolute moth density double those shown in Table 5.4. Again, using the TR_{75} rather than the full trapping radius would assure that the pest density is not underestimated.

As the sex ratio of codling moths is 1:1, the absolute density of female moths can be taken as identical to male density. The currently recommended threshold

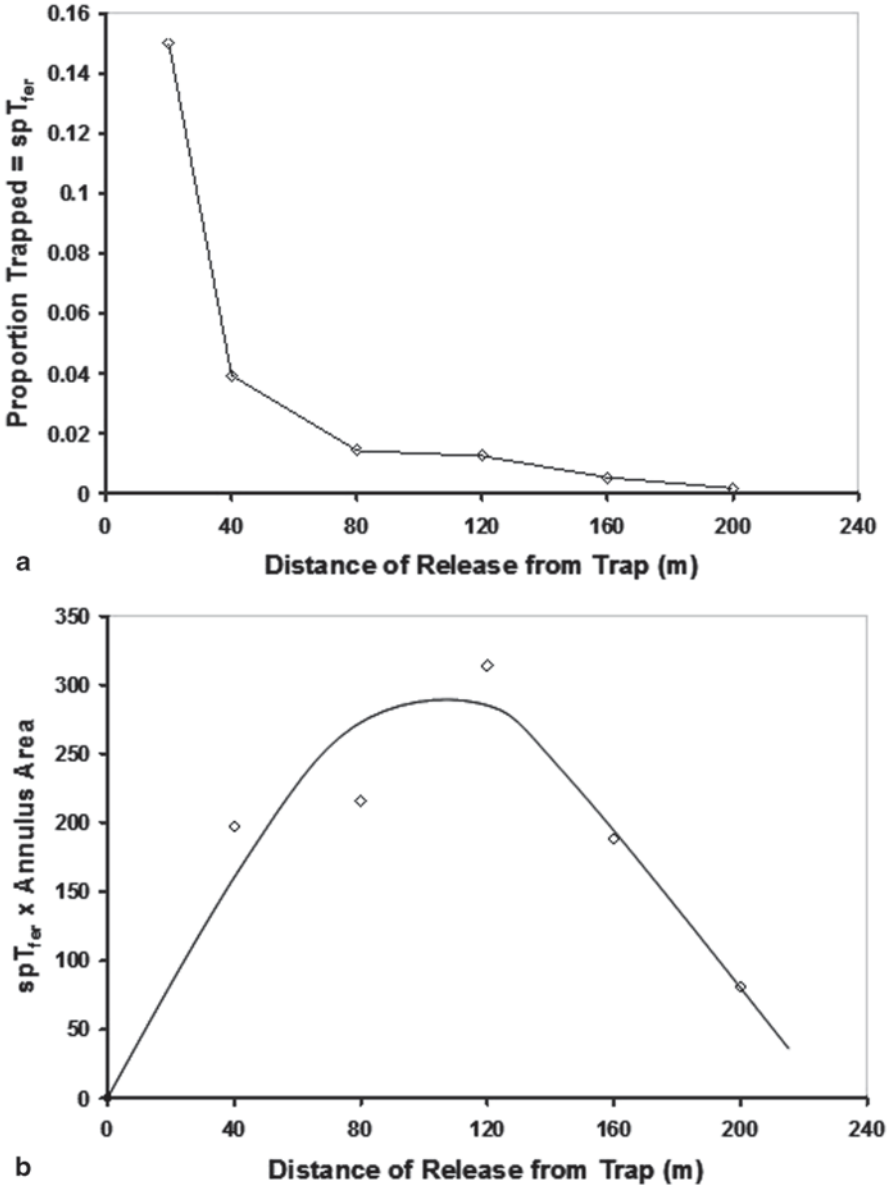

Fig. 5.7 Untransformed plot **(a)** and Miller plot **(b)** of codling moth trapping data from Table 5.2. The datum at 20 m in panel **(a)** came from a preliminary test and is included to show the shape of the curve as it extends back toward the trap. No error bars are included because only one replicate of this experiment is reported here

triggering sprays for codling moth in Michigan is 3 males/trap/wk. If catch were four, we see from Table 5.4 that about ten females would be present per ac. The following projections can then be made about maximal possible % apple infesta-

Table 5.4 An example of how catches of animals in one standard monitoring trap might translate to absolute densities scaled to differing units of area. T_{fer} for this codling moth example was taken at 0.008 and trapping radius 225 m as per the above analyses. Then male moth density was computed as density per trapping area = catch per one trap divided by T_{fer}. That density was then scaled to smaller units of area relevant to grower experience. Since the sex ratio for codling moth is 1:1, the number of females equals that of males. Warning: These numbers are preliminary and cannot safely be used for actual pest management decisions for codling moth or other such pests. These data are only instructive for how to apply the trapping approaches developed in this book

Catch per single monitoring trap	Males per trapping area (16.9 hectares)	Males per hectare	Males per acre
1	125	8	3
3	375	23	9
10	1,250	80	30
30	3,750	230	90
100	12,500	800	300

tions based upon knowledge of this moth's biology gathered by Michigan's tree-fruit extension specialists: each of the nine out of ten females successfully mating will scatter ca. 50 eggs individually near a developing apple for an estimated total of 450 eggs; 40% of these eggs are likely to produce larvae that successfully colonize apples for a total of 180 infested apples/ac. The average density of Michigan apple fruits/ac is about 150,000, thus, the estimated maximal infestation rate would be 1.2/1,000 fruits when the permissible threshold is 1 infested fruit/200 apples (0.5%). These calculations suggest that the current threshold triggering codling moth sprays is reasonable, but that it includes quite a wide safety margin. It is eye-opening to learn that Michigan growers spend about $ 60 to spray ten codling moth females per ac, or ca. $ 6 per female moth. Growers spraying whenever their monitoring traps register any catch at all are spending $ 10 per female or more. Our hope is that further field demonstrations of the validity of our trapping approach will enable growers to confidently withhold sprays when they are, in fact, not needed. Doing so will result in increased profits, enhanced levels of biological control, and greater lifespan for the valuable insecticides because of reduced selection pressure for resistance development.

Finally, the reach of the pheromone plume from the standard monitoring trap used in this codling moth test can be estimated from the MAG plot (Fig. 5.8) slope generated for responsive test organisms. The slope returned from the near-linear portion of that plot was 0.68. Figure 4.12 can then be used to interpret this slope. The first step in doing so is to locate 0.68 on the *x*-axis of Fig. 4.12 and note what plume reaches could be attributed to this given MAG slope. If the c.s.d. used by foraging codling moth were as small as 6°, we observe that the plume reach could be about 10 m. However, if these moths use a c.s.d. of 15°or more, which we judge likely, the plume reach could be as small as only several m.

The *y*-intercept was 4.0 for the near-linear phase of the MAG plot of Fig. 5.8. It can be seen from the simulations of Fig. 4.13 that such a large *y*-intercept is associated with a small plume reach. Thus, both the slope and the *y*-intercept of the MAG

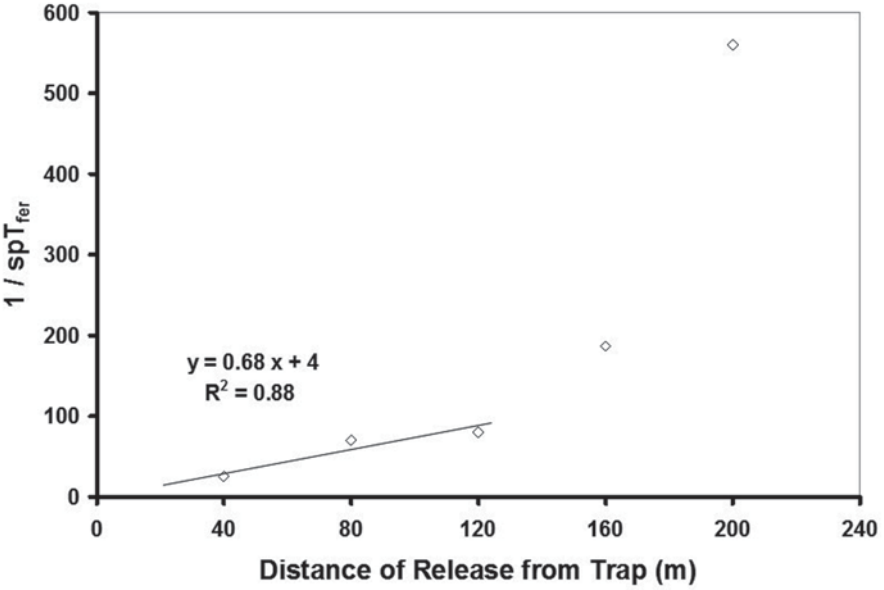

Fig. 5.8 MAG plot of the trapping data for the preliminary single-trap, multiple-release test with codling moth. Only the first three release distances were used because of up-turn evident in the MAG plot above and down-turn evident in the Miller plot (Fig. 5.5b). The corresponding plume reaches consistent with this slope of 0.68 can be read from the standard curve of Fig. 4.12

plot for codling moth argue for a small plume reach. Moreover, a previous investigation (Grieshop et al. 2010), where marked codling moths were released directly downwind of a trap and then monitored for rapid appearance in the trap, suggested a plume reach of under 10 m for this standard codling moth monitoring trap. So, the evidence is mounting that the time-averaged plume reach for the standard codling moth trap is surprisingly small.

Our second example draws upon research (Whamsley et al. 2006) conducted on the corn rootworm, a beetle whose larvae attack corn roots. This pest's annual economic impact in the USA alone is estimated at over $ 1 billion in crop losses and control costs. These investigators collected thousands of adult beetles from a natural infestation in a Kansas corn field and brought them to the laboratory for several days to standardize their physiological condition by provision of abundant foodstuffs. One hundred beetles were then released back into a corn field at each of five distances on six equidistantly spaced spokes radiating from a single Trécé™ corn rootworm trap baited with an experimental lure releasing the plant volatiles eugenol and 4-methoxy cinnamaldehyde. Beetles at each distance were dusted with a distinctively colored powder. The total number of released beetles in this nonreplicated test was 3,000 for the setup receiving the baited trap and another 3,000 for a nearby setup receiving an unbaited trap. The test ran for 3 days after which captured beetles were examined under the microscope for powder color.

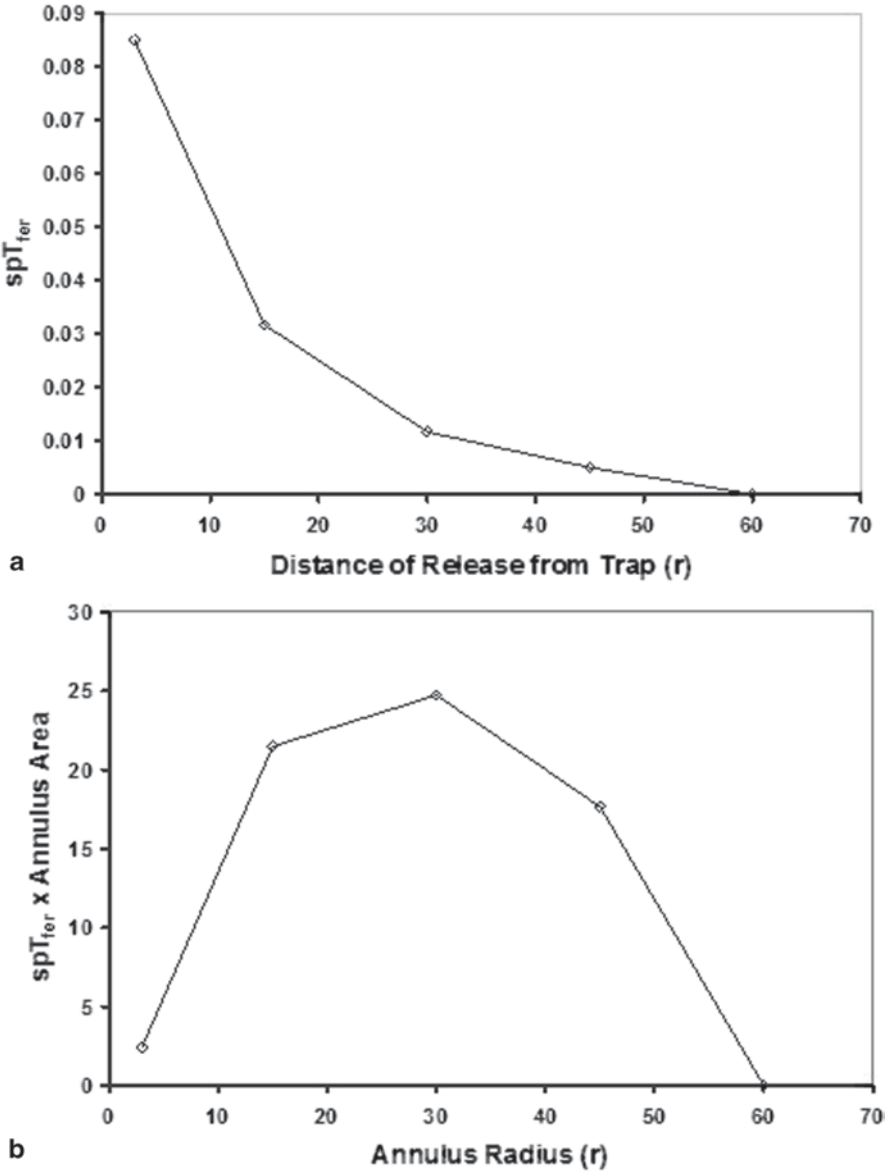

Fig. 5.9 Untransformed and Miller plot of data from a single-trap, multiple-release field study on corn rootworm conducted in a Kansas cornfield (Whamsley et al. 2006). No error bars are included because this test was not replicated

No beetles were captured in the unbaited trap, while 80 beetles total (2.7% of those released) were captured in the baited trap. Catch dropped smoothly with release distance (Fig. 5.9a) and reached zero by 60 m. The investigators rightly concluded: (i) catch in this trap does not occur without bait, (ii) maximum trapping

Table 5.5 Reinterpretation of results for the single-trap, multiple-release study on corn rootworm

Release distance (meters)	Annulus area (m^2)	spT_{fer}	spT_{fer} × annulus area
3	28	0.085	2.4
15	678	0.032	21.5
30	2,120	0.012	24.7
45	3,533	0.005	17.7
Mean	2,261	0.027	13.3

$T_{fer} = 13.3/2261 = 0.006$

Table 5.6 Translation of capture numbers in a single corn rootworm trap into numbers per the 0.5 ha trapping area or per acre when T_{fer} is taken as 0.006. Responders per trapping area was computed as catch in the trap divided by T_{fer}; then that density was scaled to the smaller unit of area

# caught	#per 0.5 ha	# per acre
1	167	67
3	500	200
10	1,667	667
30	5,000	2,000
100	16,667	6,667

radius for the 3-day test was < 60 m, and (iii) this trapping system had a short radius. However, this data set contains more information than the authors were able to harvest at the time. For example, the smoothly rising then falling Miller plot Fig. 5.9b demonstrates that these corn rootworm beetles dispersed by correlated random walks and not ballistically. A trapping radius of less than 60 m is also firmly supported, i.e., this conclusion is based on more than possible false negatives due to low sampling power. Given that the limit to the trapping radius was firm, T_{fer} for this test was calculated as per Table 5.5 at 0.006, a value remarkably similar to the 0.008 for the codling moth study above. Table 5.6 demonstrates how this trap could be used to estimate corn rootworm densities from catch data, despite its short trapping radius.

Finally, a MAG plot of the corn rootworm data (Fig. 5.10) yields an initial slope of 1.9. This slope is so steep as to be off the standard curve for interpreting plume reaches (Fig. 4.12). A firm conclusion can be drawn, however, that the plume for this trap was extraordinarily tiny (1 m or less). The very high y-intercept of Fig. 5.10 also supports this conclusion. Indeed, it is likely that the plant volatiles released by the trap functioned only as arrestants of the beetles (caused them to land) (Miller et al. 2009) rather than attractants (steer upwind in the plume). Although such a trap would be ineffective as a detection or trap-out tool, it could function well in assessing absolute densities of corn rootworms when pest pressure was high and thus could serve as an important pest management tool.

A third example draws on research from Sweden (Östrand and Anderbrant 2003) on the European pine sawfly, a wasp whose larvae feed in groups on the needles of

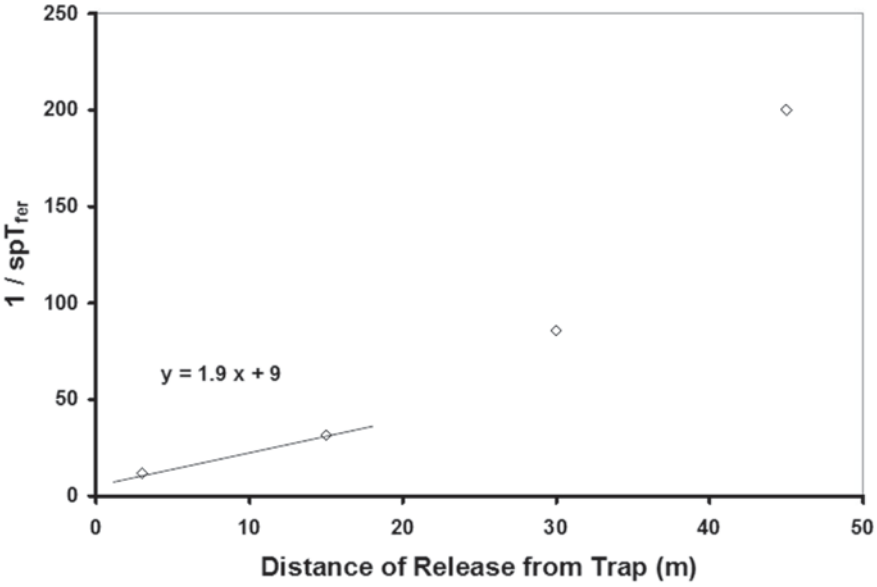

Fig. 5.10 MAG plot for corn rootworm trapping data from Fig. 5.7. Basing the slope on only two data points weakens the analysis for this case. However, the up-turn visible by 30 m and down-turning profile of Fig. 5.9b beginning at 30 m supports not including more than two data points in the MAG slope analysis

pine trees. Males of this pest are reported to respond from 50 m or more (Östrand et al. 2000) to a potent female-produced sex pheromone, and, catch in traps is well correlated with subsequent egg production and damage (Fig. 5.11). The design of this study was similar to that for the above examples, except that the intervals of release distance were enlarged with distance and not regular. This experiment was conducted in a large plantation of maturing Scots pine and is superior to the above examples because it was replicated four times. The trap was deployed at a height of 2 m; thus, the plume would largely have been wafting through the understory where the foliage of this tree species becomes sparse in maturing stands. Less physical obstruction would have been presented to the plume from this trap than for the plumes of codling moth and corn rootworm.

Our interpretations of the results support and extend those of the original investigators. The spT_{fer} values recorded declined smoothly with release distance (Fig. 5.12a). As the authors of this study were unaware that an inverse function was the more appropriate fit to their data on probability of catch vs. release distance, they used a log curve fit and then extrapolated to an estimated maximum trapping radius of 1,040 m. This step warrants reconsideration because the Miller plot of these data (Fig. 5.12b) shows no convincing decline in spT_{fer} at the largest distances of release. The recorded profile does not rule out possible near-ballistic displacement by the pine sawfly males (compare Fig. 5.12b with Fig. 5.4 c.s.d. 0°). Here is a case where

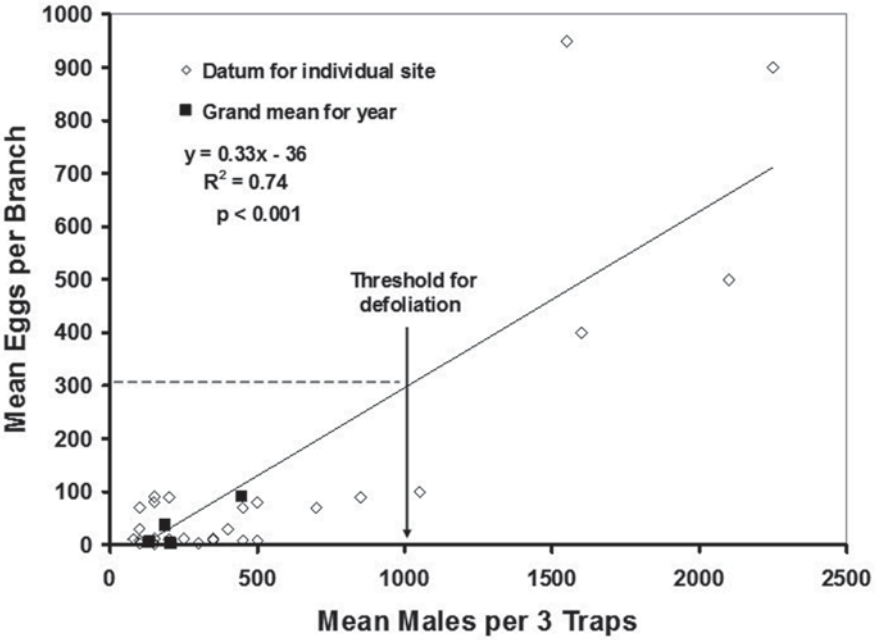

Fig. 5.11 Relationship between catch of male pine sawflies in pheromone-baited traps and density of eggs deposited at those sites. Data re-plotted from Lyytikäinen-Saarenmaa et al. (2001)

the evidence is unconvincing that the maximum trapping radius was approached by the chosen release distances for what must be a highly dispersive insect capable of appearing in a trap hundreds of meters away from the release point on the first day of the experiment. Clearly the trapping area for this insect is huge, e.g., it could have been as large as 700 ha if the trapping radius were guessed at 1,500 m, which from Fig. 5.12a is not out of the question. One wonders if the females disperse as far as males. The negative *x*-intercept of Fig. 5.11 suggests they may not.

T_{fer} for this sawfly experiment was calculated at 0.024 using the above methods. However, this value is likely inflated because the limit to trapping radius had not yet been reached; thus, T_{fer} was not reduced by spT_{fer} × annulus area values for the untested larger distances of release. Translations into density estimates via Eq. (5.1) are given in Table 5.7, when trapping radius was taken at a conservative 1,200 m. Variation around the mean densities given in Table 5.7 is expected to be similar to that shown for the large plume of Table 5.2. The current analysis supports the earlier reports that this sawfly trapping system is extremely potent and would be excellent for pest detection. Capture of a single individual/trap equates to 0.1 insects/ha for pine sawfly, while it equates to 8 and 334 insects/ha for codling moth and corn rootworm, respectively. It is not surprising then that the plume reach for this pine sawfly trap, as estimated from the MAG plot slope (0.12 Fig. 5.13) and the standard curve of Fig. 4.12 was 50 m. In this case, it is appropriate to focus only on the low c.s.d. graph because the incomplete profile of Fig. 5.12b is consistent only with a

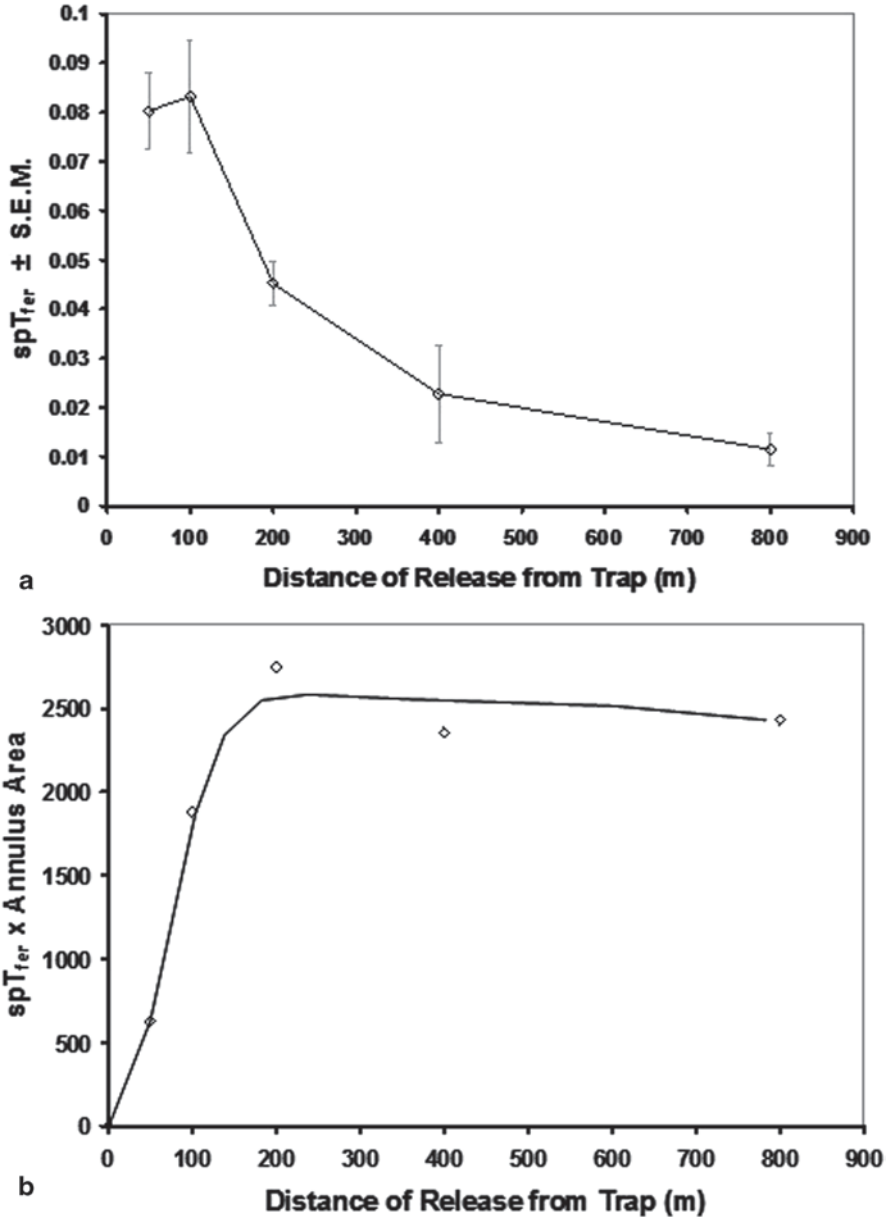

Fig. 5.12 Untransformed **(a)** and Miller plot **(b)** of data for a single-trap, multiple-release trapping study of pine sawfly (Östrand and Anderbrant 2003)

low c.s.d. value. The small *y*-intercept of 1.2 is also consistent with a large plume reach (Fig. 4.13). This estimate of plume reach agrees well with and refines that of up to 100 m arrived at by direct behavioral observations of sawflies released at various distances downwind and perpendicular to a line of traps (Östrand et al. 2000).

Table 5.7 Translation of capture numbers in a single pine sawfly trap into numbers per a 450 ha trapping area or per smaller areas within that trapping area. Trapping radius used was a conservative 120 m and the T_{fer} was 0.024

# caught	# per 450 ha	# per ha	# per acre
1	42	0.1	0.04
3	125	0.3	0.11
10	417	0.9	0.37
30	1,250	2.8	1.11
100	4,167	9.3	3.70

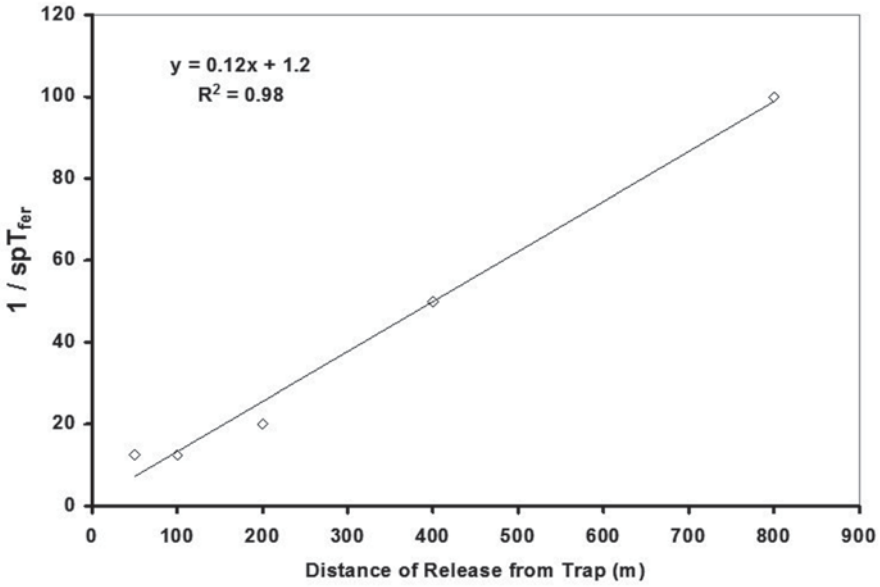

Fig. 5.13 MAG plot of pine sawfly spT_{fer} data. The lack of an up-turn is further evidence that the limit to trapping radius had not been reached

Our final detailed example comes from research (Brêthes et al. 1985) conducted on snow crabs in the Gulf of St. Lawrence, just east of Quebec, Canada. In this study, an anchor was attached to one end of a long line, and one standard commercial snow crab trap (bait unspecified but probably some type of chopped fish) was attached 100 m up the line. Bags containing 15 snow crabs each, distinctively marked for each distance, were short-tied at intervals between the anchor and the trap. The array was carefully deployed from a research vessel in a straight line more than 100 m below sea level onto the sea bed. Ingeniously, the ties on the crab bags dissolved after about 30 min, releasing the crabs to forage freely. So in this case, only a single line of release points radiated away from the trap. Traps were recovered and crabs counted after 24 h in one test and 48 h in another.

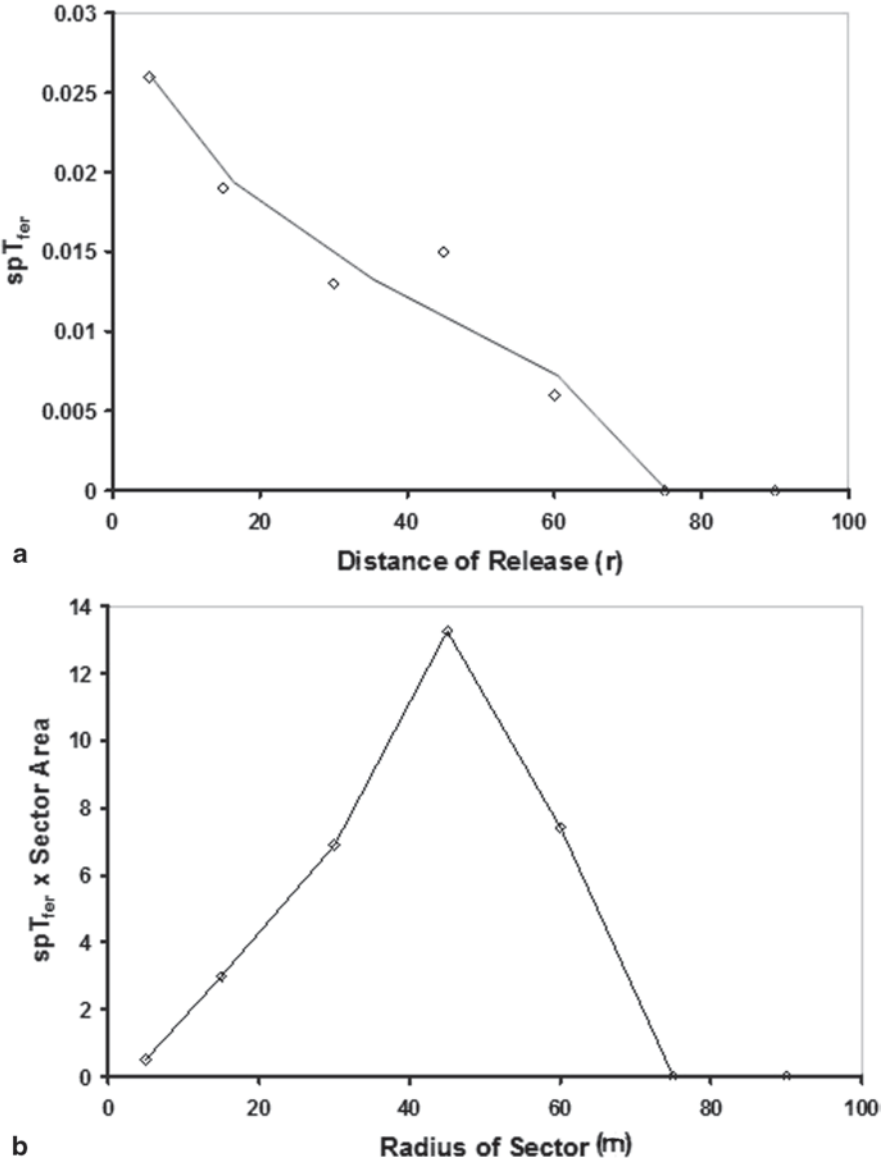

Fig. 5.14 Untransformed **(a)** and Miller plots **(b)** of data from a single-trap, multiple-release test using snow crabs (Brêthes et al. 1985). The data for several close release points at the mid-range of release distances were averaged to keep the distance increments nearly regular. As only a single line of traps was used, annulus area was divided by four to yield a sector area

Proportions of crabs caught in the 24 h test are graphed in Fig. 5.14a. The highest proportion (0.026) was caught at 5 m; catch fell from there, and no marked crabs were captured beyond 60 m. The profile of the Miller plot (Fig. 5.14b) suggests that

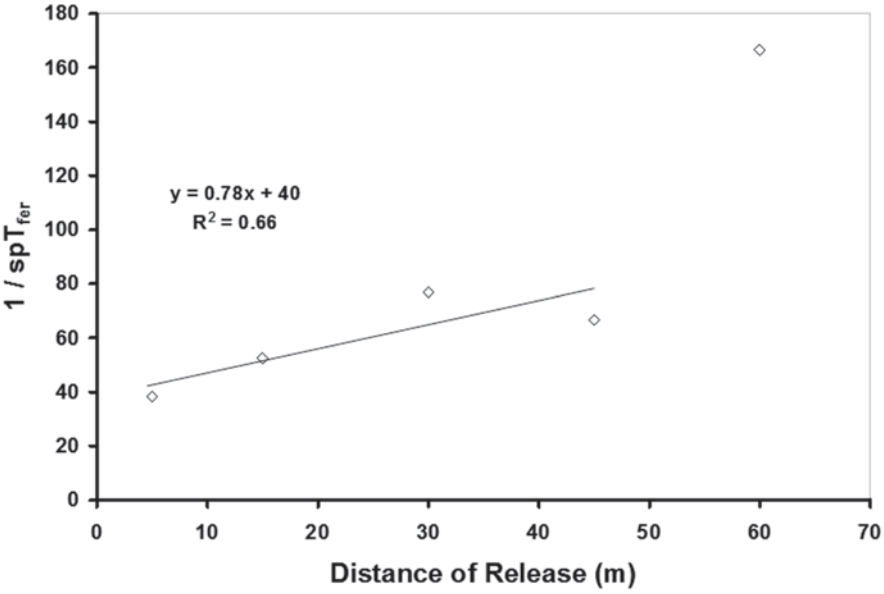

Fig. 5.15 MAG plot of spT_{fer} data from a single-trap, multiple-release trapping study of snow crabs. This case is unusual in that only a single line of traps radiated from the trap, not multiple lines in various directions as is the more standard procedure for terrestrial studies

the snow crabs displaced by correlated random walks rather than ballistically. Given that a maximum trapping radius of 60 m was evident, trapping area can be computed at just over 1 ha; T_{fer} was computed at 0.007 by the above methods, with the exception that only one quarter of the annulus area was used because of the single line of release points. Using this T_{fer} value and the 1 ha trapping area, application of Eq. 5.4 suggests that catches of 1, 3, and 10 snow crabs in one such trap over this brief interval equate to 143, 430, and 1,430 crabs/ha, if their starting distribution across the sea floor were random.

Plume reach of a baited trap is of considerable interest to fishermen, as that knowledge helps gauge appropriate trap spacing for maximizing overall catch with a minimum of equipment and travel. Thus, the data of Fig. 5.15 will be important to snow crab fishermen. The MAG slope of 0.78, as interpreted using the calibration curve of Fig. 4.12, suggests the plume emanating from the trap was detectable for only ca. 10 m under the above conditions. Such an outcome suggests little concern is justified about fishing inefficiencies due to overlapping bait plumes, unless traps would be very densely packed. The suspiciously large *y*-intercept of 40 is also suggestive of a small plume.

Table 5.8 Comparison of values for T_{fer} and estimated plume reach for a sampling of arthropods for which data from single-trap, multiple-release data have been published. Examples are sorted by ascending T_{fer}. Values for T_{fer} followed by an asterisk may be inflated because the distances of release used to establish spT_{fer} were not shown to have extended close to or beyond the full trapping radius

Common name	Species name	Reference	T_{fer}	Plum reach (m)
Western corn rootworm	*Diabrotica virgifera virgifera*	Whamsley et al. 2006	0.006	1–2
Southern pine beetle	*Dendroctonus frontalis*	Turchin and Odendaal 1996	0.05	1–2
Codling moth	*Cydia pomonella*	Adams et al. 2015	0.008	2–3
Snow crab	*Chionoecetes opilio*	Brêthes et al. 1985	0.007	5–10
Douglas fir bark beetle	*Dendroctonous pseudotsuage*	Dodds and Ross 2002	0.03	10–25
Click beetle	*Agriotes lineatus*	Sufyan et al. 2011	0.21*	10–30
Long-horned beetle	*Prionus californicus*	Maki et al. 2011	0.07*	10–50
European pine sawfly	*Neodiprion sertifier*	Östrand and Anderbrant 2003	0.024*	30–50
Sweet potato weevil	*Cylas formicarius elegantulus*	Mason et al. 1990	0.13*	30–70
		Mean	*0.06*	*19*

5.7 Patterns in T_{fer} Values and Plume Reaches for Organisms Displacing Randomly

Across these four examples, it is the displacement of the responder that comprises the preponderance of trapping radius, not the plume reach. To be successful at finding stationary traps or resources like food and mates, it appears that animals must move over a considerable area.

We located some additional studies from the literature that could be analyzed by the above methods for T_{fer} and plume reach. The expanded list appears in Table 5.8. Most of these studies yielded T_{fer} values higher than those of the experiments detailed above. The largest T_{fer} found (0.21) was for a click beetle attacking turf. However, like the pine sawfly test, none of these additional examples returning the higher T_{fer} values used release distances proven to approach or exceed the trapping radius as judged by up-turning MAG plots or down-turning Miller plots. Thus, these T_{fer} values must be taken as inflated over what would have been obtained over a full trapping area. Notably, the three T_{fer} values taken over the full trapping range and using relatively short run times (codling moth, corn rootworm, and snow crab) all fell just below 0.01. We anticipate that T_{fer} values may converge around 0.01 for various random walkers when spT_{fer} measures include the full trapping radius. T_{fer} might reflect some sampling limit given the number of movers in play. This would be fortuitous, as T_{fer} would essentially become a constant. The number of movers in play could then be easily calculated via Eq. (5.4). However, measurement of trapping radius and area would still be required for the attribution of units to this number as required for an estimate of absolute density.

The T_{fer} values of Table 5.8 appear positively correlated with both plume reach (Fig. 5.16a) and duration of the respective trapping experiment (Fig. 5.16b). These findings make sense, as both factors increase interactions of movers with the trap resulting in more intersections. However, such a conclusion must await accumulation of a more robust set of representative T_{fer} values all measured using a complete set of release distances (some returning zero catch).

5.8 This Single Trap Approach is Ready for Testing and Implementation Where Proven Reliable

Hopefully, the explanations and examples above have clearly demonstrated how Eq. (5.1) and its derivatives can be used to estimate absolute density of animals via trapping. If robust field tests across a geographical region show that trapping radius and T_{fer} are quite constant through time for given animals and trapping systems, use of Eq. (5.1) and generation of tables for catch interpretation like those above is now possible and justified. Improved pest management decisions and savings for growers will hopefully follow.

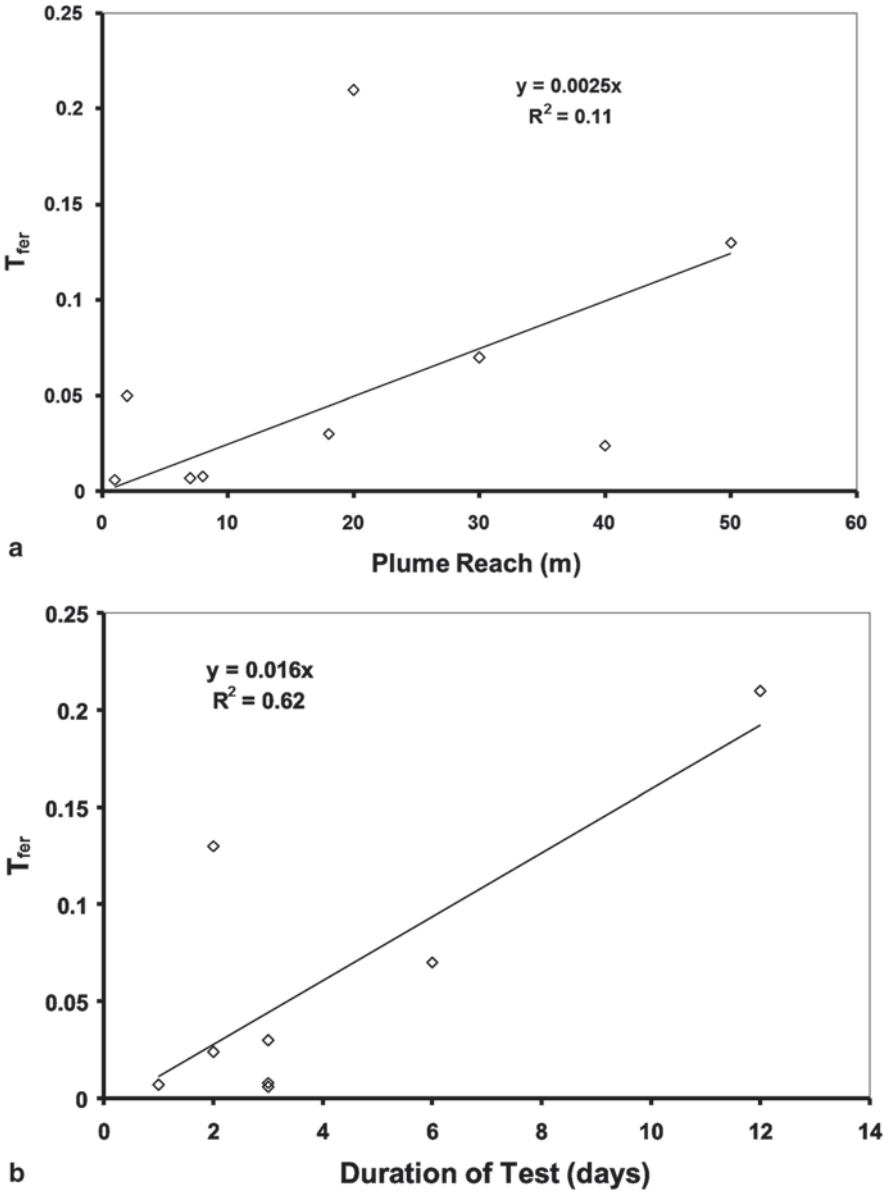

Fig. 5.16 Demonstration of positive correlations between T_{fer} values from Table 5.8 and plume reach **(a)** as well as the duration of the respective trapping tests **(b)**. The data for Douglas fir and southern pine beetles could not be included in **(b)** because the durations of trapping were not reported. Note: Most of the larger T_{fer} values are artificially inflated because release distances for the respective single-trap, multiple-release experiment did not extend to the limit of sampling radius for the trap

Implementing this approach to quantifying absolute pest density requires collection or rearing of goodly numbers of pests so that robust single-trap, multiple release experiments can be conducted to establish T_{fer} for particular growing regions. Perhaps the various private companies specializing in rearing small animals like biological control agents could fill this niche in collaboration with university researchers.

Alternatively, government agencies could facilitate laying this foundation. It will be the role of applied researchers and extension agents to understand the principles and procedures for this approach, to set protocols for how monitoring traps are deployed to maximize constancy in trapping radius and T_{fer}, and to generate the tables for translating catch into absolute pest density. Then, the connection must be made between estimated pest density and the probability of damage. For example, the translation of pest density to projected percent injury will need to be informed by reliable knowledge of pest fecundity and survivorship, as well as measures of total crop mass available to the estimated number of pests. The good news is that many pest managers are already doing a good job of integrating these factors without having a firm grip on absolute pest density. So, even better pest management decisions should be possible when inexpensive, quick, and accurate estimates of pest density become available through the use of the above tools of trapping. It is likely that growers will follow resultant extension recommendations when properly taught how to set a monitoring trap, tend it for the required time, and interpret the resulting catch. The costs in trapping materials and time will also matter, but not as much as being guaranteed good pest control and increased overall profits from applying controls only when actually needed.

5.9 A Caveat

Trapping radius and T_{fer} might vary with the activity level of the target animals. Using values of trapping radius and T_{fer} established under ideal environmental conditions for estimating M_{den} from catch data collected under inclement conditions could lead to underestimates of M_{den}. Linking catches with recorded environmental conditions (now commonplace in agriculture) should be helpful in avoiding such over-reaches. The following chapter explores how this limitation might be overcome by use of a set of competing traps to obtain estimates of trapping radius and M_{den} simultaneously from a single set of capture data.

Chapter 6
Competing Traps

6.1 Definition of Trap Competition

We define traps as competing when the presence of one or more traps reduces the catch in a given trap below what would have been measured if the additional trap or traps were not present. This effect has been sometimes labeled as interference or poaching. Wall and Perry (1978, 1980) were the first to investigate this phenomenon for attractive insect traps. Until now, the kinetics of trap competition has received surprisingly little attention.

6.2 Complete Competition

The most easily understood case of competition occurs when identical traps are deployed so closely that their plumes overlap completely without influencing each other's effective size. Under these hypothetical conditions, the number of movers arriving at the set of traps equals those arriving at a single trap. However, the catch would be split evenly between them under ample replication. If we designate some number (T_{den}) of focal traps T and some number (t_{den}) of competing traps t, then the probability of catch in the focal traps (P_T) for movers arriving at the set of completely competing traps is given by:

$$P_T = T_{den} / \left(T_{den} + t_{den}\right). \tag{6.1}$$

This situation is analogous to drawing cards from a randomized deck. Imagine that we have 1 T and 4 t in the deck, or $T_{den} = 1$ and $t_{den} = 4$. The probability of drawing T on a single draw from the randomized deck is then 1/5 or 0.2; and, the cumulative catch in the one T (C_T) with multiple draws followed by replacement is:

J. R. Miller et al., *Trapping of Small Organisms Moving Randomly,*
SpringerBriefs in Ecology, DOI 10.1007/978-3-319-12994-5_6

$$C_T = \left[\frac{T_{den}}{\left(T_{den} + t_{den}\right)} \right] \#\,\text{draws}. \tag{6.2}$$

Transitioning from cards fully back to trapping, the number of draws becomes the number of movers arriving at the set of fully competing traps (arriving *M*), or:

$$C_T = \left[\frac{T_{den}}{\left(T_{den} + t_{den}\right)} \right] \text{arriving } M. \tag{6.3}$$

Since the density of T in this situation is one, Eq. (6.3) reduces to:

$$C_T = \left[\frac{1}{\left(1 + t_{den}\right)} \right] \text{arriving M}. \tag{6.4}$$

We learned in Chap. 5 that only a small fraction (designated T_{fer}) of the total random walkers (designated M_{den}) present in a large trapping area find, get caught in, and are retained by the trap. Under no competition, $C_T = T_{fer} M_{den}$ (Eq. 5.1). The number of movers from the full trapping area that get caught in the focal trap under complete competition becomes:

$$C_T = \left[\frac{1}{\left(1 + t_{den}\right)} \right] T_{fer}\ M_{den}. \tag{6.5}$$

Finally, the brackets identifying P_T per arriving mover can be removed to yield:

$$C_T = \frac{T_{fer}\ M_{den}}{1 + t_{den}}. \tag{6.6}$$

6.3 Test for Whether or Not Competition is Complete

Plotting t_{den} on the *x*-axis vs. $1/C_T$ on the *y*-axis (designated Miller-Gut plot (Miller et al. 2006a,b)) can test whether the trap competition was actually complete. As demonstrated in Fig. 6.1, such graphs generate straight lines whose *x*-intercept is negative 1.0 when competition is complete, indicating that the catch in *T* will be halved by one competing trap (Eq. 6.4). An *x*-intercept of −2.0 (inverse = −0.5) would indicate that each *t* suppressed catch in the focal trap *T* by only half of what would be expected for a fully competing trap. Figure 6.2 offers the mathematical justification for this test of competition completeness and establishes that for a Miller-Gut plot of data from traps competing fully:

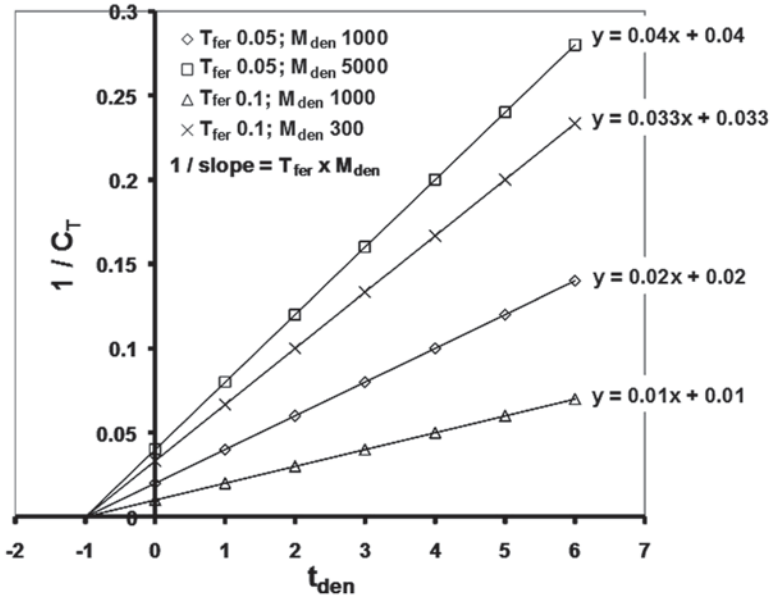

Fig. 6.1 Graphical outputs of Eq. (6.6) for several T_{fer} and M_{den} values when t_{den} is plotted vs. $1/C$, Miller-Gut plot (Miller et al. 2006 a,b). The x-intercept and its inverse return − 1.0 under complete competition

$$\text{Equation (6.6)} \quad C_T = \frac{T_{fer}\, M_{den}}{1 + t_{den}}$$

$$\text{Invert} \quad \frac{1}{C_T} = \frac{1 + t_{den}}{T_{fer}\, M_{den}}$$

$$\text{Distribute} \quad \frac{1}{C_T} = \frac{1}{T_{fer}\, M_{den}} + \frac{t_{den}}{T_{fer}\, M_{den}}$$

$$\text{Reorder} \quad \frac{1}{C_T} = \frac{t_{den}}{T_{fer}\, M_{den}} + \frac{1}{T_{fer}\, M_{den}}$$

$$\text{Format as } y = mx + b \quad \frac{1}{C_T} = \frac{1}{T_{fer}\, M_{den}}\, t_{den} + \frac{1}{T_{fer}\, M_{den}}$$

$$y = m \quad x + b$$

$$\text{x intercept} = -b/m = -\frac{\dfrac{1}{T_{fer}\, M_{den}}}{\dfrac{1}{T_{fer}\, M_{den}}} = -\frac{1}{T_{fer}\, M_{den}} \times \frac{T_{fer}\, M_{den}}{1} = -1$$

$$\frac{1}{\text{x intercept}} = -1$$

Fig. 6.2 Mathematics explaining why the Fig. 6.1 graphs yield straight lines and why the inverse of the x-intercepts must be − 1.0 when competition between T and t is complete

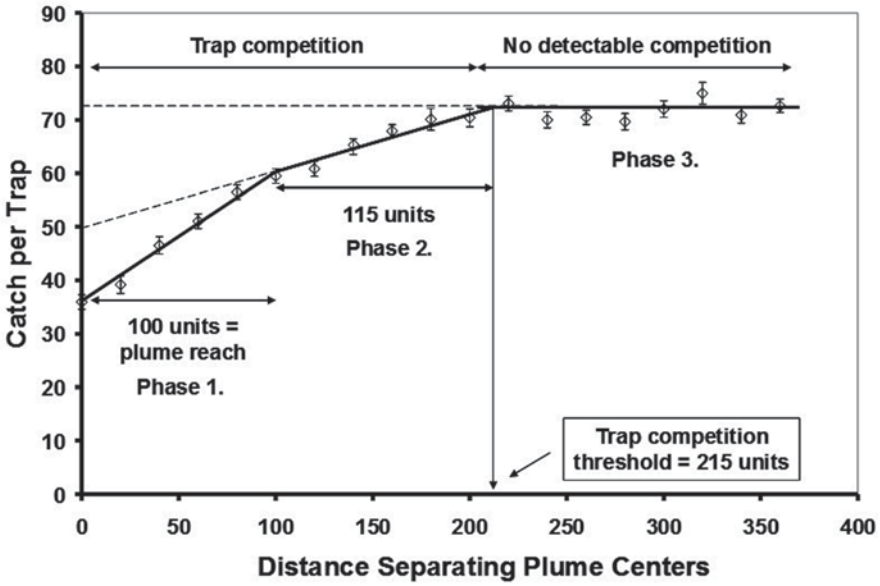

Fig. 6.3 Capture of computer-simulated random walkers as influenced by distance separating two competing traps. Twenty replicates were run for each datum; error bars = S.E.M

$$\text{Slope} = \frac{1}{T_{fer}\, M_{den}}. \tag{6.7}$$

Therefore:

$$M_{den} = \frac{1}{T_{fer}\,\text{Slope}}. \tag{6.8}$$

6.4 Incomplete Competition

Things become a bit more complex when the plumes from competing traps do not overlap completely or at all. For example, a catch of 73 ± 4 (S.E.M.) movers was realized when a trap having an elliptical plume of 100 × 10 units was deployed at the center of a large cyber space containing 5,000 uniformly distributed Weston movers operating with a c.s.d. of 15° and displacing for 1,000 steps of 1 unit. Catch in such a trap was reduced (Fig. 6.3) when two identical traps were deployed closely in this unbounded arena. When the plumes of the two traps were fully superimposed, catch was halved. As the interplume distance increased for two plumes arranged so that their long axes fell on the same straight line, captures in the competing traps increased in two distinct linear phases: 1 and 2 (Fig. 6.3). A steeper rise in catch was recorded over the first 100 units of trap separation (Fig. 6.3, Phase 1), whose

span matched the plume reach. Then, the captures increased in Phase 2 at about half the rate for Phase 1, until no competition was detectable at or beyond 215 units of separation (Phase 3).

The sampling radius for this trap interacting with these movers was measured by releasing (at varying distances) sets of 100 Weston movers in a ring centered on one end of the 100×10 plume and then rendering the capture data as a Miller plot. Figure 6.4b reveals that the trapping radius was ca. 450 units. Thus, our initial hypothesis that the threshold distance for measurable trap competition would match that for trapping radius was falsified. Rather, the radius for detectable trap competition (Fig. 6.3) was less than half of the measured trapping radius.

Understanding the above outcome requires consideration of the behavior of individual movers. The mismatch between measured trapping radius and competition radius suggests that more is required for measurable trap competition beyond the availability of some movers with the capacity to reach one trap or the other, or simply with theoretical capacity to reach both traps. Measurable competition requires a detectable reduction in catch relative to that for a trap operating alone. Thus, no competition would be measured unless Trap 2 captured movers destined to be caught in Trap 1, had Trap 2 not been present, and vice versa. Captures by Trap 2 of movers not catchable by Trap 1 cannot suppress catch of Trap 1, and vice versa. Therefore, realized competition of traps requires not only capacity of some movers to reach both traps, but also certainty that either trap would have caught any mover gone "missing."

The latter stipulation explains why the measurable competition radius proved smaller than the trapping radius. For example, the probability of a visit by a mover originating 300 units from a space that could have been occupied by one plume can be read from Fig. 6.4a as ca. 0.02. Requiring that the same mover, having arrived at this first plume, then visit another plume now 300 units away would likewise be probable at 0.02. Multiplying these individual probabilities gives the combined probability that one mover will visit both Trap 2 and Trap 1, i.e., 0.0004. This probability was apparently too tiny for an actual event to be realized given the sample sizes and power of the Fig. 6.4 experiment where no catches were registered below a probability of 0.001. However, if the distances were reduced to 200 units, the probability of visiting one trap is ca. 0.06 (Fig. 6.2 A) and that for visiting two traps in the same run would have been 0.0036, making the competition detectable in this experiment at 200 but not 300 units of plume separation.

The hypothesis that realized trap competition requires that a given mover would actually have visited the space potentially occupied by both plumes is further supported by the data in Fig. 6.5. In this experiment, individual Fig. 6.3 movers were released equidistantly from two Fig. 6.3 plumes placed at set separation distances onto the computer screen, but where neither of the plumes were endowed with the capacity to arrest movers. The individual tracks ($n = 50$ for each distance) laid down by the simulation program during runs of 1,000 steps were scored for whether the mover visited the areas under both, one, or no plumes. Obtaining a straight line beyond a separation distance of 100 units (plume reach) with an x-intercept (210) very similar to the detectable competition threshold of Fig. 6.3 (215) supports the idea

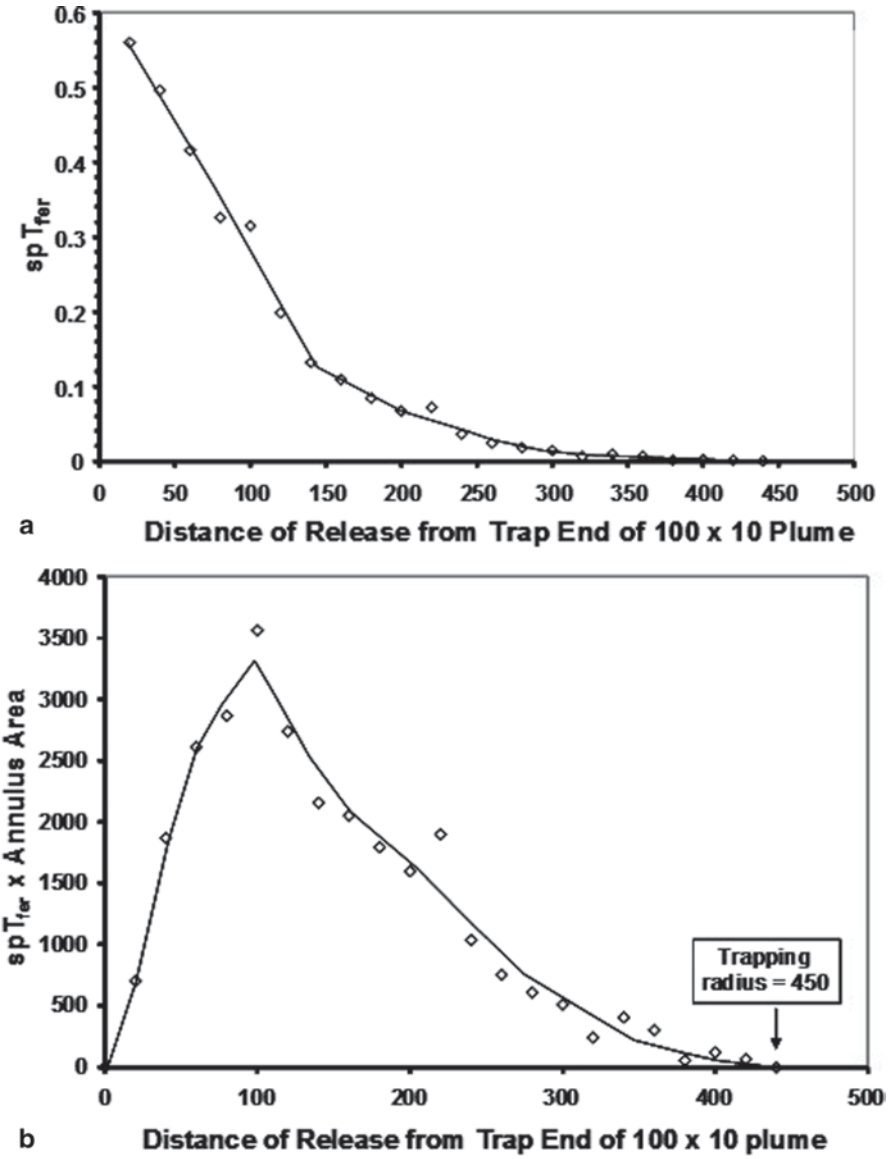

Fig. 6.4 Untransformed **(a)** and Miller plot **(b)** of data for Weston movers having a c.s.d. of 15° and displacing for 1,000 steps of 1.0. These data support a trapping radius of 450 units; and, they returned a T_{fer} value of 0.047 computed as per Chap. 5

that the trap competition measured in Fig. 6.3 resulted only from the events where there was certainty that the plumes from both competing traps would have been contacted had the competitor not been present.

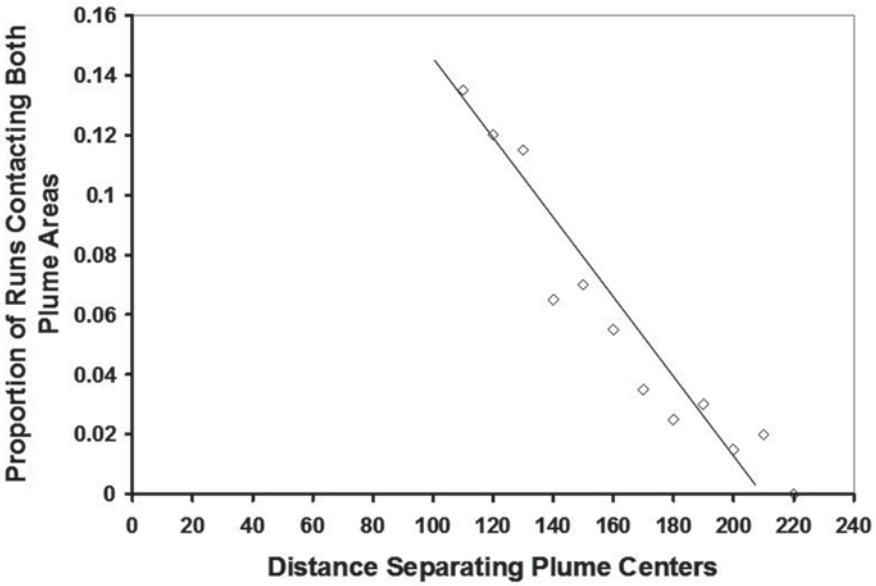

Fig. 6.5 Graph of the proportion of runs Fig. 6.1 movers contacted both competing plumes as a function of plume separation distance. The shape of this profile and its limit of 210 units is a good match to the Phase 2 result of Fig. 6.1

6.5 Trapping Radius Does Not Equate to Competition Threshold

The above result demonstrates that using the competition threshold to estimate trapping radius would badly underestimate the latter and particularly trapping area which increases by πr^2. Rather, trapping radius for biological random walkers can exceed competition radius by a factor of two. This fact was not recognized in previous studies of trap competition (e.g., Wall and Perry 1978, 1980) and will require a revision of some previous measures of trapping radius taken as equivalent to competition radius.

6.6 Equation for Incompletely Competing Traps

We conducted simulation experiments like the following to determine how Eq. (6.6) fitting completely competing traps must be modified to fit data from incompletely competing traps. The conditions were those of the Fig. 6.3 experiment, except that either 1, 2, 3, or 4 trap plumes were deployed singly, one horizontal plume above another (2 traps), three horizontal plumes arranged vertically (3 traps), or as a 2×2 grid (4 traps). Plume centers were spaced 110 units apart. Each trap density was run

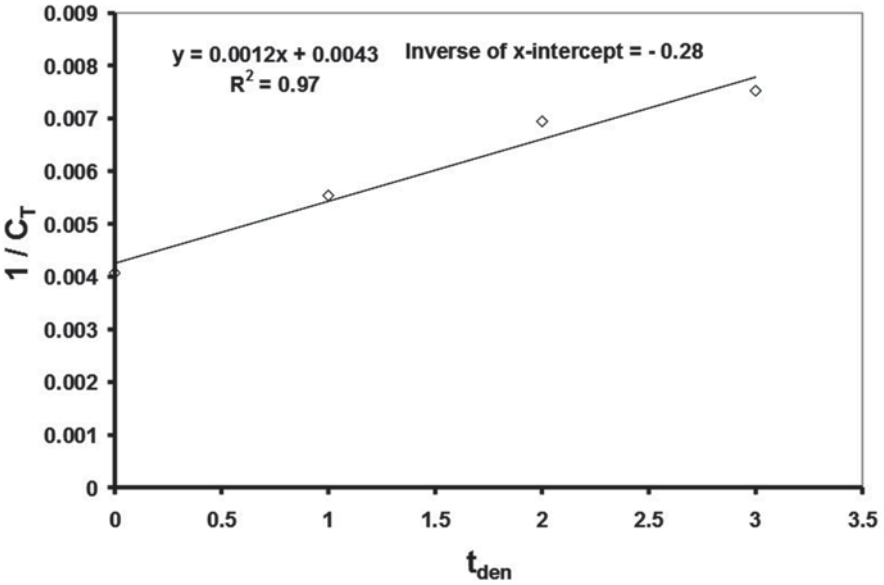

Fig. 6.6 Miller-Gut plot of data for runs of 6,000 steps using 1, 2, 3, and 4 traps where one of these traps was considered the focal trap *T* and the remainder were considered competing traps *t*

for 300, 1,000, 2,000, 3,000, 4,500, and 6,000 steps of 1.0 unit (10 replicates of each condition). We also measured maximum net dispersive distance for each runtime for these Weston movers operating with a c.s.d. of 15° after releasing 300 movers from a point at the edge of the computer screen. Trapping radius and area could then be computed. Numbers of randomly seeded movers per trapping area were then counted for computations of T_{fer} for each run time. Results of a typical run are shown in Fig. 6.6. All such plots yielded straight lines suggesting that the equation fitting incomplete competition had a form similar to that of Eq. (6.6), as explained in Fig. 6.2. The inverse of all *x*-intercepts was well less than −1.0, as expected, when traps experienced no plume overlaps. For example, the absolute value of the inverse of the *x*-intercept for Fig. 6.6 was 0.28, indicating that the level of competition per *t* was only 28% of that for a completely overlapping trap. It became evident by inspection that Eq. (6.6) needed only the below modification to fit these data for incomplete trap competition:

$$C_T = \frac{T_{fer} M_{den}}{1 + \frac{1}{x - \text{int}} t_{den}}. \tag{6.9}$$

Nevertheless, a mechanistic explanation for this relationship was desired—what phenomenon did an inverse of *x*-intercept value like 0.28 from Fig. 6.6 actually represent? One approach to this puzzle was exploration of how the inverse of *x*-intercept varied with duration of trapping runs. As shown in Fig. 6.7a, the inverse of *x*-intercept rose according to the number of steps raised to the power of 0.74.

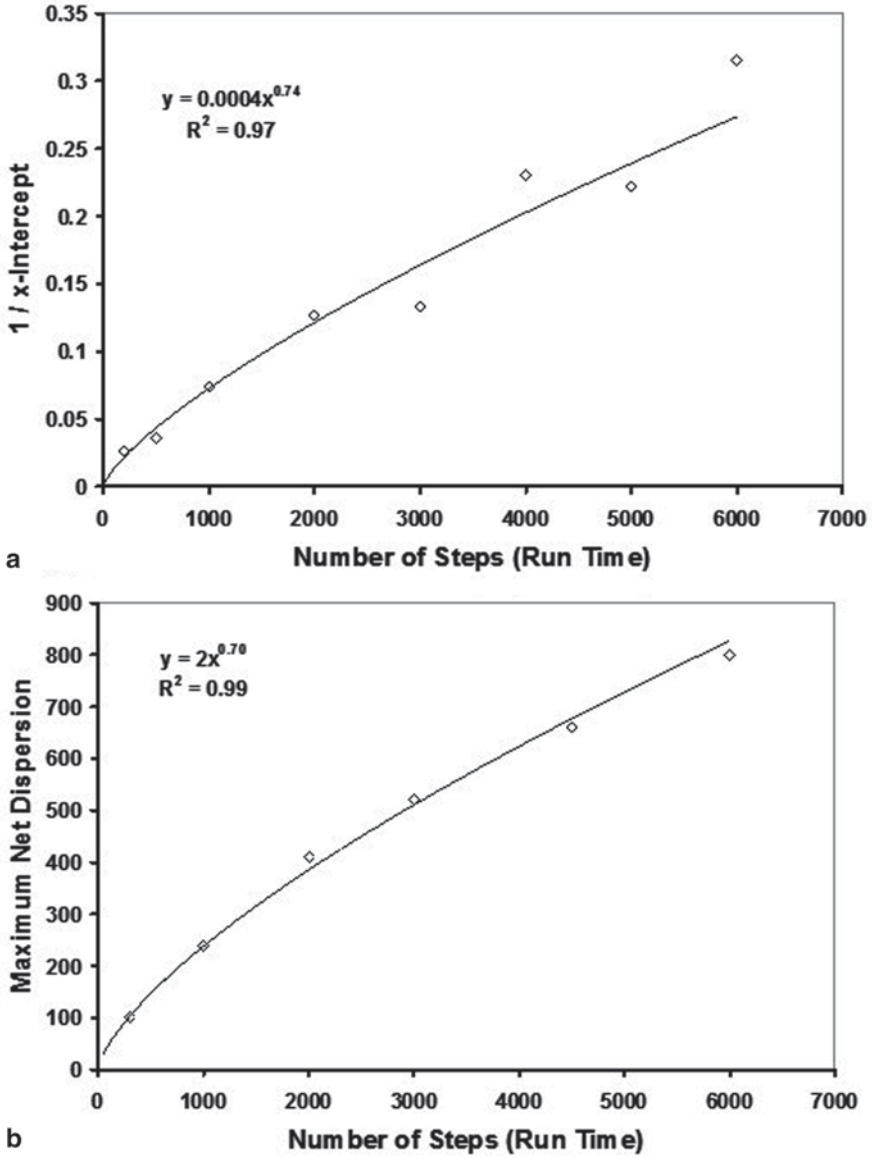

Fig. 6.7 Demonstration using Fig. 6.3 movers and plumes that the inverse of *x*-intercept. **(a)** Maximum net displacement of movers. **(b)** Both rise with the number of steps raised to the 0.7 power

In light of Fig. 3.4, such an outcome suggested that the inverse of *x*-intercept was closely tied to the maximum net dispersion of movers; this match was confirmed in Fig. 6.7b and solidified by Fig. 6.8.

Based on the findings of Chap. 5, we reasoned that the parameter likely to vary most dramatically (at least initially) with run time of a trapping experiment was T_{fer}.

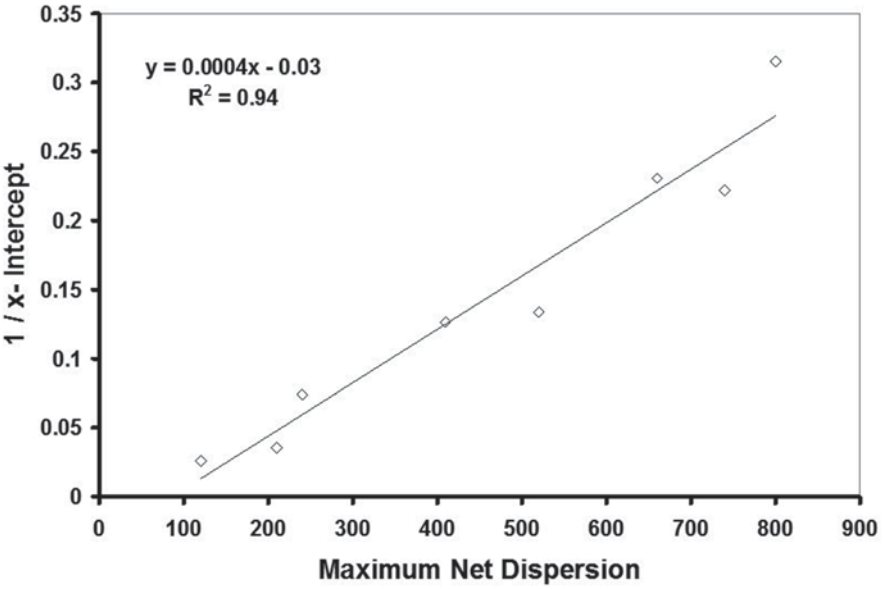

Fig. 6.8 Proof that the inverse of *x*-intercept was well correlated with maximum net displacement of movers

For the current experimental conditions, T_{fer} initially dropped precipitously with increasing run time (Fig. 6.9a) and then stabilized upon approaching 0.05. A graph of $1/T_{fer}$ vs. run time (Fig. 6.9b) bore a striking resemblance to Fig. 6.7a and returned an exponent of 0.70 that we take as matching the exponent of 0.74 for 1/*x*-intercept vs. run time (Fig. 6.7a). This match led to the hypothesis that:

$$\frac{1}{x-\text{intercept}} = \frac{\text{unknown parameter}}{T_{fer}}. \tag{6.10}$$

We then sought to identify an unknown parameter whose numerical value might provide hints for a mechanism leading to the above quantitative relationships. To this end, the expression *unknown parameter*/T_{fer} was substituted for *1/x-intercept* in Eq. (6.9) and then solved for after plugging in all other terms, each known from experimental measurements detailed above. The solution returned for *unknown parameter* for all run times with *t* densities > 0 turned out to be a value close to 0.02. Further inspection of this data set revealed that the product of 0.02 × M_{den} for the trapping area associated with each respective run time nearly matched the difference between catch in a trap under no competition and catch under competition from one *t*. We concluded that this *unknown parameter* (hereafter designated P_t) is the proportion of all movers populating a trapping area that will be captured per competing trap *t* that otherwise would have appeared as part of the catch in the focal trap *T*. The inverse of the *x*-intercept for a Miller-Gut plot can then be taken as:

$$\frac{1}{x-\text{intercept}} = \frac{P_t}{T_{fer}}. \tag{6.11}$$

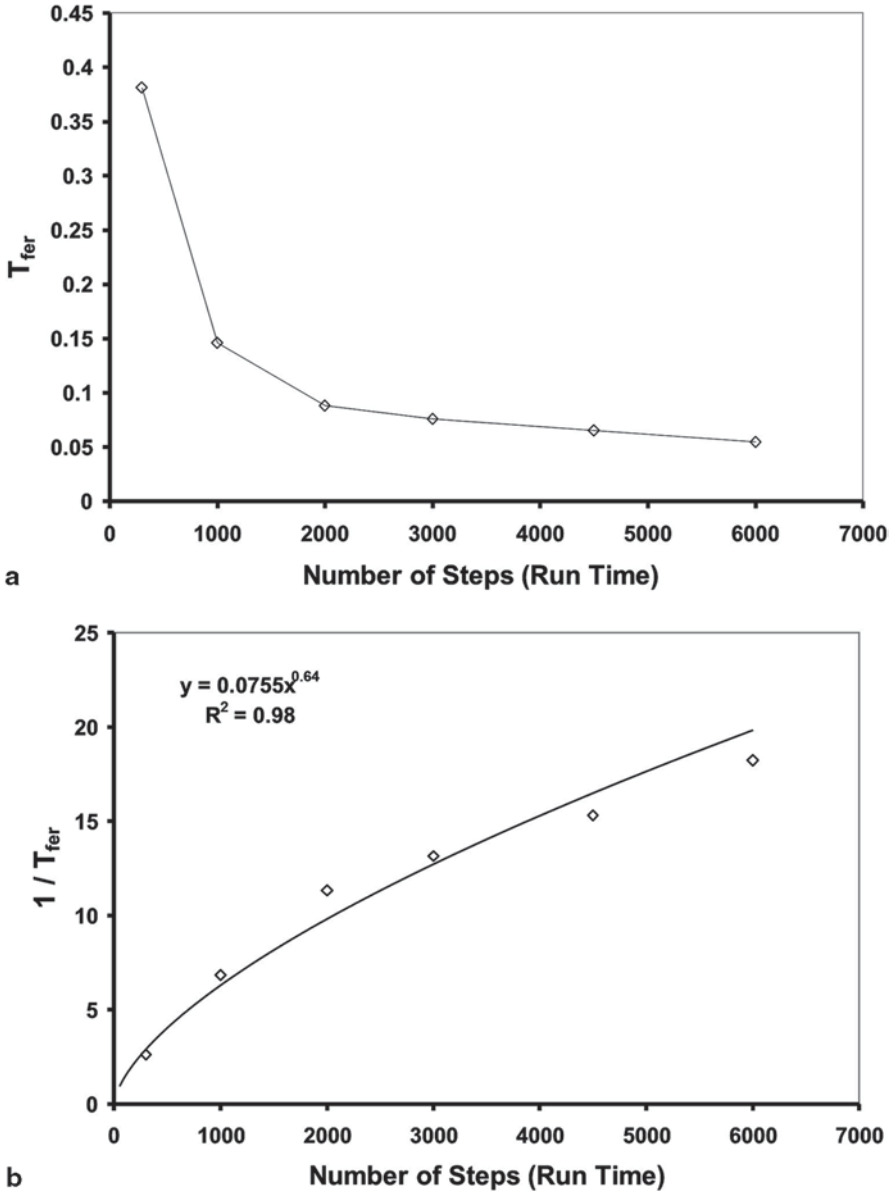

Fig. 6.9 T_{fer} (**a**) and $1/T_{fer}$ (**b**) as a function of run time for Weston movers with a c.s.d. of 15° and a trap having elliptical plume dimensions of 100 × 10 computer units

The number of movers approaching T from the trapping area is given by:

$$\text{Movers approaching } T \;=\; T_{fer} \times M_{den} \tag{6.12}$$

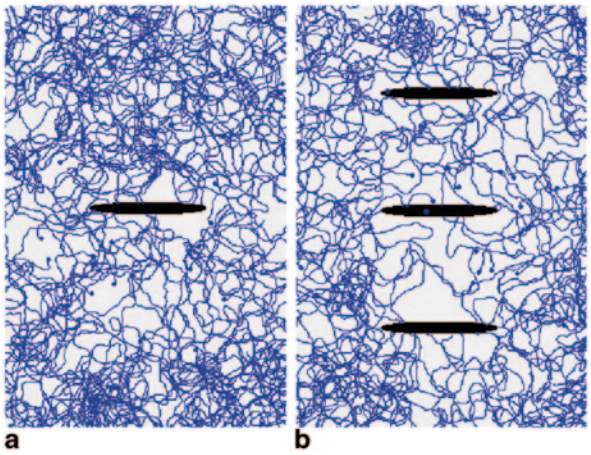

Fig. 6.10 Tracks of Weston movers displacing for 1,000 steps of 1.0 with c.s.d. 15° in the vicinity of a trap under no competition (**a**) and when competing incompletely (**b**). The *small solid circles* indicate the starting points for randomly seeded movers. Any intersection of a track with the *dark elliptical plume* yielded a capture. Note that captures were fewer on the sides of plumes that were shielded from incoming movers by a competing trap. The shielding effect of each trap operating under these given conditions reduced catch in a focal trap by about 20% on average and yielded a P_t value of 0.017

and the number of approaching movers pilfered by t is given by:

$$\text{Approaching movers pilfered} = P_t \times M_{den}. \tag{6.13}$$

It follows that:

$$\frac{\text{approaching movers pilfered}}{\text{movers approaching } T} = \frac{P_t \times M_{den}}{T_{Fer} \times M_{den}} = \frac{P_t}{T_{fer}} = \frac{1}{x\text{-intercept}}. \tag{6.14}$$

Here, then is the first-principles explanation for the inverse of x-intercept: it is the proportion of movers incoming to T that are intercepted and pilfered by one t. Deploying competing traps near the focal trap screens T from some but not all approaching movers (Fig. 6.10). Packing additional competing traps around the central T of Fig. 6.10 translates into more movers pilfered. However, the inverse of x-intercept quantifies the proportion of movers incoming to T that are pilfered per t. Values for P_t shifted only from 0.017 to 0.023 across simulation runs of duration 200–5,000 steps.

Now an equation fitting incompletely competing traps can be offered with terms precisely defined. When: T = one focal trap; t = a trap placed close by so as to compete with T; M_{den} = number of entities per trapping area; T_{fer} = proportion of all movers in a trapping area caught by T when under no competition; P_t = proportion of all movers in the trapping area caught by t while on their way to T and that otherwise

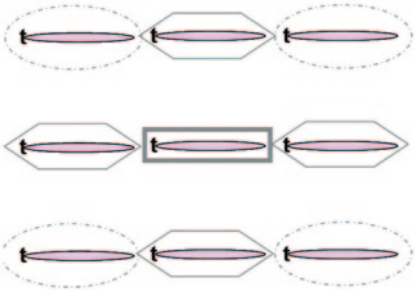

Fig. 6.11 One suggested array of incompletely competing traps that could serve to simultaneously estimate trapping area and M_{den} via Eq. (6.13). The level of competition as influenced by trap position (corner, mid-edge, and center) is suggested by the boldness of each respective imaginary symbol drawn around the elongated elliptical plumes emanating from each competing trap *t*

would have been caught by *T*; and C_T = cumulative catch in the focal trap *T* per trapping interval; then:

$$C_T = \frac{T_{fer} \times M_{den}}{1 + \frac{P_t}{T_{fer}} t_{den}}. \tag{6.15}$$

Equation (6.15) can be viewed as the general equation for all trap competitions; Eq. (6.6) for complete competition becomes a special case where $P_t = T_{fer}$ and P_t / T_{fer} thus becomes invisible because it is 1.0.

6.7 Estimating Mover Numbers and Trapping Area Simultaneously by Competitive Trapping

A central goal of this book is development of quick, inexpensive, but valid methodologies for accurately estimating absolute density of random walkers from trapping data. A possible limitation of the methods outlined in Chap. 5 is that the experimental conditions extant for a particular trapping run might not always match those in effect when T_{fer} and trapping area were established using the single-trap, multiple-release technique. For example, inclement weather might truncate animal activity to yield a smaller than expected trapping area and a larger than expected T_{fer}. The resulting M_{den} estimate would then be falsely low. The ideal situation would be to obtain a measure of trapping area and T_{fer} concurrently while collecting a catch number from which the M_{den} would be calculated.

Equation (6.15) could be the gateway to such procedures. We suggest that a small array of traps (e.g., Fig. 6.11) could be deployed simultaneously to compete incompletely at multiple strengths of competition. If an appropriate t_{den} value could be assigned to the strengths of competition for respective trap positions in the grid,

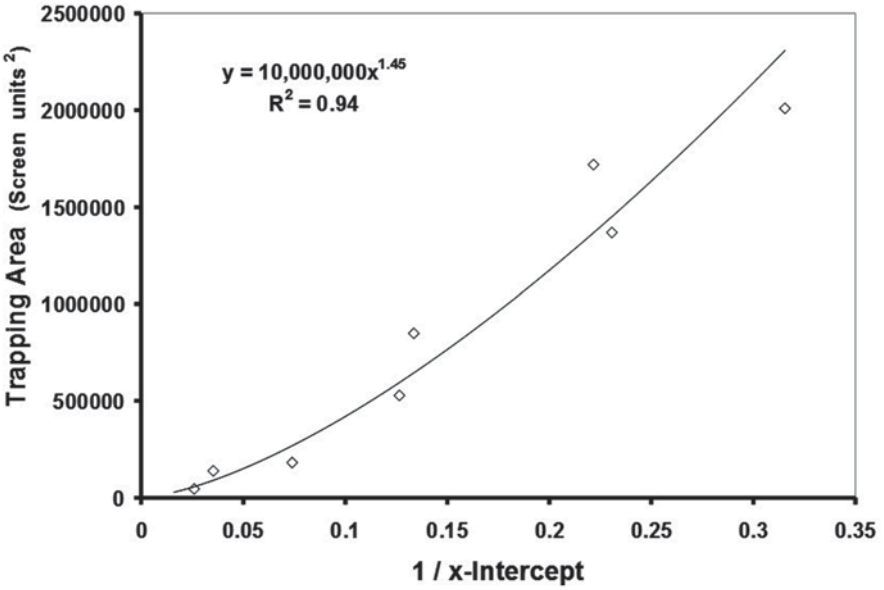

Fig. 6.12 Demonstration that values for trapping area recorded in the experiment of Fig. 6.7 correlate well with 1/*x*-intercept

those values plotted on the *x*-axis against $1/C_T$ on the *y*-axis will yield a straight line and an *x*-intercept, the magnitude of whose inverse would be pivotal to assigning a trapping area. As demonstrated in Fig. 6.7a, values for 1/*x*-intercept can serve as proxy for elapsed time of the trapping run. In that experiment, values of 0.05 vs. 0.3 for 1/*x*-intercept indicate very short and long trapping runs, respectively. Thus, 1/*x*-intercept can function as a clock for trapping runs. Importantly, this clock operates independently of M_{den}. The inverse of *x*-intercept correlates well with trapping area as demonstrated in Fig. 6.12. After such experimental calibrations, an experimenter would be able to calculate trapping area via a regression equation like that of Fig. 6.12, but unique to the given set of plume and mover characteristics.

The T_{fer} value for a given competitive-trapping experiment can be obtained when the relationship between *x*-intercept and T_{fer} has been calibrated as in Fig. 6.13 for the Fig. 6.7 experiment using 100×10 plumes. Once T_{fer} and trapping area are estimated for a competitive trapping run, M_{den} can be found by using Eq. (6.18) or (6.19) offered in Fig. 6.14 showing equations derivable from Eq. (6.13) and its graphical outputs. We anticipate that the competitive-trapping method of estimating M_{den} will prove more robust than always relying on Eq. 5.1 and an historically established estimate of trapping area and T_{fer}.

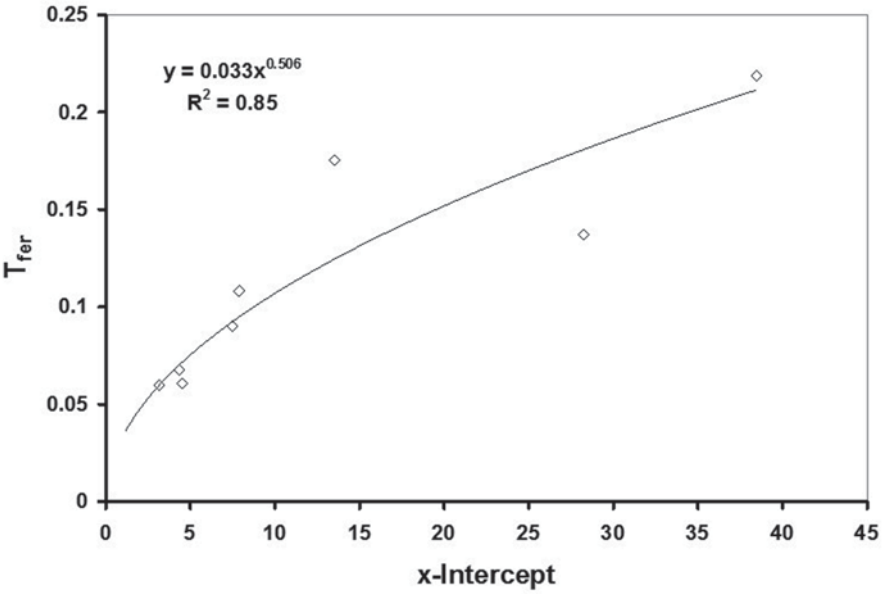

Fig. 6.13 Demonstration that T_{fer} is well correlated with the x-intercept of a plot of t_{den} on the x-axis vs. $1/C_T$ on the y-axis

Equation (6.15) $$C_T = \frac{T_{fer} M_{den}}{1 + \frac{pt}{T_{fer}} t_{den}}$$

Invert $$\frac{1}{C_T} = \frac{1 + \frac{pt}{T_{fer}} t_{den}}{T_{fer} M_{den}}$$

Distribute $$\frac{1}{C_T} = \frac{1}{T_{fer} M_{den}} + \frac{\frac{pt}{T_{fer}} t_{den}}{T_{fer} M_{den}}$$

Reorder $$\frac{1}{C_T} = \frac{\frac{pt}{T_{fer}} t_{den}}{T_{fer} M_{den}} + \frac{1}{T_{fer} M_{den}}$$

Simplify $$\frac{1}{C_T} = \frac{pt}{T_{fer}^2 M_{den}} t_{den} + \frac{1}{T_{fer} M_{den}}$$ Equation (6.16)

$y = m x + b$

Substitute 1/x-int for pt/T_{fer} in Equation (6.16) $$\frac{1}{C_T} = \frac{1}{\text{x-int } T_{fer} M_{den}} t_{den} + \frac{1}{T_{fer} M_{den}}$$ Equation (6.17)

Slope = 1 / (x-int T_{fer} M_{den})

M_{den} = 1 / (slope T_{fer} x-int) Equation (6.18)

y-int = 1 / (T_{fer} M_{den})

M_{den} = 1 / (y-int T_{fer}) Equation (6.19)

Fig. 6.14 Equations derivable from Eq. (6.15) enabling calculation of M_{den} from experimental data once x-intercept, T_{fer} is measured, and trapping area are estimated

6.8 Computer Simulations Demonstrating How Absolute Density of Biological Random Walkers Can Be Estimated by Competitive Trapping under Variable Run Times

This example builds upon the foundation laid thus far in this chapter for traps having 100 × 10 elliptical plumes and movers taking steps of 1.0 while executing a 15° c.s.d. The competing-trap array utilized was the 3 × 3 grid of Fig. 6.11 under a trap spacing of 110 units. The last piece of groundwork needed is calibration of the appropriate t_{den} value to assign to traps at the corner, mid-edge, and center of the array (Fig. 6.11) such that t_{den} values to be plotted on the x-axis occurred in increments of one t against $1/C_T$. To this end, mean captures in corner, mid-edge, and center traps were recorded after 6,000 steps for 10 replicate runs of the 3 × 3 grid of traps deployed in a field of 5,000 randomly seeded Weston movers as above. Then, the regression equation of Fig. 6.6 was used to solve for the t_{den} corresponding to the catch recorded for each trap position. The corner, mid-edge, and center traps returned t_{den} values of 3.3, 8.2, and 20.9, respectively. A t_{den} value of about 3 is understandable for a corner trap, because two competing traps lie at right angles and a third occurs diagonally between these two competitors. However, as additional competing traps were added into the array their competitive effect became more than additive. For example, a mid-edge trap in a 3 × 3 array is surrounded by only five competing traps, yet the t_{den} value for this configuration was slightly above 8. A center trap is surrounded by eight competing traps and returned a t_{den} value of over 20. As competing traps increasingly surround a focal trap, they apparently interact to choke off an increasing proportion of the overall access to the focal trap. But, once understood and accounted for, this lack of linearity is no impediment to competitive trapping.

With this background information in place, we randomly seeded various densities of movers into an unbounded cyberspace and determined M_{den} after various run times between 300 and 6,000 steps. The steps of this analysis were:

1. For a given run using a 3 × 3 trapping grid, record the mean catch for corner traps, mid-edge traps, as well as the single value for the central trap.
2. Plot the inverse of catch on the y-axis against the t_{den} values of 3.3, 8.2, and 20.9 for corner, mid-edge, and center traps, respectively.
3. Compute the x-intercept for the graph by dividing the y-intercept by the slope.
4. Compute 1/x-intercept.
5. Use the regression equation of Fig. 6.12 to compute trapping area.
6. Use the regression equation of Fig. 6.13 to compute T_{fer}.
7. Use Eq. 6.18 to compute M per trapping area.
8. Scale all outcomes to a common area (one computer screen) to facilitate comparisons.

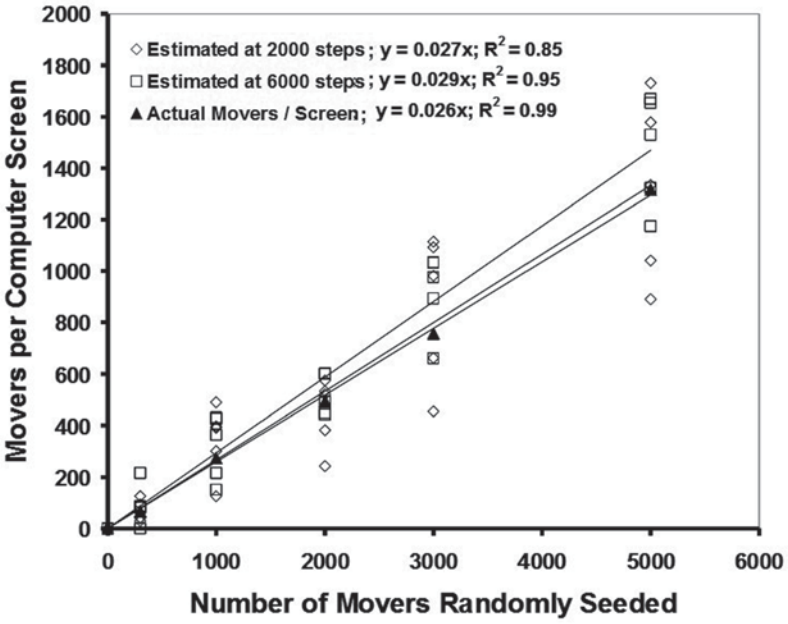

Fig. 6.15 Results from computer simulations estimating M_{den} of Weston movers (using a c.s.d. of 15˚ and steps of 1.0 unit) via competitive trapping using a 3×3 trapping grid and plumes of 100×10 units. Each datum is the outcome from a single run of designated duration for the indicated seeding density. Five valid replicate runs are shown for each condition

Estimated M_{den} values for both short (2,000 steps) and long (6,000 steps) run times proved to be linearly related to the actual values (Fig. 6.15). Precision was a bit better for longer vs. shorter run time, as evidenced by values for shorter runs usually bracketing those for longer runs for a given seeded M_{den} (Fig. 6.15). Encouragingly, precision and accuracy of the method did not rapidly degrade under low numbers of randomly seeded movers. However, evidence for a lower limit to the utility of this method was noted. Zero catch was recorded for the center trap in three of ten instances when the number of seeded movers was 1,000 or less. This meant that the analysis could proceed only using the data for corner and mid-edge traps, which was not a problem. However, in 4 out of the 50 determinations comprising Fig. 6.15, nonsense values resulted primarily for the lowest mover densities, usually because the *x*-intercept returned a positive rather than a negative value. In one case, the slope of the Miller-Gut plot was negative rather than positive. Such outcomes are not unexpected when the catch numbers for corner traps fall to less than ten per trap. Nonsense values were easy to identify among a majority of reliable values. Overall, this method shows real potential. Indeed, the potential problem of unknown run time effects can be overcome by competitive trapping.

6.9 Suggested Plan for Employing Competitive Trapping Under Field Conditions

Although now recommended for basic research studies, it is unlikely that growers could afford to deploy nine traps as per Fig. 6.11 to estimate pest density at one given location. Instead, we recommend that growers deploy their monitoring traps singly or in small multiples to increase accuracy by increasing overall plume reach as explained in Chap. 5. Rather than relying only on historically established estimates of trapping area and T_{fer} to derive M_{den}, we envision that a few competitive trapping tests could be ongoing under the care of extension personnel responsible for a growing region. Growers could use the historical values to compute M_{den} from their catch numbers as per Chap. 5 unless alerted to more appropriate real-time estimates arising from the ongoing and rapidly shared competitive-trapping assays for the region.

6.10 Summary

This chapter has established that, although the outcomes of trap competition can be somewhat counter-intuitive, their kinetics can be captured in a few relatively simple equations. This knowledge provided an opportunity for the development of competitive trapping, a novel method for computing M_{den} from capture data that is unencumbered by unknown time of the trapping run. Competitive trapping can be accomplished only after the following background information has been laid for a given pest and trapping system: (1) plume reach must be estimated via results from a single-trap, multiple-release experiment (as per Chap. 5); (2) the c.s.d. for the given pest should be estimated (upcoming in Chap. 7), and if this is not possible, c.s.d. can be reasonably guessed at approximately 15–20° (Chap. 5); (3) computer simulations of trapping under various run times would be conducted as demonstrated in this chapter so as to establish the quantitative relationships among x-intercept, trapping area, and T_{fer}; (4) the relationships arising from step 3 would be tested by further computer simulations to ascertain precision and accuracy of M_{den} determinations from a trapping grid; and (5) the simulation results would be corroborated by actual field tests using the given pest. The authors were recently funded by the U.S. National Science Foundation to accomplish this step for codling moths.

Chapter 7
Experimental Method for Indirect Estimation of c.s.d. for Random Walkers via a Trapping Grid

7.1 The Idea

The research of Chap. 6 with grids of traps suggested a means for experimental measurement of the circular standard deviation (c.s.d.) being used by random-walkers before they encounter the plume from a trap. For example, the c.s.d. of a population of movers released at one point outside of a regular grid of traps might be obtained via analysis of the pattern in resultant catch across the array. Figure 7.1 shows one such trap configuration we explored in some depth for that purpose. As demonstrated in Fig. 7.2, movers executing a small c.s.d. populate edge traps more evenly and penetrate the grid more deeply than those using a large c.s.d.

The next step was converting capture data from across the grid into an objective dependent variable for constructing a standard curve for c.s.d. such that it could be back-calculated once the dependent variable was measured experimentally. This was not difficult. It required use of only the data for the traps labeled 1–5 in Fig. 7.3a. Catch for traps in a given position was first normalized (this step optional) to catch in Trap 1—the corner trap nearest the release point for 100 movers. Plots of mean catch for a given trap position against a trap position number on the *x*-axis (Fig. 7.3b) proved a better fit to an exponential curve than any other model examined. Conveniently, the magnitude of the decay constant returned for graphical plots resulting from a given combination of plume reach, plume spacing, mover population, and run time for the simulation proved to be linearly correlated with c.s.d. (Fig. 7.4) to generate a useful standard curve with no need for transformations.

J. R. Miller et al., *Trapping of Small Organisms Moving Randomly,*
SpringerBriefs in Ecology, DOI 10.1007/978-3-319-12994-5_7

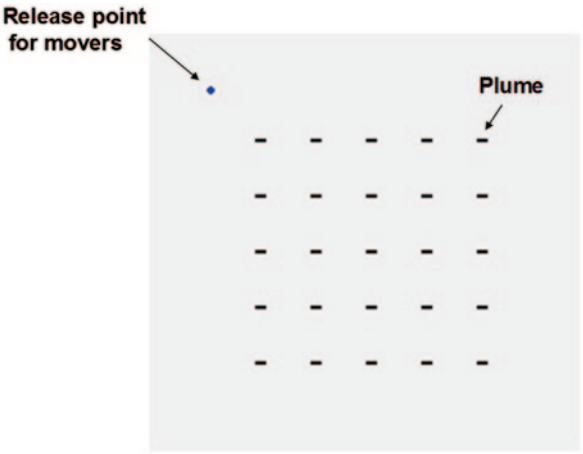

Fig. 7.1 One of various possible configurations of traps explored for potential to estimate random-walker c.s.d. via the resultant pattern in catch across an array of traps

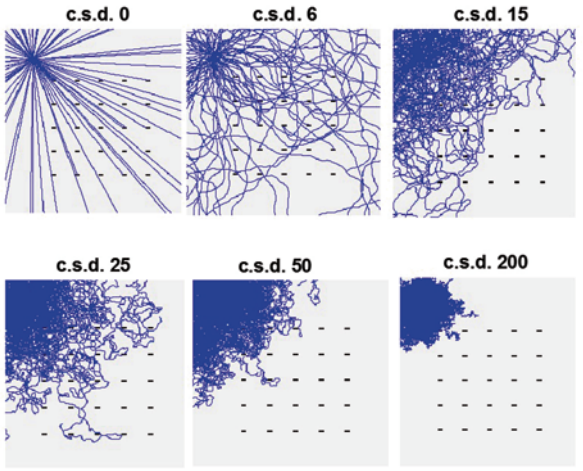

Fig. 7.2 Visual demonstration of differences in penetration of a 5 × 5 grid of traps by 100 Weston movers displacing for 1,000 steps of 1 unit while executing various c.s.d. values. The setup and release point was that of Fig. 7.1. Plume reach was only 5 units so as to mimic that for codling moth and intertrap distance was 30 units

7.2 Translation of the Idea to Field Tests with Real Organisms

We suggest that this trapping-grid approach could be used by field researchers to estimate the c.s.d. for real biological random walkers. The plume reach and maximum dispersive radius must first be estimated for a given organism using the single-trap, multiple-release, and associated techniques of Chap. 5. Spacing of traps in a 5 × 5 grid would then be set to at 1.5 times plume reach so that the standard curves of Fig. 7.4 can be utilized. The elapsed time for the trapping run would be kept short to capture mainly the initial flux of movers through the grid. The techniques of Fig. 7.3 would be used to obtain the decay constant from the trapping outcomes.

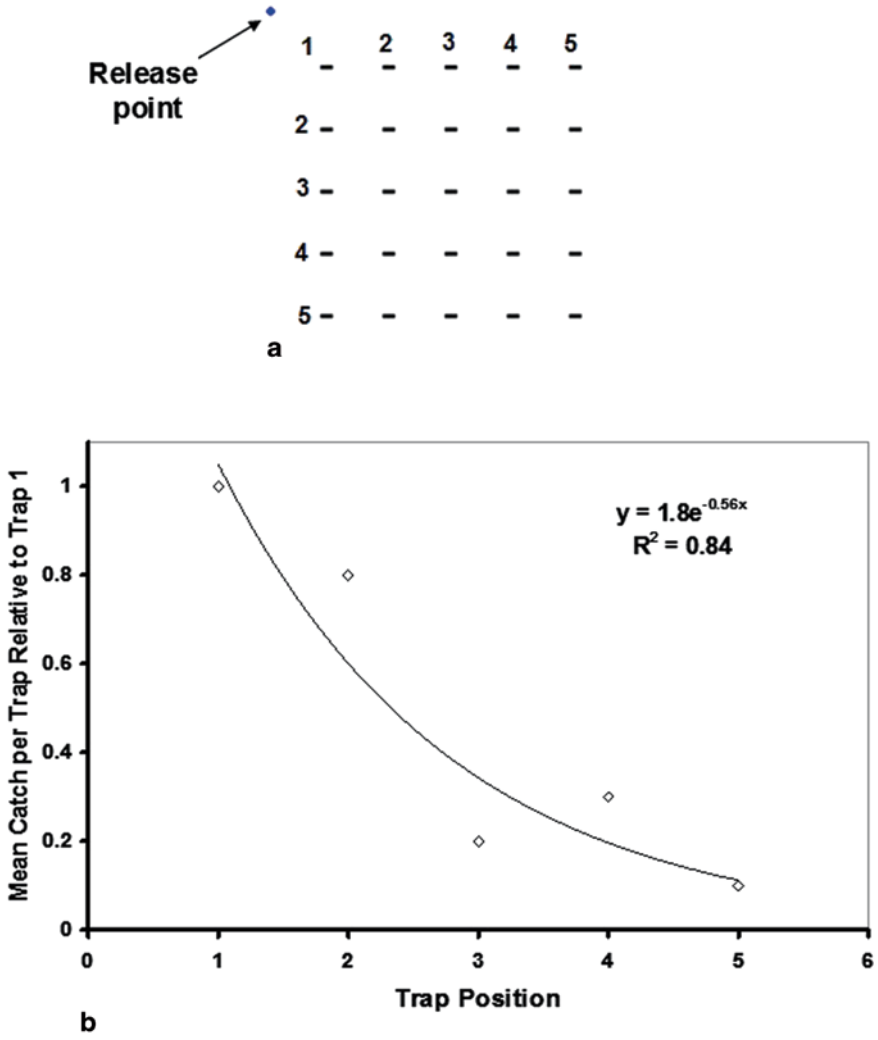

Fig. 7.3 **(a)** Numbering system for positions of traps whose capture data were analyzed to produce a dependent variable well-correlated with c.s.d. **(b)** Plot of capture results 1,000 steps after a *single* corner release of 100 Weston movers taking steps of 1.0 unit and operating with a c.s.d. of 10°. The negative exponent in the regression equation above (*decay constant*) served as a suitable measure for generating a standard curve for back-calculating c.s.d. from experimental data

Finally, the standard curves of Fig. 7.4 having the appropriate plume reach would be used to translate decay constant into a measure of c.s.d. At least five replicate runs of such an experiment would be required to produce error bars as tight as those of Fig. 7.4. If sufficient numbers of test organisms are available, simultaneous re-

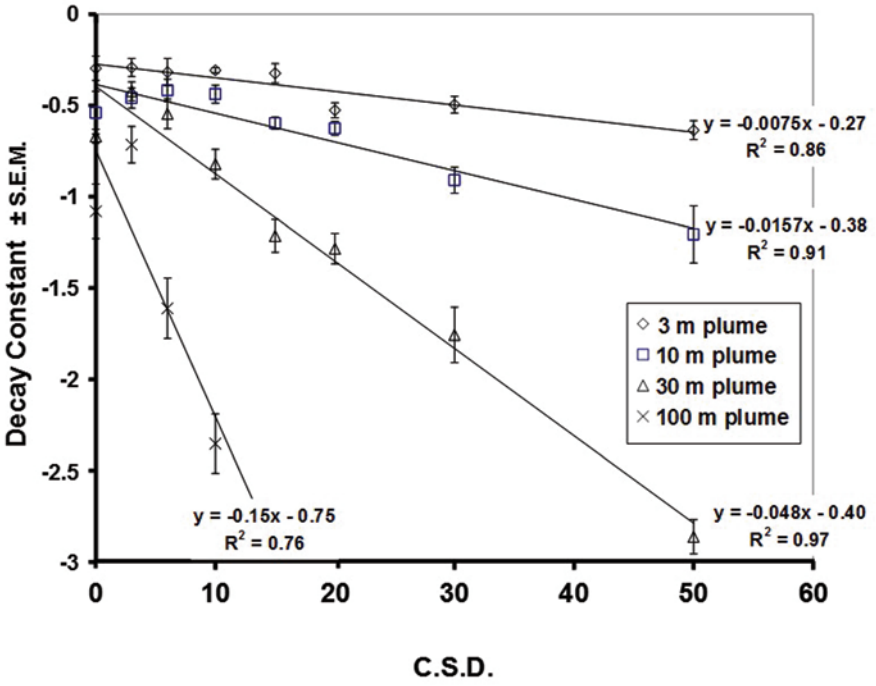

Fig. 7.4 Standard curves for c.s.d. determinations when elapsed time for the trapping simulations was short (1,000 *steps*) and trap spacing in a 5 × 5 grid was 1.5 times the plume length. The decay constants came from the exponents of regression equations like that shown in Fig. 7.3. Error bars reveal S.E.M. values when $n = 5$ for each treatment combination. Additional simulations established that the slopes of graphs for the respective plume reaches diminished slightly as run times increased and movers had appreciable time to double back upon the trapping grid. For this reason, such experiments should be brief

leases bearing distinctive marks could be made at all four corners of the grid both to improve statistical power and to assess whether there was any directional effects during the trapping run.

We believe this approach has the potential to reveal important data on c.s.d. never previously harvested because of the difficulty in directly observing small foraging animals, some of which fly at night. An experiment currently underway with codling moth in Michigan apple orchards using the 5 × 5 array of traps on a 15 m spacing has revealed that the relationship between catch and distance of release is indeed a negative exponential. It also suggests that this insect forages with a c.s.d. of ca. 30–40°, which is somewhat above the theoretical optimum for a resource with a plume having an average reach of less than 10 m (Chap. 5). Perhaps being forced to fly around the many obstructions offered by the branches and foliage of apple trees elevates the realized c.s.d. over the theoretical value measured by our computer simulations under no obstructions.

Chapter 8
Trapping to Achieve Pest Control Directly

8.1 The Idea

As noted in Chap. 2, traps are sometimes explored as instruments to reduce pest populations to tolerable levels without additional control measures. In the field of entomology, this tactic goes by various names (Knipling 1979; El-Sayed et al. 2006), e.g., mass trapping (the term we will use); trap out; and trap-and-remove. Such insect traps are usually baited with an attractant to improve their findability, but some like an electrically charged bug-zapper operate without bait. The core idea is to quickly remove the pest from the environment where it has appeared and begun causing damage by e.g., feeding, inoculating a host with a disease agent, or mating and producing damaging progeny. The lure-and-kill approach operates similarly (El-Sayed et al. 2006); however, the pest is enticed to carry away a lethal dose of poison without requiring capture in a trap per se. Nevertheless, the dynamics of such a system match those of mass trapping.

8.2 Time-Dependency and Dynamics of Mass Trapping

Crop damage is influenced by the time a pest interacts with its environment (Miller and Cowles 1990); or:

$$\mathbf{Damage} \propto \mathbf{Pest}_{\mathbf{den}} \times \mathbf{Time} \tag{8.1}$$

It follows that equivalent damage can be done by few pests active for a prolonged time or many pests active briefly. Thus, the speed with which pests are removed matters for pest control. Pesticides usually act very quickly and kill a high proportion of all individuals in the system. The elapsed time the few survivors are active after treatment typically becomes inconsequential for conventional pesticides. Their

J. R. Miller et al., *Trapping of Small Organisms Moving Randomly,*
SpringerBriefs in Ecology, DOI 10.1007/978-3-319-12994-5_8

efficacy is then said to be pest-density-independent, which is a highly desirable trait for any control tactic. However, behavioral controls usually require time to take effect. Byers (1993) conducted pioneering research on the dynamics of mass trapping using computer simulations similar to the Weston simulations featured in this book. As first documented by Byers and redemonstrated in Fig. 8.1 for our Weston movers, the proportion of simulated movers removed by a trap deployed for a constant time in a closed arena representing a crop field from which they do not depart is independent of M_{den}; thus, the proportion of individuals removed by a trap is pest-density-independent. However, the time required for a trap to lower the pest density to a level that would be nondamaging rises with M_{den} (Byers 1993; and Fig. 8.2). As seen in Fig. 8.3, the level of interaction of pest and crop, and thus damage shown by amount of coloration per panel, rises nearly linearly with pest abundance. It follows that control by mass trapping or other similar behavioral tactics requiring appreciable time to take effect becomes pest-density-dependent once elapsed time to remove the pests is considered in addition to the proportion of the population removed.

It has long been understood (e.g., Knipling 1979) that behavioral control tactics, such as mass trapping or mating disruption using sex attractant pheromones (Thacker 2002), are best-suited for suppressing the growth of pest populations once they are already reduced by a pest-density-independent means like a pesticide. Moreover, some authors (El-Sayed et al. 2006) suggest that mass trapping and mating disruption are well-suited for eradicating low-density pest populations because their efficacy increases as pest density approaches zero.

8.3 Damage Suppression as Influenced by Trap Number and Spacing: Simulations

As a starting point for exploring how best to deploy traps for direct pest control, we used computer simulations to quantify what impact a single trap can have on damage when deployed in a crop under high pest pressure. For this heuristic exercise, satisfactory control was arbitrarily taken as a reduction in cumulative track density to the level equal to or less than the track density seen in the Fig. 8.3 panel for 16 movers. As shown in Fig. 8.4, where the panel for one trap should be compared to the panel for zero traps, a single trap under high pest density provided no control, as evidenced by only a few flecks of white around the trap and no noticeable diminution in the intensity of blue throughout the arena. The single trap removed only 3% of the movers from the overall population and the area around it was continuously inundated by movers from all directions. Such a result is consistent with the experience of some homeowners who use Japanese beetle traps baited with sex pheromone and floral odors (Potter and Held 2002) in an attempt to protect their landscape plantings. Although these traps may capture hundreds or sometimes thousands of beetles, it is difficult to show that they actually protect nearby plants. Some authors warn that use of the Japanese beetle trap may actually increase damage by attracting more insects than are caught. Clearly, deploying a single trap into a space

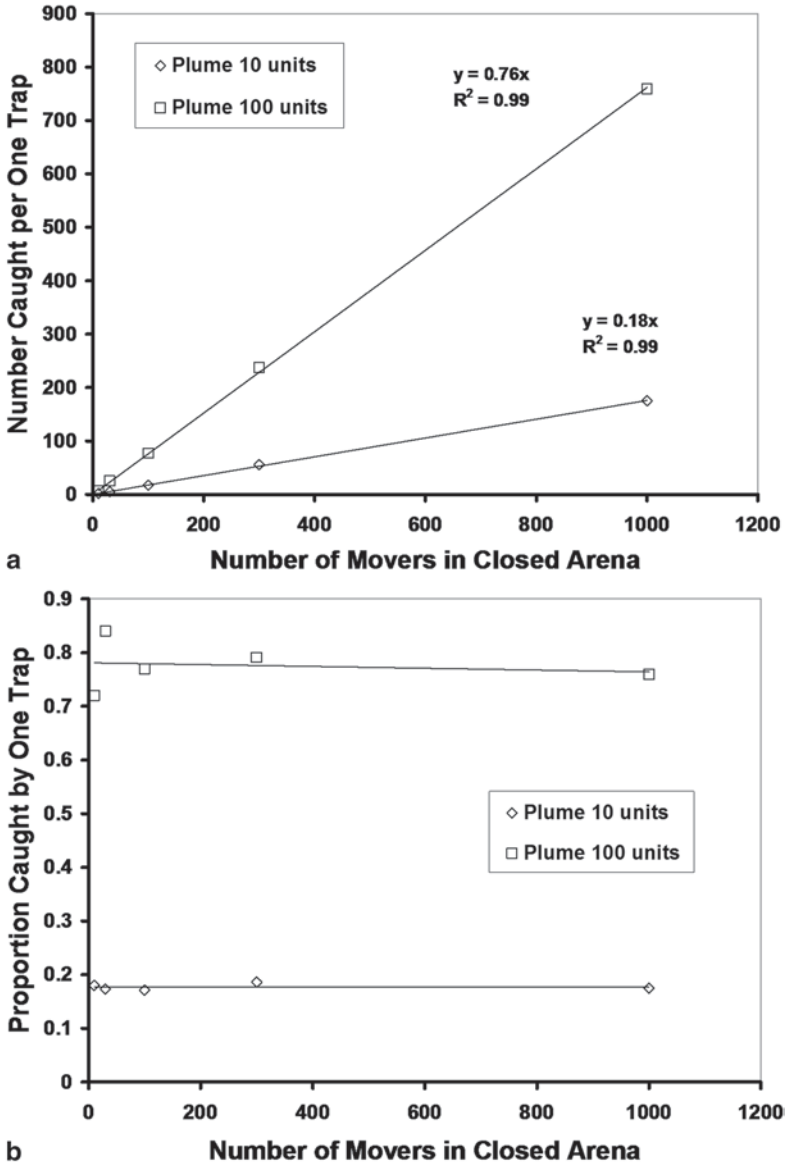

Fig. 8.1 Number (**a**) and proportion (**b**) of movers caught when varying numbers of randomly seeded Weston movers displaced for 5,000 steps of 1.0 and c.s.d. 15° in a 500 × 300 unit bounded arena. Movers were reflected back into the arena when encountering a wall. Trap plumes measured either 10 × 2 or 100 × 10 units

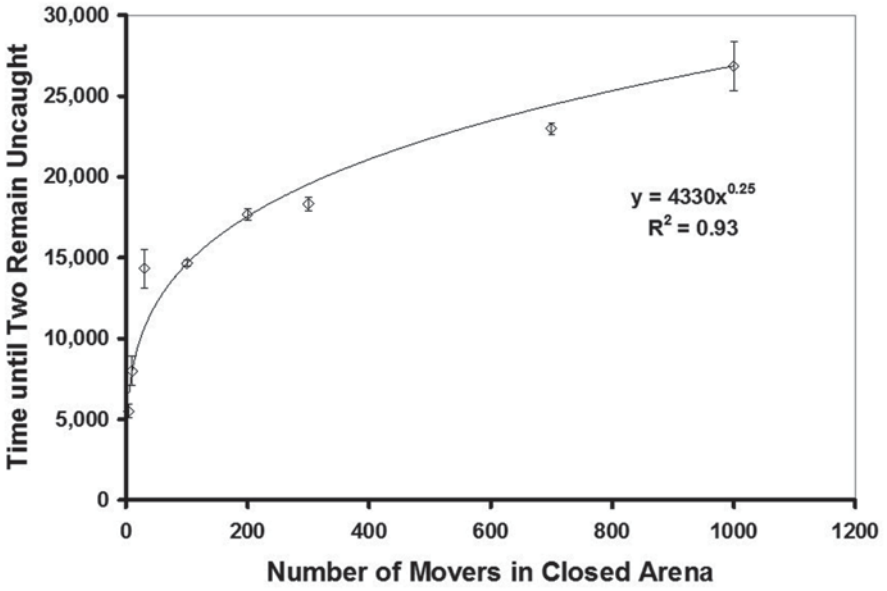

Fig. 8.2 Relationship between the number of steps (*time*) required to catch all but two movers in one trap with a 100 × 10 plume as influenced by number of randomly seeded movers under conditions very similar to those of Fig. 8.1

where the trap plume will occupy only a small fraction of the area from which a mobile pest is being recruited is not a fruitful approach.

The same conclusion holds for deploying a pair of traps in close proximity (Fig. 8.4). However, now one sees the first hint that deploying multiple traps near one another may lead to synergism, i.e., the number of white flecks around two traps is slightly greater than twice the number around a single trap. But, control improved dramatically when traps were arranged as a grid (Fig. 8.4). A 3 × 3 grid of traps generated a small patch of control at its center that approached our target of tracks no more dense than for 16 movers in Fig. 8.3. Then that area of acceptable control expanded with the size of trapping grids maintaining the same spacing. But, control as defined by this example could never be complete, because some of the randomly seeded pests always originated within the trapping grid.

These simulation results suggest that two important and complementary effects are at play when traps are arrayed as a large and close grid. First, the interior of the grid is rapidly *cleared* of movers. Then, the traps on the perimeter shield the interior (also documented in Chap. 7) from recolonization so that the cleared interior is *held*. Single traps, a tiny grid of traps, or traps spaced more than two plume reaches apart (Fig. 8.5) fail to thoroughly clear any areas and fail to prohibit repopulation of the grid interior by immigrants. Each widely spaced trap functions as a stationary solitary soldier. Each is unable to effectively clear any area of the enemy, and no soldier is close enough to effectively guard another's back. The parallels between the mass trapping problem and the soldier-survival problem are obvious and suggest that the

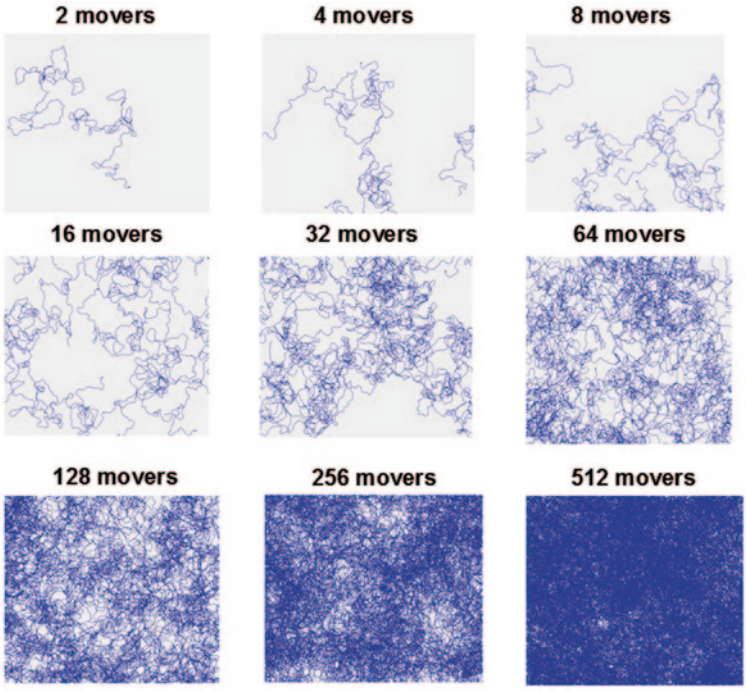

Fig. 8.3 Demonstration of the amount of interaction (*cumulative tracks shown in blue*) simulated movers accumulated in a 1,000 × 600 unit plot of crop during 2,000 steps of 1.0 unit and c.s.d. 15° as influenced by number of randomly seeded movers

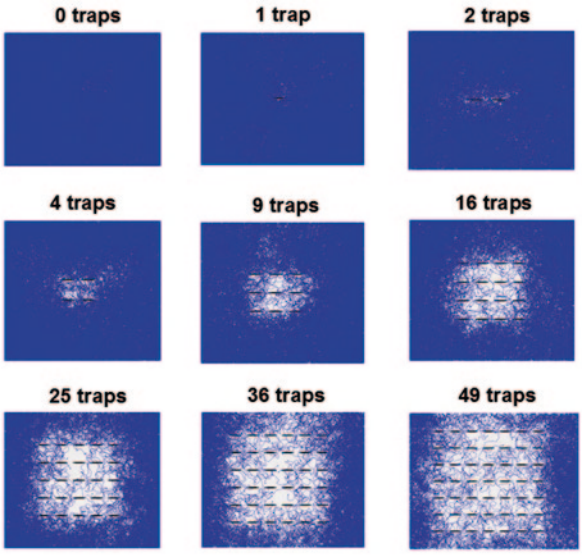

Fig. 8.4 Demonstration of the amount and location of damage protection (*clear zones*) as influenced by the number and placement of traps. These computer simulations used 300 randomly seeded Weston movers displacing for 5,000 steps of 1.0 and c.s.d. of 15° in an enclosed 1,000 × 600 unit arena. The *black ellipses* represent 50 × 5 unit trap plumes. Traps were spaced at 80 units. Intensity of *blue equates* to intensity of accumulated mover tracks and can be interpreted as likelihood of damage

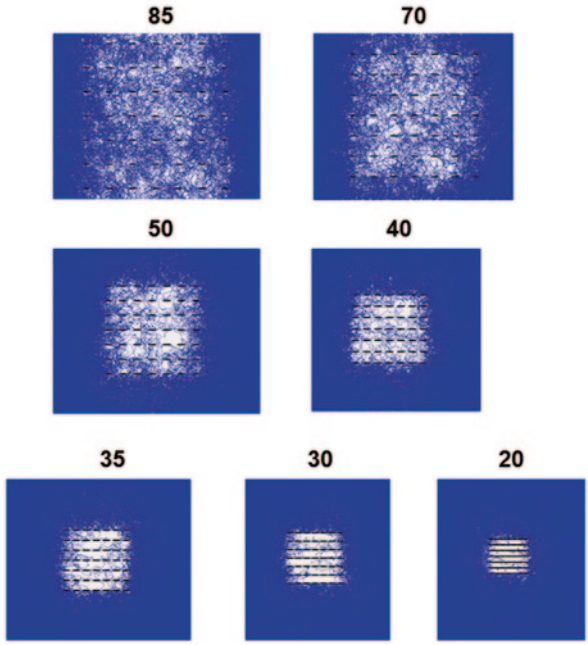

Fig. 8.5 Influence of trap grid spacing on control by mass trapping. Numbers above panels indicate trap spacing in computer units. In these simulations, plumes (*black ellipses*) measured 30 × 5 to make them visible. Other conditions were as for Fig. 8.4

rich history of military experience may inform the optimal deployment and use of traps for direct pest control. "*Clear-and-hold*" is a well-recognized counter-insurgency tactic (http://en.wikipedia.org/wiki/Clear_and_hold; Marston and Malkasian 2008) heavily used in current and recent wars. It is the best tactic we have found to date for simulated mass trapping using stationary traps.

Byers (1993) demonstrated that the exact placement of traps for mass trapping may be of little consequence, so long as they are spread out and their plumes do not overlap. For example, randomly seeded traps produced mass-trapping results nearly as good as an evenly spaced trapping grid. Nevertheless, we suggest that a trapping grid is sensible and may be easier to deploy in row crops than some more irregular design. Our simulations indicate that the optimal trap spacing for control by a mass trapping grid will be ca. 1.5 times the elliptical plume reach of the given trap. Thus, it will be important that pest managers use the tools for determining plume reach as developed in Chaps. 4 and 5. In contrast to the report that c.s.d. has negligible impact on mass trapping outcomes (Byers 1993), we found that mass trapping efficacy does degrade somewhat when the c.s.d. of movers departs from ca. 20°, (Fig. 8.6) the zone where gain (Chap. 4) was maximal for the plume sizes encountered for typical insects. Fortunately, the selective pressures that maximize the foraging efficiency of pests for plumes from potential mates will likewise have optimized foraging efficiency for plumes from traps.

We close this section with a clear demonstration of the extent to which pest control by a behavioral tactic like mass trapping is pest density-dependent. In the simulations of Fig. 8.7, we used the optimal spacing (1.5 × plume reach) for a trapping grid as arrived at from Fig. 8.5. Then we varied only pest density. By the standard

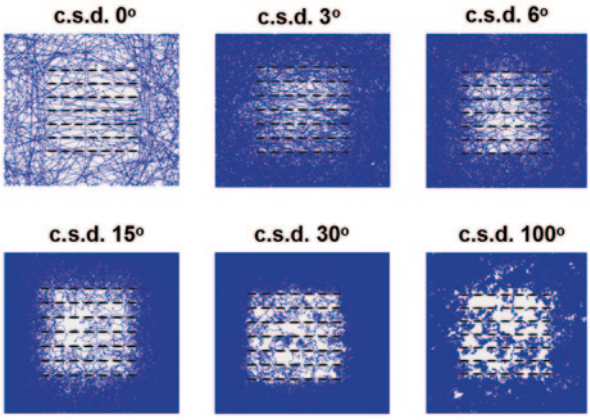

Fig. 8.6 Control by a mass trapping grid as influenced by c.s.d. of movers. Conditions as per Fig. 8.4. Note: the density of tracks for c.s.d. zero is reduced because these ballistic movers accumulated at the field border not shown at this magnification

of cumulative tracks no denser than the panel for 16 movers in Fig. 8.3, control by mass trapping was possible for a population density at or below (but not above) 300 movers/arena (Fig. 8.7). Efficacy of mass trapping or mating disruption is usually judged by the suppression of catch in one standard monitoring trap placed within the treated crop plot relative to one trap in an equivalent but untreated plot. It may startle some readers to see that the percent suppression of catch was virtually identical for all panels in Fig. 8.7; yet, control was certainly not identical. Incongruence between percent catch suppression and control has been the bane of mating disruption research since its inception 40 years ago and could be equally confusing when judging efficacy of mass trapping. To our knowledge, the cause of this troublesome mismatch has never been clearly identified. It occurs because the ratio of catch for one trap operating alone vs. one trap operating within the grid of traps is time-independent and thus pest density-independent. However, damage is pest density-dependent as shown above. A time-independent measure of efficacy (percent catch suppression) will not correlate well with a time-dependent (percent infestation) measure of efficacy across a wide range of pest densities. Expecting a good match between these efficacy measures is a misconception that needs to be laid to rest.

Figures 8.8 and 8.9 offer insight into how percent crop infestation varies with time of interaction with pests. This relationship is not linear. Percent infestation initially rises rapidly with elapsed time; but then the rate of increase slows and only asymptotically approaches 100 % infestation. These two factors are related in much the same way as are the number of movers in an arena and the time it takes for most of them to be removed by traps (Fig. 8.2). In both cases, the object being sought is in diminishing supply. The severity of the bow in the curves of Fig. 8.9 diminishes with pest density. Yet, plots of crop under behavioral controls that modestly reduce pest density relative to untreated control plots can, over long-running experiments, register similar high levels of damage as the damage curve for the former eventually catches up with that of the latter. Such outcomes have perplexed many investigators who found little difference in percent infestations while simultaneously recording pronounced differences in percent catch suppression. Such incongruence is most pronounced under high pest populations, as seen in Fig. 8.9.

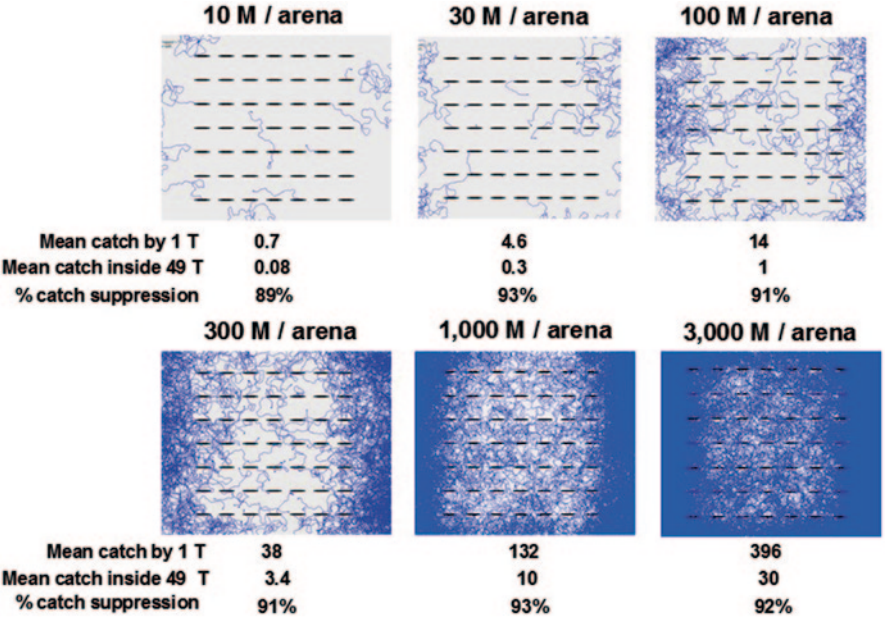

Fig. 8.7 Control (*white zones*) of an optimized mass trapping grid as influenced by the density of simulated pests in the crop. Conditions for these simulations match those of Fig. 8.4. Percent catch suppression is computed as (1 − (catch of a trap inside the 49 T/catch by a single trap operating in an untreated plot)) × 100

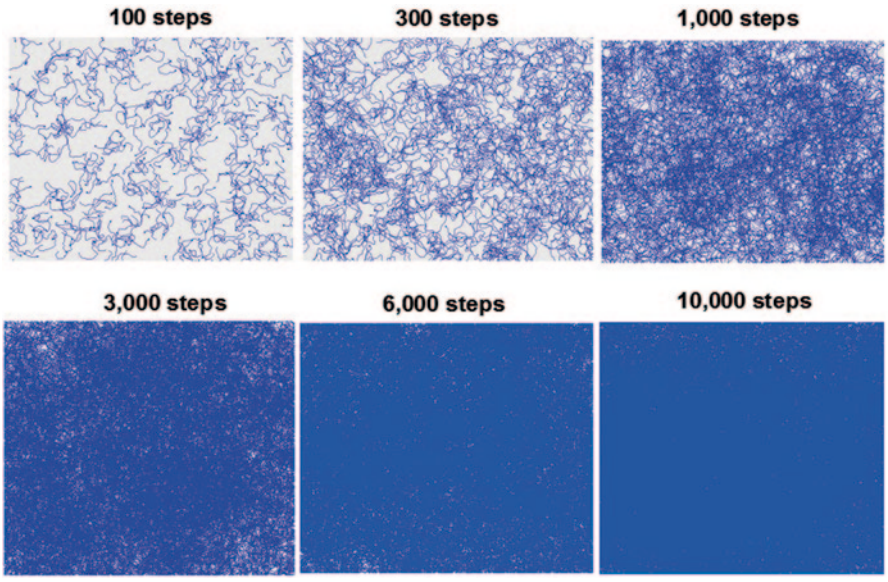

Fig. 8.8 Proportion of crop visited (*blue*) vs. unvisited (*white*) as influenced by elapsed time of the simulation run measured in number of steps taken. The number of movers randomly seeded was 500 and no traps were deployed; other conditions were identical to those of Fig. 8.4

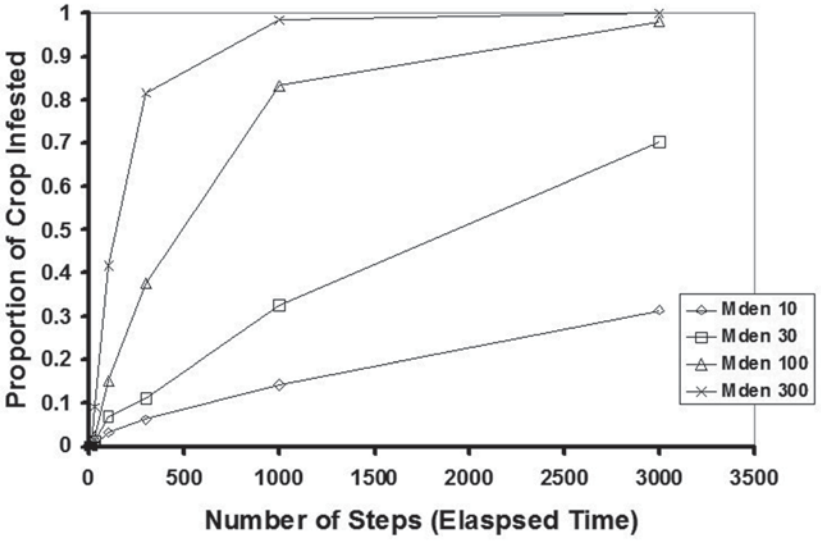

Fig. 8.9 Simulation results showing the proportion of a crop plot infested vs. elapsed time measured as number of steps taken in the simulation. The measure of proportion of crop infested was taken as the proportion of traps (20 × 2 *unit plumes*) out of a 7 × 7 trapping grid (*widely spaced in a* 1,000 × 600 *arena*) that were visited when movers were not arrested by the traps

8.4 Examples of Successful Pest Control by Mass Trapping

Such examples remain few. El-Sayed et al. (2006) aptly summarized the best cases for insects. They emerge where: (i) pest densities are low, (ii) reproductive capacity of the pest is not extraordinarily high, (iii) the plants or animals to be protected are at least somewhat isolated from sites generating new immigrants, (iv) potent attractants exist for the pest species and their chemistry is well elucidated both qualitatively and quantitatively, (v) lures and traps are not terribly costly and are effective for months, (vi) traps experience high findability, efficiency, and retention (cannot saturate), (vii) pests are sufficiently mobile to rapidly find the plumes of nearby traps, but not so mobile that they rain down upon a crop from elevations where they would not encounter a perimeter of traps, and (viii) cheap labor is available for trap manufacture, deployment, and servicing. In fact, the cost/benefit ratio has everything to do with the feasibility of mass trapping. It is not surprising, then, that examples of effective and economical mass trapping (El-Sayed et al. 2006) have been reported from locations where labor in inexpensive, i.e., pink bollworm, *Pectinophora gossypiella*, in Brazilian cotton: certain weevil pests of palm trees in the Middle East and in Central America: and the West Indian cane weevil. A recent study (Samson and Kirk 2013) on control of western flower thrips, *Frankliniella occidentalis*, concluded that use of pheromone-baited blue sticky traps will be economical for control of this pest in isolated locations producing cut flowers and

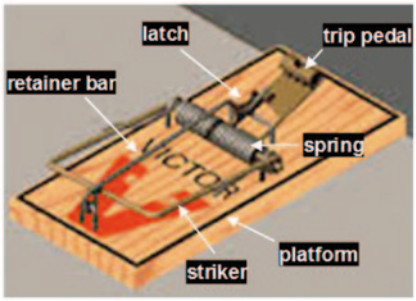

Fig. 8.10 An example of the dominant design of traps sold across the globe for mass trapping of mice in homes and businesses. Key features are labeled. This trap based on the Mast patent is manufactured by Woodstream Corp. of Lititz, PA, USA

vegetables, where insecticide residues are highly undesirable. Mass trapping is also expected to find a viable niche in control of stored food pests (Phillips 1994) where pesticide use is restricted. Mass trapping will likely be a viable option for management of some insect pests in organic agriculture.

Large sums of money are justified if mass trapping or lure-and-kill formulations can eradicate a serious new invasive pest, as has been accomplished for the Mediterranean fruit fly, *Ceratitis capitata*, in California (Myers et al. 2000) using a lure-and-kill approach where malathion was widely sprayed with a sugar bait. Here, the up-front costs pale in light of the long-term savings.

Mass trapping is also a viable pest control option for some vertebrate pests. The following examples deal with pests whose foraging behaviors may not conform fully to the patterns described for biological random walkers in earlier chapters of this book. Nevertheless, it is informative to consider the similarities and differences in mass trapping outcomes between such movers and random walkers. Trapping of mice invading houses, businesses, etc. seems to be the hallmark of successful pest control by mass trapping, as judged by user satisfaction, profits reaped by trap suppliers, and longevity of this market. Dagg (2011) elegantly traced the history of the modern mouse trap while using it as an example for addressing principles of cultural evolution pertaining to the controversy of intelligent design. As evidenced by pictographs, human use of mouse- and rat-traps predates the Bronze Age. Thereafter, interest in "the better mousetrap" never subsided. Between 1996 and the inception of the US Patent Office in 1,838, 4,400 mousetrap patents were awarded (Jackson 2011). This number sets the all-time record for patents surrounding any single US technology. Although thousands of designs have competed for a share in an estimated 50 million unit annual international market, the designs retaining more than 60% of the market are only slight variants of that shown in Fig. 8.10. This design was apparently converged upon simultaneously at the turn of the twentieth century by John Mast of Lancaster, PA, USA, and James Atkinson of Leeds, Yorkshire, England. Such traps were originally priced at just pennies per copy but have now inflated to about a dollar or substantially more if the trip pedal is made from plastic infused with a long-lasting attractive odorant. The senior author can personally attest that investment in traps like that of Fig. 8.10 is well worth the benefits of restored domestic tranquility each fall when cold weather drives mice indoors. The number of traps required for effective mass trapping in this particular

Michigan farmhouse over ca. 4 weeks is 4–6 and the annual harvest is ca. 12 mice. Our threshold for control is zero mice or mouse droppings. And, each trap lasts for years. This is an example of unequivocally successful mass trapping.

Larger traps like that in Fig. 8.10 have played an important role for many years in mass trapping of rats around businesses like farms. And they were recently investigated as agents for protecting Hawaiian crops of macadamia nuts from roof rat damage (Tobin et al. 1993). Some 40 ha of nut trees received traps in a grid pattern (trap every 4th tree) at 40 traps/ha. Traps were baited with coconut and deployed on low horizontal branches where the rats were known to be most active. The layout and spacing of traps appeared to approach the *clear and hold* standards detailed above from computer simulations. More than 1,700 rats were captured in the 1,600 traps in 1 year of this study. Satisfyingly, rat damage to the crop was reduced from ca. 4 to 1 %. But, it remains to be seen whether this method will be adopted when the program costs approached $ 250/ha. Another concern was that the traps injured birds.

By contrast, trapping of bandicoot rats for control of deepwater rice in Bangladesh is reported to be highly effective and practical (Islam and Karim 1995). Here, live traps worked better than snap traps and each one was deployed on a floating platform among the deeply flooded rice stems. Rats swimming among the flooded rice plants tired and were attracted to the floating platforms holding the traps. Thus, the drawing power to each trap was much increased over random encounter as was likely for the macadamia nut mass trapping research.

Trapping of vertebrate pests such as raccoons, skunks, and ground moles remains an important component of wildlife pest control in the home and garden setting (Salmon et al. 2006). It is also an important source of income for pest control companies. Having one skunk in the back yard is no small problem when one's dog is released from the back door to relieve himself and he bolts off into the night. Trapping of this sort is rarely referred to as mass trapping because relatively few traps are used per site. Instead the elapsed time that a pest is subjected to trapping is extended until it is no longer productive. Nevertheless, the goal is the same—reduce the pest problem to acceptable levels by traps alone (rather than e.g., poisons). In many cases, live traps are employed that do not harm the wildlife. But, as some of us can attest when a pest control company traps our lawns for ground moles, one reevaluates the threshold for acceptable pest density as the bill for this service mounts over the weeks or months when eradication clearly has not been attained. The standards for humane treatment of animals by homeowners and vertebrate pest control operators are appropriately rising through time (Fall and Jackson 1998).

Mass trapping using large cage traps contributes to successful management of the sea lamprey, *Petromyzon marinus,* an eel-like parasite of sport fish species throughout the Great Lakes (McLaughlin et al. 2007). Although not nearly as effective as lampricides directed against the worm-like immature sea lamprey developing as sedentary feeders in stream beds leading into the lakes, mass trapping helps reduce the density of spawner runs recolonizing streams each spring. The hope that synthetic sex pheromones (in this case released from the gills of males preparing nests) would greatly increase captures of female lamprey over unbaited traps as they do for male insects, unfortunately, has not been fulfilled (Johnson et al. 2013). To

Fig. 8.11 Michigan State University's patented Micro-Trap developed for mass trapping of small moth pests of fruit like codling moth and perhaps extendable to other insect pests. This trap measures only 4 cm on a side, while a standard monitoring trap (Fig. 1.3) is nearly 30 cm long

date, baiting traps with pheromone increases lamprey capture by less than twofold. The current hypothesis is that the pheromone is increasing trap entry (raising trap efficiency) but not findability. Nevertheless, the benefit of modestly increased captures is tentatively considered worth the cost of the rather expensive pheromone. Mass trapping is an especially appealing approach in the lamprey system having a great advantage that the pests are forced to follow stream channels; thus traps can be deployed so that their targets must repeatedly pass them before reaching the spawning grounds. Only then can damage result by the production of offspring. However, this advantage is offset by the disadvantage that this species is an extreme r-strategist. Each female produces tens of thousands of eggs. Thus, the proportion of spawners that must be removed by mass trapping to reduce final larval populations in the limited zones of suitable larval habitat must be extremely high. So, this is yet another case where mass trapping is not a stand-alone pest management tactic. As in most other cases, trapping is considered a component of an overall IPM program for sea lamprey.

8.5 New Approaches to Mass Trapping

An impediment to the practical development of mass trapping for insects has been that standard monitoring traps are frequently used for mass trapping research. Each of these traps is designed to collect dozens of insects without saturating, and therefore their trapping surface must be large. However, if mass trapping is conducted under low pest densities and dozens of traps will be used per ha, large trap size is wasteful because large traps will never saturate. They represent design overkill. This realization prompted the Michigan State University team of Reinke et al. (2012) to develop a small trap more appropriate to a mass trapping role for codling moth. This patented MicroTrap (Fig. 8.11) is an enclosed cube measuring only 4 cm on a

side. A sex pheromone lure is contained inside the trap whose inner walls are coated with nonodorous glue that does not inhibit insect entry. Twelve-mm diam holes on cube faces permit airflow through the trap, ample release of pheromone, and quick entry of male moths into the trap interior where they are permanently ensnared. MicroTraps caught similarly to the standard codling moth monitoring trap and, when mass-produced, will cost far less per copy than the standard monitoring trap.

In a test (Reinke et al. 2012) conducted using 0.2 ha plots of apple and a grid of traps spaced at 4 m, mass trapping with MicroTraps yielded 92 % catch suppression of codling moth males that was superior to the best mating disruption product on the market (71 %). Mass trapping of the obliquebanded leafroller, *Choristoneura rosaceana*, under similar conditions also suppressed catch in monitoring traps more strongly (85 %) than did mating disruption (58 %) (Reinke et al. 2012). Moreover, damage of this pest to young shoots was reduced to 1 % by mass trapping relative to 4 % measured in control plots. We therefore conclude that mass trapping is more efficacious than mating disruption when the mechanism of disruption is competitive (Miller et al. 2006a, 2010)—point sources act as false females attracting the males.

We suggest that the mass trapping tactic has substantially more to offer to pest control than has been realized to date because the fundamentals of the method (like reach of attractive plumes and required spacing based on plume reach) are only now being uncovered. With more effort on research and development, it is likely that the costs of small traps used for insects could drop substantially. If mass trapping is to be adopted in developed countries, the high labor costs associated with trap deployment will need to be solved by automating deployment. For example, the Tangler® (http://www.goodfruit.com/the-tangler/) bolas technique (patent pending by RidgeQuest) shows great promise as a method for securing small devices launched by pressurized gas into tree canopies. Commercial opportunities remain wide open to entrepreneurs who grasp the science behind effective trapping, are sufficiently creative to invent, engineer, and manufacture effective trap designs and deployment techniques, and who can develop effective marketing and servicing networks.

Chapter 9
Automated Systems for Recording, Reporting, and Analyzing Trapping Data

9.1 Need for Such Systems

Crop production in the global economy is highly competitive. Profit margins have become remarkably thin and are likely to remain so indefinitely. Market forces drive agriculture to adopt economies of scale and to cut costs wherever possible. Labor is one segment of the cost equation being squeezed to its minimum. Thus, it is not surprising that growers and pest management consultants question whether they can afford the time it takes them or their employees to deploy the recommended density of monitoring traps for pests and to visit all of them at recommended intervals to collect the data. This dissatisfaction combined with the availability of powerful new information technologies that are becoming ever cheaper makes it sensible and inevitable that trapping, reporting, and analysis of data will become automated.

9.2 History of Insect Trap Automation

With the invention of the first light trap for insects in 1927 (http://wwwrci.rutgers.edu/~insects/njtrap.htm), entomologists became interested in when during the diel cycle insects were responding. Such studies initially required investigators to tend their experiments continuously for 24 h to change collecting jars under traps at regular intervals to record when catch began, peaked, and ceased. Clever minds soon devised machinery for doing this sleep-depriving job. In 1934, Seamans and Gray developed a turntable that automatically switched the collecting vessels at regular intervals. Many publications on that theme followed.

When sex pheromones became available in the 1970s for baiting insect traps, the turnabout idea was again soon utilized for assessing the timing of responses. One such device (Comeau 1971) simply mounted a large pizza pan to the hour hand of a large wind-up mechanical clock so that it made one revolution every 12 h. A cutout equivalent to 1 h of travel over a sticky disk permitted moths to become ensnared after approaching a sex pheromone lure mounted immediately over the opening.

J. R. Miller et al., *Trapping of Small Organisms Moving Randomly,*
SpringerBriefs in Ecology, DOI 10.1007/978-3-319-12994-5_9

Such devices conveniently permitted investigators to graph activity level over time, including a full day with one clock switch.

In the mid-1980s, insect trap automation advanced beyond simple mechanical technology when Hendricks (1985) incorporated a portable infrared (IR) detector into an inverted cone trap baited with sex pheromones targeting the medium-sized moth pests of cotton in South Texas, tobacco budworm (*Heliothis virescens*), and cabbage looper (*Trichoplusia ni*). The traps were powered by an ordinary lantern battery and operated in remote open fields subject to ambient wind, rain, fog, and dust. The records of moth transit into the trap reservoir were translated into ink dots deposited on a time-stamped revolving paper disk. The results were excellent; captures in the automated traps were 95 % correlated with those recorded from nonautomated traps. No serious problems were experienced with the electronics or mechanics of this trap.

Recognizing the great potential of automated traps and apparently permitting his inventions to remain in the public domain, Hendricks (1989) quickly proceeded to use a portable computer to receive the tone-coded radio frequency pulses emitted by the traps upon moth entry. Count data could then be provided in easily understood format to a farm manager. This system was 92 % accurate in counting moths and 100 % accurate in reporting the detection of single moths as a first event each night. Again, the system proved highly robust under the full range of field conditions.

Other researchers (Schouest and Miller 1994), working with the cotton pest pink bollworm (*Pectinophora gossypiella*), extended this effort by linking various computers to receive trapping data from multiple sites and then transmit the cumulative data over phone lines to a central location where it could be analyzed and potentially translated into control decisions appropriate to each field.

Tseng et al. (2006) used a high-voltage electrocution system to record visits of Taiwanese diamondback, *Plutella xylostella*, moths to traps baited with sex pheromone. But the notable advancement was the demonstration that the global system for mobile communication (GSM) and short message service (SMS) could successfully transmit the collected data over long distances to a central location where data could be processed for pest management decisions. Based on performance testing on over 915 data transmissions, the one-way SMS transmission time for a field monitoring platform to a host-control platform was reported to be 10–15 s, while the average transmission time of a field monitoring platform to host-control command was about 30 s, both tolerable time delays. The correctness of the data sent by the GSM-SMS system was judged at 100 %. The rate of data loss was about 1 % and that was entirely due to the service quality of the commercial telecommunication company used. Notably, this system simultaneously collected and transmitted environmental data along with the capture data from the monitoring traps, a development that will appropriately facilitate integration of weather with capture data. Two years later, this research group demonstrated (Jiang et al. 2008) that a similar system worked well for collecting and transmitting trapping data for the oriental fruit fly, *Bactrocera dorsalis*. In this case, an optical sensor was used to count flies entering

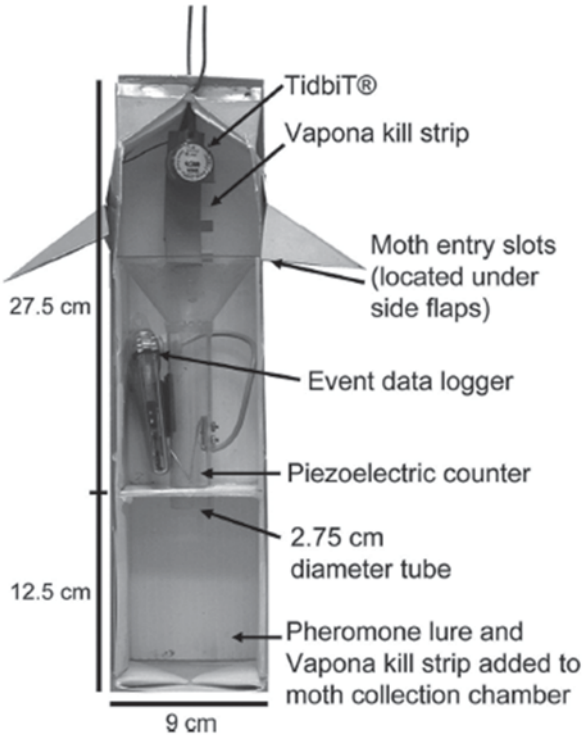

Fig. 9.1 Design of the milk carton trap modified for automated recording of captures of male gypsy moths (Tobin et al. 2009). As they pass through the tube toward the source of the sex pheromone, moths displace the piezoelectric counter for which the date–time stamp is recorded by an event data logger

the trap. Moreover, this trap employed a pneumatic "inhaler" that overcame a previous problem of multiple counts of the same arriving fly.

Reports of other kinds of automated traps, some also simultaneously collecting environmental data, are appearing in the literature (Beerwinkle 2001; Tabuchi et al. 2006; Tobin et al. 2009). Such a trap has been developed by the United States Department of Agriculture (USDA) Animal and Plant Health Inspection Service for gypsy the moth, *Lymantria dispar*, a devastating forest pest toward which the US Forest Service has directed much research and management effort. This modified milk carton trap (Fig. 9.1) baited with (+) disparlure counts male gypsy moths via a piezoelectric counter interfaced with an event data logger giving each capture a time and date stamp. The trap also contains a HOBO TidbiT temperature data logger. However, this trap lacks any capacity to transmit data. Researchers must visit each trap and physically download the data from the respective recorders onto a portable computer for transport and analysis. Nevertheless, the accuracy of this automated gypsy moth trap shows great promise (Figs. 9.2 and 9.3).

Another promising technology for automatically recording insect appearance in traps is digital photography. Kondo et al. (1994) demonstrated that this technique allowed accurate counts of arrivals into traps of the Asiatic rice stemborer, *Chilo suppressalis*, and the Oriental leafworm moth, *Spodoptera litura*. Guarnieri et al. (2011) improved the method by incorporating a smartphone into a pheromone-baited trap

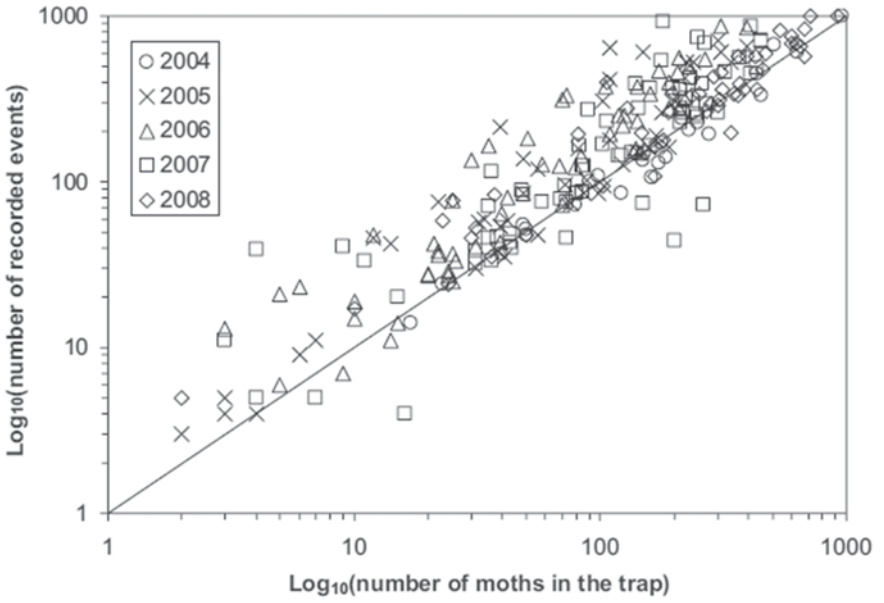

Fig. 9.2 Data from Tobin et al. (2009) demonstrating that the number of captures recorded by the automated gypsy moth trap is very well correlated with the actual catch recorded by visual inspection. The *solid diagonal line* indicates a 1:1 relationship

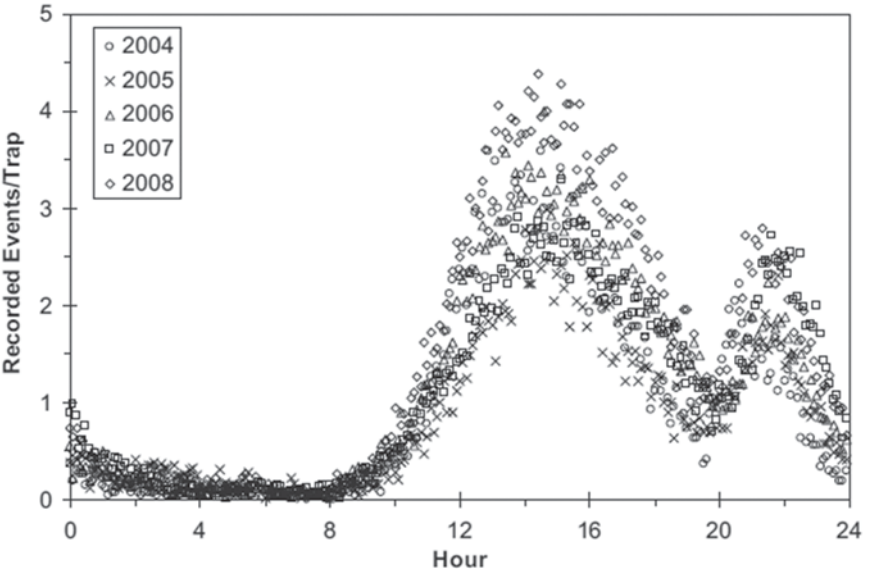

Fig. 9.3 Remarkably consistent pattern in diel responsiveness of male gypsy moths to sex pheromone as measured by the automated gypsy moth trap (Tobin et al. 2009)

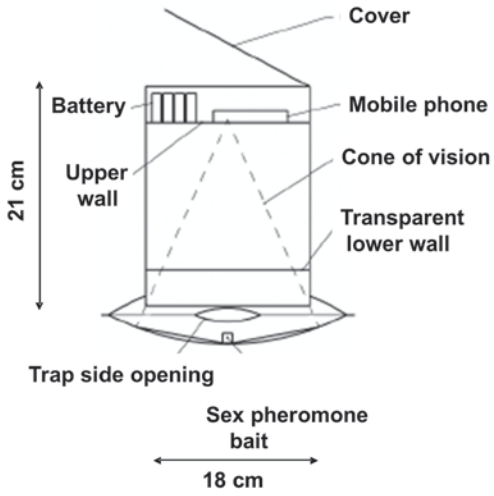

Fig. 9.4 Design of the codling moth trap incorporating a smartphone to snap and periodically transmit images of the sticky liner. Redrawn from Guarnieri et al. (2011)

for codling moth, *Cydia pomonella*, and programmed to wirelessly transmit updated images to any location for processing (Fig. 9.4). The battery pack used permitted the system to operate continuously for 20 days. Image resolution was sufficient to guarantee that only codling moths were counted. Moreover, use of a highly species-specific pheromone and the trap design make catches of nontarget organisms highly improbable.

9.3 Recent Developments and Future Prospects

Capture and transmission of visual images from traps is becoming the favored method for automated data flow as judged by recent publications (López et al. 2012). Rapid advances are being made in reducing the power (and thus cost) required to run these systems and increasing the speed and reliability of data transmission. Smart traps using visual imaging are becoming commercially available. The model shown in Fig. 9.5a is sold by Trapview (http://www.trapview.com/en). It is manufactured by EFOS informacijske resitve d.o.o. of Slovenia, a company specializing in software and technologies advancing environmental and food safety. Spensa Technologies of West Lafayette, IN (USA) also offers a smart trap (Fig. 9.5b) along with a complete analysis system. The speed with which such automated trapping systems are adopted by pest managers and growers remains to be seen and will be highly influenced by pricing. We predict that smart traps will remove much of the labor costs associated with pest monitoring and a few inexpensive versions will inevitably sweep the market in developed countries. Evidence is mounting that the marketing strategy of companies promoting this technology is to bundle the traps and transmission systems with data storage (already includes cloud storage and retrieval) and analysis systems.

Fig. 9.5 Smart traps purchasable from Trapview (**a**) and Spensa Technologies (**b**). Both companies offer analysis systems or services. (Images and permission to use theme here were provided by the respective companies)

No peer-reviewed publications were found on smart trap technologies for arthropods such as lobsters and crabs. However, they are soon to arrive. A web article (http://www.halfbakery.com/idea/smart_20shrimp_20crab_20pots) reports attachment of an underwater camera to a crab or shrimp pot. A floating data cable delivered images to an radio frequency (RF) transmitter attached to a buoy that periodically transmitted the images to a base-station where the images were used to determine whether or not to visit the trap for collecting the harvest and/or rebaiting. Smart mouse traps are currently available. Some models even send the tender a text message or an email notifying them that the trap has caught and needs to be serviced.

To our knowledge, the possible benefits of mobile vs. stationary monitoring traps for pests have not yet been explored, probably because costs for achieving trap mobility are thought to be prohibitive. However, our preliminary explorations using computer simulations show that capture rate of a single trap moving in a circular orbit in a field of insectlike Weston movers rises approximately linearly with trap speed for any plume reach. Intersections of movers with plumes can rise substantially when trap speed exceeds the movers' net speed such that the plume sweeps over the movers in addition to having the movers fly into the passing plume. In essence, the trap then becomes a mobile rather than sit-and-wait predator. Encounter rates of mobile predators with prey are well known to be substantially higher than those for stationary predators (see Gurarie and Ovaskainen 2013, and references therein). In today's world where increasingly inexpensive and reliable unmanned aircraft are becoming available for civil uses (Nonami 2007), it seems appropriate that mobile monitoring traps receive their due attention, because they could offer decided advantages in pest detection and sampling efficiency.

9.4 Wrap-Up

Our hope is that the principles of trapping set forth in this book will become an integral part of modern trapping systems. Clearly, companies selling traps and pest managers will want to know the plume reaches and trapping radii of their traps so as to optimize deployment spacing. Conversion of catch numbers into absolute pest density will surely become a key part of any sophisticated analysis system. Smart traps will be a boon to collection, speed of analysis, and sharing of competitive trapping data (Chap. 7) so as to simultaneously measure trapping area as well as catch. Such information, combined with other data streams on past and future weather conditions, crop loads, and projected prices attainable for the developing crop, will all become part of an overall decision system that will increasingly become automated and centralized. In the end, software and computer systems, rather than pencil-pushing humans, will be crunching the numbers and suggesting optimized actions and their timing. Considerable efficiency will be gained in this process. Hopefully, those gains will translate into a safer, less expensive, and sustainable food supply.

References

Adams CG, McGhee PS, Gut LJ, Miller JR (2015) Trapping radius and plume reach for the standard monitoring trap for codling moth, *Cydia pomonella*. (In preparation)

Arora R, Singh B, Dhawan AK (eds) (2012) Theory and practice of integrated pest management. Scientific Pub. Jodhpur, India, 529 p

Batiste WC, Olson WH, Berlowitz A (1973) Codling moth: influence of temperature and daylight intensity on periodicity of daily flight in the field. J Econ Entomol 66:883–892

Beerwinkle KR (2001) An automatic capture-detection time-logging instrumentation system for boll weevil pheromone traps. Appl Eng Agric 17:893–898

Bell WJ (1991) Searching behaviour: the behavioural ecology of finding resources. Chapman and Hall, New York, 358 p

Berg HC (1993) Random walks in biology. Princeton University Press, Princeton, N.J., 152 p

Billingsley P (1956) The invariance principle for dependent random variables. Trans Am Math Soc 83:250–268

Breman JG, Egan A, Keusch GT (2001) The intolerable burden of malaria: a new look at the numbers. Am J Trop Med Hyg 64:iv–vii

Brêthes JC, Bouchard R, Desrosiers G (1985) Determination of the area prospected by a baited trap from a tagging and recapture experiment with snow crabs (*Chionoecetes opillo*). J Northwest Atl Fish Sci 6:37–42

Byers JA (1993) Simulation and equation models of insect population control by pheromone-baited traps. J Chem Ecol 19:1919–1956

Byers JA, Anderbrant O, Löfqvist J (1989) Effective attraction radius: a method for comparing species attractants and determining densities of flying insects. J Chem Ecol 15:749–765

Comeau A (1971) Physiology of sex pheromone attraction in Tortricidae and other Lepidoptera. Ph. D. Dissertation, Cornell University

Dagg JL (2011) Exploring mouse trap history. Evo Edu Outreach 4:397–414

Dodds KJ, Ross DW (2002) Sampling range and range of attraction of *Dendroctonus pseudotsugae* pheromone-baited traps. Can Entomol 134:343–355

Donsker MD (1951) An invariance principle for certain probability limit thermos. Mem Am Math Soc 6:1–10

Elkinton JS, Childs RW (1983) Efficiency of two gypsy moth (Lepidoptera: Lymantriidae) pheromone-baited traps. Environ Entomol 12:1519–1525

El-Sayed AM, Suckling DM, Wearing CH, Byers JA (2006) Potential of mass trapping for long-term pest management and eradication of invasive species. J Econ Entomol 99:1550–1564

Fall MW, Jackson WB (1998) A new era of vertebrate pest control? An introduction. Int Biodeterior Biodegrad 42:85–91

Feller W (1968) An introduction to probability theory and its applications, vol 1. Wiley, New York, 528 p

J. R. Miller et al., *Trapping of Small Organisms Moving Randomly,*
SpringerBriefs in Ecology, DOI 10.1007/978-3-319-12994-5

Feynman RPl Leighton RG Sands M (1963) Feynman, Lectures on physics, vol 1. Addison-Wesley, Reading, Massachusetts, USA

Grieshop MJ, Brunner JF, Jones VP, Bello NM (2010) Recapture of codling moth (Lepidoptera: Tortricidae) males: influence of lure type and pheromone background. J Econ Entomol 103:1242–1249

Guarnieri A, Maini S, Molari G, Rondelli V (2011) Automatic trap for moth detection in integrated pest management. Bull Insectol 64:247–251

Gurarie E, Ovaskainen O (2013) Toward a general formulation of encounter rates in ecology. Theor Ecol 6:189–202

Gut LJ, Stelinski L, Thompson D, Miller JR (2004) Behavior-modifying chemicals: prospects and constraints in IPM. In: Koul O, Dhaliwal GS, Cuperus GW (eds) Integrated pest management: potential, constraints, and challenges. CABI Press, New York, pp 73–121

Hendricks DE (1985) Portable electronic detector system used with inverted-cone sex pheromone traps to determine periodicity and moth captures. Environ Entomol 14:199–204

Hendricks DE (1989) Development of an electronic system for detecting *Heliothis* spp. moths (Lepidoptera: Noctuiidae) and transferring incident information from the field to a computer. J Econ Entomol 82:675–684

Hermes DA, McCullough DG (2014) Emerald ash borer invasion of North America: history, biology, ecology, impacts, and management. Annu Rev Entomol 59:13–30

Islam Z, Karim ANMR (1995) Rat control by trapping in deepwater rice. Int J Pest Manage 41:229–233

Jackson N (2011) Mousetraps: a symbol of the American entrepreneurial spirit. The Atlantic, Mar 28, 2011

Jiang JA, Tseng CL, Lu FM, Yang EC, Wu ZS, Chen CP, Lin SH, Lin KC, Liao CS (2008) A GSM-based remote wireless automatic monitoring system for field information: a case study for ecological monitoring of the oriental fruit fly, *Bactrocera dorsalis* (Hendel). Comput Electron Agric 62:243–259

Johnson NS, Siefkes MJ, Wagner CM, Dawson H, Wang H, Steeves T, Twohey M, Li W (2013) A synthesized mating pheromone component increases adult sea lamprey (*Petromyzon marinus*) trap capture in management scenarios. Can J Fish Aquat Sci 70:1101–1108

Judd GJR, Gardiner MGT (1997) Forecasting phenology of *Orthosia hibisciguenée* (Lepidoptera: Noctuiidae) in British Columbia using sex-attractant traps and degree-day models. Can Entomol 129:815–825

Justus KA, Murlis J, Jones C, Cardé RT (2002) Measurement of odor-plume structure in a wind tunnel using a photoionization detector and a tracer gas. Environ Fluid Dyn 2:115–142

Knipling EF (1979) The basic principles of insect population suppression and management. Agriculture Handbook 512. USDA, Washington DC, 659 p

Kogan M (1986) Ecological theory and integrated pest management practice. Wiley-Interscience, New York, 362 p

Kondo A, Sano T, Tanaka F (1994) Automatic record using camera of diel periodicity of pheromone trap catches. Jap J Appl Entomol Zool 38:197–199

Krebs CJ (1999) Ecological methodology. Addison-Welsey Educational Publishers, Inc., Menlo Park, 620 p

Kuz'zima GV Conformal radius of a domain. Encyclopedia of mathematics. http://www.encyclopediaofmath.org/index.php?title=Conformal_radius_of_a_domain&oldid=18740

Lincoln FC (1930) Calculating waterfowl abundance on the basis of banding returns. Circular 118. United States Department of Agriculture, Washington DC

López O, Rach MM, Migallon H, Malumbres MP, Bonastre A, Serrano JJ (2012) Monitoring pest insect traps by means of low-power image sensor technologies. Sensors 12:15801–15819

Lyytikäinen-Saarenmaa P, Varama MC, Anderbrant O, Kukkola M, Hedenström E, Högberg HE (2001) Predicting pine sawfly population densities and subsequent defoliation In: Liebhold AM, McManus AM, Otvos LS, Fosbroke SLC (eds) Proceedings: integrated management and dynamics of forest defoliating insects, pp 108-116; 1999 August 15-Victoria, B.C. Gen. Tech. Rep. NE-277, Newton Square, PA; US Dept. Agric, Forest Service, NE Research Station

Maki EC, Millar JG, Rodstein J, Hanks LM, Barbour JD (2011) Evaluation of mass trapping and mating disruption for managing *Prionus californicus* (Coleoptera:Cerambycidae) in hop production yards. J Econ Entomol 104:933–938

Marston D, Malkasian C (eds) (2008) Counterinsurgency in modern warfare. Osprey Publishing, 304 p

Mason LJ, Jansson RK, Heath RR (1990) Sampling range of male sweetpotato weevils (*Cylas formicarius elegantulus*) (Summers) (Coleoptera:Curculionidae) to pheromone traps: influence of pheromone dosage and lure age. J Chem Ecol 16:2493–2502

McLaughlin RL, Hallett A, Pratt TC, O'Connor LM, McDonald DG (2007) Research to guide use of barriers, traps, and fishways to control sea lamprey. J Great Lakes Res 33:7–19

Miller JR, Cowles RS (1990) Stimulo-deterrent diversion: a concept and its possible application to onion maggot control. J Chem Ecol 16:3197–3212

Miller JR, Gut LJ, de Lamé FM, Stelinski LL (2006a) Differentiation of competitive vs. noncompetitive mechanisms mediating disruption of moth sexual communication by point sources of sex pheromones: (Part 1) Theory. J Chem Ecol 32:2089–2114

Miller JR, Gut LJ, de Lamé FM, Stelinski LL (2006b) Differentiation of competitive vs. noncompetitive mechanisms mediating disruption of moth sexual communication by point sources of sex pheromones: (Part 2) Case studies. J Chem Ecol 32:2115–2143

Miller JR, Siegert PY, Amimo FA, Walker ED (2009) Designation of chemicals in terms of the locomotor responses they elicit from insects: an update of Dethier et al. (1960). J Econ Entomol 102:2056–2060

Miller JR, McGhee PS, Siegert PY, Adams CG, Huang J, Grieshop MJ, Gut LJ (2010) General principles of attraction and competitive attraction as revealed by large-cage studies of moths responding to sex pheromone. PNAS 107:22–27

Mora C, Tittlensor DP, Adi S, Simpson AGB, Worm B (2011) How many species are there on earth and in the ocean? PLoS Biol (8):e1001127. doi:10.1371/journal.pbio.1001127

Muirhead-Thomson RC (1991) Trap responses of flying insects: the influence of trap design on capture efficiency. Academic Press, New York, 287 p

Murlis J, Elkinton JS, Cardé RT (1992) Odor plumes and how insects use them. Ann Rev Entomol 37:505–532

Myers J, Simberloff D, Kuris AM, Carey JR (2000) Eradication revisited: dealing with exotic species. Trends Ecol Evol 15:316–320

Newman CM, Wright AL (1981) An invariance principle for certain dependent sequences. Ann Prob 9:671–675

Nonami K (2007) Prospect and recent research and development for civil use autonomous unmanned aircraft as UAV and MAV. J Syst Design and Dynam 1:120–128

Östrand F, Anderbrant O (2003) From where are insects recruited? A new model to interpret catches in attractive traps. Agric For Entomol 5:163–171

Östrand F, Anderbrant O, Jönsson P (2000) Behaviour of male pine sawflies, *Neodiprion sertifer*, released downwind from pheromone sources. Entomol Exp Appl 95:119–128

Phillips TW (1994) Pheromones of stored-product insects: current status and future perspectives. In: Highley E, Wright EJ, Banks HJ, Champ BR (eds) Stored product protection, pp 479-486. Proceedings of the 6th International Working Conference on Stored-Product Protection, 17-23 April 1994, Canberra, Australia. CAB International, Wallingford, UK

Pimentel D (2005) Environmental and economic costs of the application of pesticides primarily in the United States. Environ Dev Sustain 7:229–252

Potter DA, Held DW (2002) Biology and management of the Japanese beetle. Annu Rev Entomol 47:175–205

Reinke MD, Miller JR, Gut LJ (2012) Potential of high-density pheromone-releasing microtraps for control of codling moth, *Cydia pomonella*, and obliquebanded leafroller, *Chroistoneura rosaceana*. Physiol Entomol 37:53–59

Roelofs WL, Cardé RT (1977) Responses of Lepidoptera to synthetic sex pheromone chemicals and their analogues. Annu Rev Entomol 22:377–405

Salmon TP, Whisson DA, Marsh RE (2006) Wildlife pest control around gardens and homes, 2nd edn. U.C. Ag. and Nat. Res. Publication 21385, Univ. CA Publications

Sampson C, Kirk WDJ (2013) Can mass trapping reduce thrips damage and is it economically viable? Management of the western flower thrips in strawberry. PloS One. doi:10.1371/journal.pone.0080787

Schouest LP Jr, Miller TA (1994) Automated pheromone traps show male pink bollworm (Lepidoptera: Gelechiidae) mating response is dependent on weather conditions. J Econ Entomol 87:965–974

Seamans HL, Gray HE (1934) Design of a new type of light trap to operate at controlled intervals. 25th and 26th Repts. Quebec Soc. Prot. Plants. 1933–1934, pp 39–46

Southwood TRE, Henderson PA (2000) Ecological methods: with particular reference to the study of insect populations. Chapman and Hall, New York, 575 p

Spitzer F (1964) Electrostatic capacity, heat flow, and Brownian motion. Z Wahracheinlichkeit 3:110–121

Sufyan M, Neuhoff D, Furlan L (2011) Assessment of the range of attraction of pheromone traps to *Agriotes lineatus* and *Agriotes obscurus*. Agric For Entomol 13:313–319

Tabuchi K, Moriya S, Mizutani N, Ito K (2006) Recording the occurrence of the bean bug *Riptortus clavatus* (Thunberg) (Heteroptera:Alydidae) using an automatic counting trap. Jap J Appl Entomol Zool 50:123–129

Taylor LR (1974) Insect migration: flight periodicity and the boundary layer. J Anim Ecol 43:225–238

Thacker JRM (2002) An introduction to arthropod pest control. Cambridge University Press, Cambridge, UK, 337 p

Tobin ME, Koshler AE, Sugihara RT, Ueunter GR, Yamaguchi AM (1993) Effects of trapping rat populations and subsequent damage and yields of macadamia nuts. Crop Prot 12:243–248

Tobin PC, Klein KT, Leonard DS (2009) Gypsy moth (Lepidoptera: Lymantriidae) flight behavior and phenology based on field-deployed automated pheromone-baited traps. Environ Entomol 38:1555–1562

Tseng CL, Jiang JA, Lee RG, Lu FM, Ouyand CS, Chen YS, Chang CH (2006) Feasibility study on application of GSM-SMS technology to field data acquisition. Comp Electron Agric 53:45–59

Turchin P, Odendaal FJ (1996) Measuring the effective sampling area of a pheromone trap for monitoring population density of southern pine beetle. Environ Entomol 25:582–588

Wall C, Perry NJ (1978) Interactions between pheromone traps for the pea moth, *Cydia nigricana* (F.). Entomol Exp Appl 24:155–162

Wall C, Perry NJ (1980) Effect of spacing and trap numbers on interactions between pea moth pheromone traps. Entomol Exp Appl 28:313–321

Wamsley C, Wilde GC, Higgins R (2006) Preliminary results of use of a mark-release-recapture technique for determining the sphere of influence of a kairomone-baited lure trap attractive to adult western corn rootworm (Coleoptera: Chrysomelidae). J Kansas Entomol Soc 79:23–27

Weston PA (1986) Experimental and theoretical studies in insect chemical ecology: ovipositional biology of *Delia* flies and simulation modeling of insect movement. Ph. D. Dissertation, Michigan State University

Witzgall P, Bäckman AC, Svensson M, Koch U, Rama F, El-Sayed A, Brauchli J, Arn H, Bengtsson M, Löfqvist J (1999) Behavioral observations of codling moth, *Cydia pomonella*, in orchards permeated with synthetic pheromone. BioControl 44:2011–237

Wolf WW, Kishaba AN, Toba HH (1971) Proposed method for determining density of traps required to reduce and insect population. J Econ Entomol 64:872–877

Yudelman M, Rattu A, Nygaard D (1998) Pest management and food production: looking to the future. Food, Agriculture, and the Environment Discussion Paper 25. International Food Policy Research Institute